Action of the Bacterial Alarmones (p)ppGpp on Translational GTPases

DOCTORAL THESIS

Submitted in Fulfillment of the Requirements

of a Doctoral Degree in Chemistry

(Dr. rer nat.)

to the Department of Chemistry,

Philipps-Universität Marburg

presented by

M.Sc. Mohamad Majkini

from Syria

Marburg an der Lahn, 2021

Vom Fachbereich Chemie

der Philipps-Universität Marburg (Hochschulkennziffer 1180)

als Dissertation am _____angenommen.

Erstgutachter: Prof. Gert Bange

(Fachbereich Chemie der Philipps-Universität Marburg)

Zweitgutachter: Prof. Andreas Seubert

(Fachbereich Chemie der Philipps-Universität Marburg)

Tag der Einreichung: 01/12/2021

Tag der Disputation: / /2022

Scientific Career

Family Name, First Name: **Majkini, Mohamad**

Date, Place of Birth: 1st January 1987, Aleppo

Email: majkini1987@gmail.com

Education

08/2017 - 04/2021 Doctoral thesis

"Action of the bacterial alarmones (p)ppGpp on translational GTPases"

Prof. Dr. G. Bange, Philipps-University Marburg & SYNMIKRO, Germany

01/2010 - 05/2015 Master in Organic Chemistry

"Isolation and determination of some active chemical components from leaves and fruits of Morus Nigra"

Prof. Dr. A. Kattah, Aleppo University, Syria

10/2005 - 10/2009 Biochemistry study

Faculty of Science Chemistry Department at Aleppo University, Syria

Wissenschaftlicher Werdegang

Name, Vorname:	**Majkini, Mohamad**
Geburtsdatum und -ort:	01. Januar 1987, Aleppo
E-mail:	Majkini1987@gmail.com

Ausbildung

08/2017 - 04/2021 Doktorarbeit

„Wirkung der bakteriellen Alarmone (p)ppGpp auf translationale GTPasen“

Prof. Dr. G. Bange, Philipps-Universität Marburg & SYNMIKRO, Deutschland

01/2010 - 05/2015 Master in Organischer Chemie

"Isolierung und Bestimmung einiger aktiver chemischer Komponenten aus Blättern und Früchten von Morus Nigra "

Prof. Dr. A. Kattah, Fakultät für Naturwissenschaften der Universität Aleppo, Syrien

10/2005 - 10/2009 Studium der Biochemie

Fakultät der Naturwissenschaften der Universität Aleppo, Syrien

Statutory Declaration

I hereby declare that I have worked on this thesis independently. Furthermore, it was not submitted to any other examining committee. All sources and aids used in this thesis, including literal and analogous citations, have been identified.

Mohamad Majkini Marburg, 01st December 2021

Eidesstattliche Erklärung

Ich versichere, dass ich die hier vorgelegte Dissertation selbst und ohne fremde Hilfe verfasst, keine anderen als die angegebenen Quellen oder Hilfsmittel benutzt, alle vollständig oder sinngemäß übernommenen Zitate als solche gekennzeichnet sowie die Dissertation in der vorliegenden oder einer ähnlichen Form noch bei keiner anderen in- oder ausländischen Hochschule im Rahmen eines Promotionsgesuches oder zu anderen Prüfungszwecken eingereicht habe.

Mohamad Majkini Marburg, 01. Dezember 2021

Acknowledgements

This work was established at the research group of **Professor Dr. Gert Bange**, which is part of the interdisciplinary LOEWE Center for Synthetic Microbiology (Synmikro) and the department of Chemistry, located at the Philipps-University-Marburg.

I am grateful to **Professor Dr. Gert Bange**. It has been an honour working in his research group andunder his supervision.

I am deeply thankful to **Dr. Wieland Steinchen** for his support and advice during the project and for the performance of the HDX and HPLC measurements.

Sincere thanks to **Professor Dr. Andreas Seubert** and **Professor Dr. Olalla Vazquez** for the examination of this work.

Special thanks to **Anja Paulus** for her support, **Pietro Giammarinaro** who contributed to the construction of a suitable model to solve the protein structures used, and **Anita Dornes** for performing the translation assays.

My warmest thanks belong to my colleagues, you made the laboratory more than just a workplace.

My deepest gratitude belongs to my family who always supported me not only during this work but during the whole period of my studies.

Mohamad Majkini

Abstract

Ribosomes are intricate and highly complex macromolecular structures. Their maturation into fully functional entities is aided by a vast number of accessory proteins, many of which belong to the class of GTPases. GTPases do furthermore play pivotal roles during protein biosynthesis, during which the genetic code in the form of transcribed mRNA is translated into functional proteins.

The nutritional alarmones ppGpp and pppGpp, collectively abbreviated as (p)ppGpp or alarmones, are nucleotide-based second messenger molecules, the synthesis of which is linked to the onset of numerous unfavorable environmental conditions, in particular limitations in the availability of amino acids. Owing to the similarities of the (p)ppGpp compounds with the GTPase-directed GTP and GDP molecules, a direct regulation of ribosomal and translational GTPases is highly conceivable and documented in literature. However, a structural and mechanistic understanding of the action of (p)ppGpp and how precisely they interfere with GTPase functionality, are less well understood. This work aimed to fill this gap of knowledge.

Selected ribosomal and translational GTPases were purified and probed for their ability to interact with (p)ppGpp. The crystal structure of *Escherichia coli* elongation factor Tu (EF-Tu) could be obtained in presence of ppGpp and provides a rationale for inhibition of translation elongation by (p)ppGpp. Furthermore, alarmone binding to three GTPases involved in maturation of the prokaryotic ribosome was substantiated by various biophysical approaches evidencing that (p)ppGpp should interfere with their cellular function through competition with the natural substrate GTP. Although further implications of (p)ppGpp interference with ribosomal GTPases could not be substantiated in this work, it settles the stage for further in-depth mechanistic and functional studies on these target proteins.

Zusammenfassung

Ribosomen sind hoch komplexe Makromoleküle, deren vollständige Assemblierung in funktionale Einheiten eine Vielzahl von akzessorischen Proteinen und Faktoren bedingt. Viele dieser Maturierungsfaktoren gehören der Proteinfamilie der GTPasen an. Im Kontext des Ribosoms sind GTPasen weiterhin an der Translation, der Übersetzung des genetischen Codes in Form von DNA-abhängig transkribierter mRNA in funktionale Proteine, beteiligt.

Die Stressmoleküle ppGpp und pppGpp, oft auch als (p)ppGpp oder ‘Alarmone’ bezeichnet, sind nukleotidbasierte *second messenger*, deren Synthese den Beginn der bakteriellen Stressantwort auf eine Vielzahl von ungeeigneten Umweltbedingungen, insbesondere des Mangels an Aminosäuren, markiert. Aufgrund der strukturellen Ähnlichkeit von (p)ppGpp mit den Guanosinnukleotiden GTP und GDP ist eine direkte Regulierung von GTPasen naheliegend und in der Literatur dokumentiert. Ein tiefgründiges strukturelles und mechanistisches Verständnis der Wirkungsweise von (p)ppGpp, und dabei insbesondere wie diese die Funktionalität von GTPasen beeinflussen, fehlt bislang. Diese Arbeit versucht einen Beitrag zu einem verbesserten Verständnis beizutragen.

Ausgewählte in der Maturierung von Ribosomen und Translation am Ribosom beteiligte GTPasen wurden gereinigt und auf ihre Fähigkeit zur Interaktion mit (p)ppGpp geprüft. Die Kristallstruktur des translationalen Elongationsfaktors Tu (EF-Tu) aus *Escherichia coli* konnte dargestellt werden und lieferte strukturelle Erkenntnisse über die Art und Weise, wie (p)ppGpp die Translation inhibiert. Weiterhin wurde die Bindung von Alarmonen an drei GTPasen, welche in der Maturierung von prokaryotischen Ribosomen beteiligt sind, durch verschiedene biophysikalische Methoden manifestiert. Diese Experimente zeigten, dass (p)ppGpp die untersuchten GTPasen durch kompetitive Inhibition mit deren natürlichem Substrat GTP in ihrer Funktion hemmt. Obwohl keine strukturellen Erkenntnisse über die genaue Art und Weise der Inhibition dieser GTPasen gewonnen werden konnten, ebnet diese Arbeit den Weg für weitere mechanistische und funktionelle Analysen an dieser Proteinklasse.

Publications

During my work in the lab of Prof. Gert Bange, I contributed to the following publication:

Steinchen W, Ahmad S, Valentini M, Eilers K, **Majkini M**, Altegoer F, Lechner M, Filloux A, Whitney JC, Bange G (2021). Dual role of a (p)ppGpp- and (p)ppApp-degrading enzyme in biofilm formation and interbacterial antagonism. *Molecular Microbiology.*

Contents

List of Figures

Abbreviations

Chemical symbols, SI units and one-letter for amino acids were used without further reference. Abbreviations for bacterial species are given in the text. All other abbreviations employed in this work are listed below:

Å	Angstrom (= 0.1 nm)
AC	Affinity chromatography
ADP	Adenosine 5’-diphosphate
AMPPNP	Adenosine 5'-[(β,γ)-imido]triphosphate
APS	Ammonium persulfate
ATP	Adenosine 5’-triphosphate
ADP	Adenosine 5’-diphosphate
AMP	Adenosine 5’-monophosphate
AMPCPP	α,β-Methyleneadenosine 5’-triphosphate
bp	Base pairs
Cryo-EM	Cryo-electron microscopy
CV	Column volume
CTD	C-terminal domain
Da/Dalton	Da/Dalton (1.660538×10^{-27} kg)
ddH_2O	Double-distilled water
DMSO	Dimethyl sulfoxide
DNA	Deoxyribonucleic acid
dsRNA	Double-stranded RNA
DTT	Dithiothreitol
EDTA	Ethylenediaminetetraacetic acid
EF-Ts	Elongation factor Ts
EF-Tu	Elongation factor Tu
EF-G	Elongation factor G
GTP	Guanosine 5’-triphosphate
GDP	Guanosine 5’-diphosphate
GMP	Guanosine 5’-monophosphate
GMPPNP	Guanosine 5'-[(β,γ)-imido]triphosphate
His_6	Hexa-histidine
HPLC	High Performance Liquid Chromatography
HDX	Hydrogen-deuterium exchange
HDX-MS	Hydrogen-deuterium exchange coupled to mass spectrometry
HEPES	4-(2-Hydroxyethyl)-1-piperazineethanesulfonic acid
IPTG	Isopropyl-β-D-1-thiogalactopyranoside
IMP	Inosine 5'-monophosphate
IF-1	Initiation factor 1
IF-2	Initiation factor 2
IF-3	Initiation factor 3
LB	Lysogeny broth
L11	Ribosomal protein L11
L10	Ribosomal protein L10
mRNA	Messenger RNA

MWCO	Molecular weight cut-off
MR	Molecular replacement
MS	Mass spectrometry
NTP	Nucleoside triphosphates
NTD	N-terminal domain
OD	Optical density
PAGE	Polyacrylamide gel electrophoresis
PCR	Polymerase chain reaction
PDB	Protein data bank, www.pdb.org
pGpp	Guanosine 5'-monophosphate 3'-diphosphate
ppGpp	Guanosine 5'-diphosphate 3'-diphosphate
pppGpp	Guanosine 5'-triphosphate 3'-diphosphate
pNppGpp	Guanosine 5'-[(β,γ)-imido]triphosphate 3'-diphosphate
(p)ppGpp	ppGpp and pppGpp
PCR	Polymerase chain reaction
PEG	Polyethylene glycol
PTC	Peptidyl transferase centre
RNA	Ribonucleic acid
rRNA	Ribosomal RNA
RF1	Release factor 1
RF2	Release factor 2
RF3	Release factor 3
RSH	Rel-SpoT-Homolog
RNA	Ribonucleic acid
RNAP	RNA polymerase (α2ββ'ω-subunits)
rRNA	Ribosomal RNA
SDS	Sodium dodecyl sulfate
SEC	Size-exclusion chromatography
SF	Stringent factor
SAH	Small alarmone hydrolase
SAS	Small alarmone synthase
SDS-PAGE	Sodium dodecyl sulfate polyacrylamide gel electrophoresis
SR	Stringent response
TEMED	Tetramethylethylenediamine
tRNA	Transfer RNA
TF	Transcription factor
TBE	Tris/Borate/EDTA
Tris	Tris-(hydroxymethyl)-aminomethane
σ	Sigma factor

1 Introduction

1.1 The dogma of molecular biology

The expression of gene requires several steps, in which phenotypically identifiable expression can be achieved by encoded genetic information for the nucleotide sequence of DNA [1]. This process belongs to the central dogma of molecular biology, which inherits and transmits information in the form of nucleic acids. Through heredity, the double helix of DNA is duplicated semi-conservatively into two identical copies and divided into separating cells. In a two-stage cycle, the information contained in the DNA is processed into functional proteins. In the first stage, transcription, the DNA double-stand serves as a template for the generation of a single-stranded messenger RNA (mRNA) through RNA polymerases [1][2][3][4]. In the second stage, translation, the mRNA sequence is decoded at the ribosome into proteins by adding amino acid to the carboxyl end of carboxyl group of the growing peptide chain, whereby this read-out requires the aid of numerous proteinacious and non-proteinacious factors, e.g. tRNA, ribosomal RNA (rRNA) and elongation factors [3][4].

1.2 Protein biosynthesis

Proteins are biological molecules that consist of amino acids connected by a peptide bond between the carboxyl and amino groups of adjacent amino acid residues. They have plenty of functions in the organisms, such as catalyzing metabolic reactions, responding to stimuli, transporting molecules, or replicating DNA. Translation of mRNA into proteins at the ribosome is an intricate process, which can be divided into three functionally distinct steps: initiation, elongation of the polypeptide chain, and termination of mRNA translation, all of which are described in further detail below [3][4].

1.2.1 The ribosomes

Ribosomes are a large macromolecular complex, which consists of rRNA and a large number of proteins, organized in two subunits: a 30S subunit and a 50S subunit in prokaryots corresponding to 40S and 60S in eukaryots. They are found in prokaryotic and eukaryotic cells, and are considered a factory for synthesizing proteins in the cells [4][5].

In 1955, George E. Palade discovered ribosomes and described them as small particles in the cytoplasm [6]. In *Escherichia coli,* the ribosome has a molecular mass of approximately 2,500 kDa, and a diameter of roughly 20 nm [7]. Ribosomes consist of 66% RNA and about 34% of proteins. The association of the two ribosomal subunits of *E. coli,* which are characterized by sedimentation coefficients of 50S (large subunit) and 30S (small subunit), leads to formation the entire ribosome with a sedimentation coefficient of 70S. The large subunit consists of 34 different proteins and 23S, 5S rRNA, while the small subunit contains 21 proteins and 16S rRNA [4][5][8].

The large 50S subunit of prokaryotic cells contains the peptidyl transferase center that catalyzes the formation of peptide bond between the new amino acid and the nascent peptide chain. The small 30S subunit in contrast is thin and flexible, harboring the mRNA decoding center which ensures that the tRNA is bound to the ribosome and is combined with an mRNA codon at the correct anti-codon [9].

Roughly, around 100 factors are involved in the assembly of ribosomes and implicated in cleavage, re-modification, and chaperoning of intermediates of 50S and 30S [10]. It was demonstrated that (p)ppGpp is capable of regulating many of the factors that are implicated in the maturation of ribosomes. In *S. aureus*, it was found that (p)ppGpp is a target for some of ribosome biogenesis associated GTPases Era, RbgA, HflX, RsgA, and ObgE [11].

1.2.2 Transfer ribonucleic acid

Transfer RNA (tRNA) is the fundamental adaptor molecule that participates in the protein biosynthesis, and is characterized mainly by its length of 76-99 nucleotides with an average of approximately 76 nucleotides depending on the species and type of tRNA. The fraction of tRNA of the total pool of RNAs, being represented by rRNA, mRNA, and tRNA, is only 10-15% [4][12][13]. The pivotal function of tRNA, the delivery of amino acids to the ribosome, was first discovered by Hoagland et al in 1958 [14].
Common to all of tRNA molecules is that they harbor a conserved CCA motif at their 3'-end. Off the ribosome, tRNAs are loaded at this 3' CCA-end with their corresponding amino acids by dedicated aminoacyl-tRNA synthetases through the formation of an ester bond between the carboxy moiety of the amino acid and the 3' phosphate of the tRNA [15][4][16]. Specifically, 20 different aminoacylating tRNA synthetases are

present in *E. coli* that catalyze the aminoacylation reaction under the consumption of one molecule of ATP [17][4]. At the ribosome, the charged, i.e. aminoacylated, tRNAs bind to their cognate anticodon presented by the mRNA in the decoding center of the ribosome with the aid of the elongation factor Tu (EF-Tu) in the form of a ternary complex [15].

Besides its essential function in translation, in prokaryotes tRNA furthermore plays a role in the regulation of enzyme synthesis, such as the regulation of messenger RNA transcription for enzymes related to its amino acid biosynthesis [15].

1.2.2.1 Structure of tRNA

A high number of genes are coding tRNA. The tRNA is characterized mainly by their length of 76-99 nucleotides [13]. The tRNA has two effective parts, the first part is the terminal 3′ hydroxyl group which is able to bind with amino acids and form aminoacyl tRNA (aa-tRNA). The second part is anticodon, which interacts with codon in mRNA during the biosynthesis of proteins. There are also the D-arm and T-arm that are important for its specificity and efficiency [4][8].

In addition, a variable loop as discovered holding less than 20 nucleotides between the T-loop and the anticodon loop. According to the length of this variable arm, tRNAs are divided into two groups. The class I, which has four or five nucleotides in the variable arm and class II tRNAs, which has long variable arm, consisting of 10 or more nucleotides [18].

It was demonstrated that the last three bases of the end 3’ end of tRNA, where the amino acids are attached, are always cytosines-cytosines-adenine base, as well as the acceptor arm, which contains segments of the 5’ end of the tRNA, with a stretch of 7-9 nucleotides from opposite ends of the molecule base pairing with each other. It contains an anticodon loop, which interacts with codon in mRNA during the protein synthesis and acts as a key for recognition with aminoacyl-tRNA synthetase, moreover, it contains D-arm and T-arm that include stretch of nucleotides that base pair with each other and a loop that is single stranded [4]. tRNA has a secondary structure, which includes the acceptor region, D- and T-arms and the anticodon loop resembling a cloverleaf [4].

There is also tertiary structure of tRNA, which forms after folding the tRNA which appears ,as L-shaped with the acceptor stem and T-arm, which forms an extended helix, the anticodon loop and D-arm similarly make another extended helix [4][8].

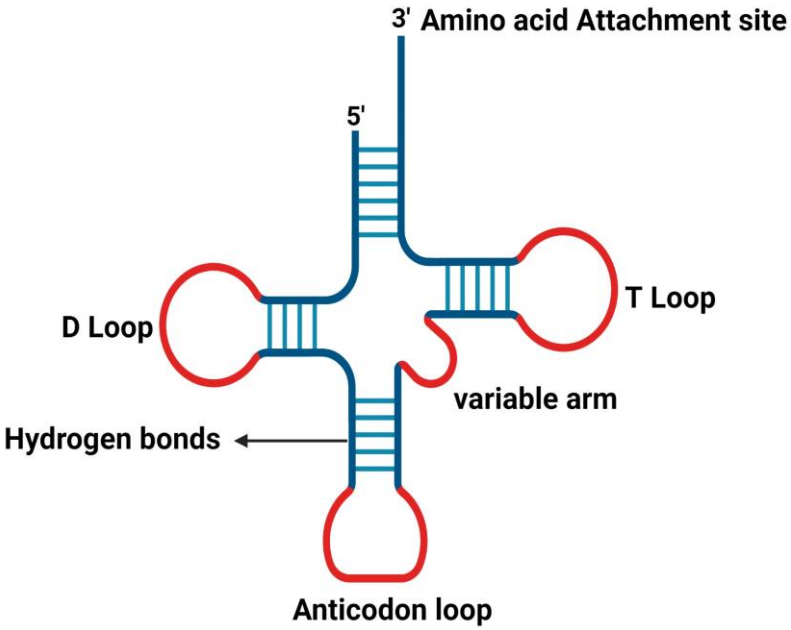

Figure 1. The secondary structure of tRNA.

1.2.2.2 Aminoacylation of tRNA by aminoacyl-tRNA-synthetases

For exact translation, two recognition mechanisms are required. The right selection of the correct amino acid for covalent linkage to the corresponding tRNA and the selection of the amino acid-loaded tRNA specified by the mRNA. The first step is catalyzed by the highly specific aminoacyl-tRNA synthetases for the corresponding amino acid and tRNA. These only distantly related enzymes recognize individual structures, usually on the inner surface of the L-shaped tRNA. In some cases, the anticodon is an essential recognition feature. In the ATP-dependent reaction, the amino acid is first converted to an aminoacyl-AMP intermediate then linked via the carboxyl group to the 2' or 3' hydroxyl group of the ribose at the 3' end of the tRNA forming an activated amino acid ester, as in figure (2), which explains the reaction of the formation of aminoacyl-tRNA [3][4].

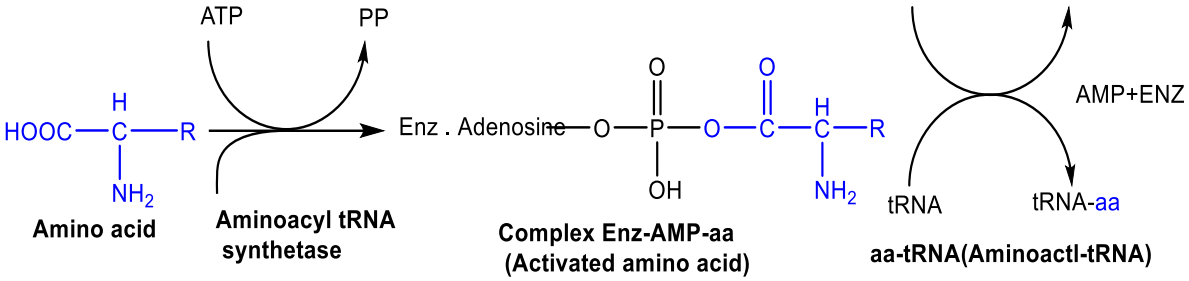

Figure 2. The reaction of the formation of aminoacyl-tRNA.

1.2.3 The translation

Translation has been divided to the three steps of initiation, elongation, and termination, which are described in further detail in the following chapters.

1.2.3.1 Initiation

During translation initiation, the ribosomal subunits, with the aid of initiation factors, assemble onto an mRNA molecule at the correct start point, which is marked by an initiator tRNA loaded with formylmethionine (fMet-tRNA) onto the mRNA's start codon. In details, initiation begins by a binding the mRNA with a complex of IF-2, GTP and fMet-tRNA onto the 30S subunit of the ribosome to form the 30S initiation complex [1][3][19]. The 16S rRNA protrudes from the ribosome with a pyrimidine-rich portion near the P-site. By base pairing with a purin-rich sequence of 3-10 nucleotides of the mRNA, the Shine-Dalgarno sequence gets centered about 10 nucleotides upstream of the start codon, allowing the ribosome to position itself on the start codon correctly [20]. This process is supported by the ribosomal GTPase IF-2. Through hydrolysis of the GTP bound by IF-2 to GDP + Pi, the ribosomal 50S subunit and the 30S subunit combine to form the 70S initiation complex, as seen in figure (3) illustrating the formation of the initiation complex. IF-1 and IF-3 are released when the 50S subunit binds to the 30S subunit forming 70S ribosome. Upon completion of polypeptide synthesis, the 50S and 30S subunits of ribosome remain linked as an inactive 70S ribosome. The initiation factors IF-1 and IF-3 cause the dissociation of the complex [21][22][4].

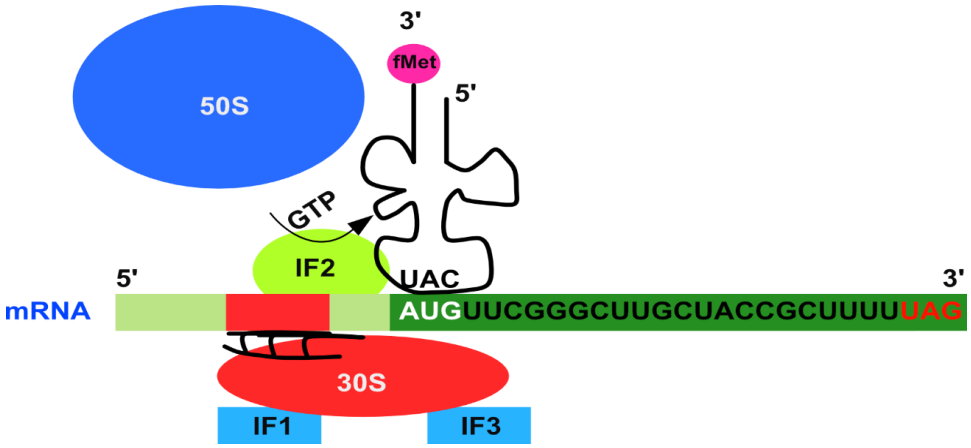

Figure 3. The formation of initiation complex.

1.2.3.2 Elongation

The second step of protein biosynthesis is translation elongation, which is initiated after the formation of the 70S complex. It contains three reaction steps: After the positioning of an aminoacyl tRNA at the A site by EF-Tu, which is followed by the formation of a peptide bond (transpeptidation) by peptidyl transfer, the elongation factor EF-G mediated the translation of the growing peptide chain. Repeating rounds of these three steps lead to an extension of the polypeptide chain by addition of amino acids to the C-terminus of polypeptide chain. EF-Tu plays a key role during this process because it delivers the required aminoacylated tRNAs to the translating ribosome [8].

The aminoacyl tRNA, which is delivered to the ribosome as the ternary complex EF-Tu/GTP/aa-tRNA by EF-Tu, is positioned on the cognate anticodon of mRNA at the A site of the ribosome. Upon doing so, the GTPase activity of EF-Tu is enhanced causing GTP hydrolysis, which subsequently causes the dissociation of the elongation factor Tu from the ribosome. Further delivery of aminoacylated by EF-Tu is only possible after reloading of EF-Tu with GTP reconverting the protein to its form able to coordinate aminoacylated tRNA. This reaction is mediated by the elongation factor Ts by displacement of GDP from EF-Tu, as seen in figure (4) [23][24].

When the peptide bond is formed by the peptidyl transferase activity of the ribosome, the amino group of the aminoacyl-tRNA displaces the tRNA at the P-site, thus, the nascent peptide chain of the peptidyl-tRNA at the P-site is transferred to the tRNA of the A-site and gets extended by one amino acid. The deacylated tRNA of the P-site is released after short-term binding to the exit site (E-site). The A-site peptidyl tRNA is

translocated to the P-site along with the codon-anticodon-linked mRNA [25][26]. For this process, an elongation factor G-dependent hydrolysis of GTP takes place. After hydrolysing the GTP of elongation factor EF-G, afterwards, either a new round of elongation or termination can occur [27][3].

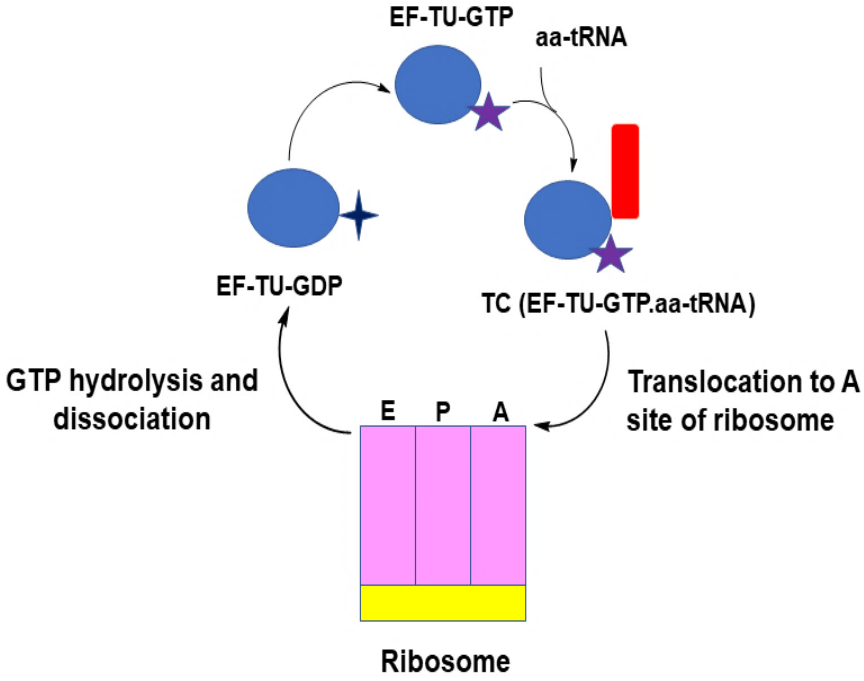

Figure 4. The cycle of elongation factor Tu.

1.2.3.2.1 Elongation factors Tu

The bacterial elongation factor EF-Tu is a G-protein, which means that it binds GTP or GDP. It is an essential protein in the cell. The main role of EF-Tu lies in the biogenesis of proteins through translation as a universal carrier of aa-tRNA [28]. It represents about 5 to 10% of all proteins in the cell highlighting its importance [29]. It was discovered by Gilman *et al.* that Mg^{2+} is cofactor of EF-Tu as described as well for other G-proteins [30]. Translation elongation EF-Tu in its GTP-bound form coordinates aa-tRNA, which is subsequently guided to a translating ribosome. The interactions between codon and anticodon lead to hydrolysis GTP on EF-Tu to GDP resulting in the release of P, inducing changing of the conformation of EF-Tu to GDP-bound state. EF-Tu/GDP leaves the ribosome and its nucleotide exchange of GDP to GTP aided by

EF-Ts which allows for another round of aa-tRNA binding and delivery to the ribosome [31][32].

1.2.3.2.2 Structure of elongation factors Tu

The crystal structures of EF-Tu from *E. coli* bound to GDP [33][34][32] and EF-Tu from *Thermus thermophilus and Thermus aquaticus* with GDP and GDPNP bound [35][36] illustrate the major conformational differences between the GDP and GTP-bound states of EF-Tu.

E. coli EF-Tu consists of 394 amino acids which are arranged into three domains. The N-terminal domain consists of 200 amino acids and is also referred to as the G-domain or domain I. It represents the catalytic part of EF-Tu and contains the binding site for GTP or GDP. The domains II (residues 201-300) and III (residues 301-393) succeed the G-domain [34]. The cofactor of EF-Tu is Mg^{2+}, which is essential for binding and hydrolysis of GTP [30]. In *E. coli* EF-Tu, the Mg^{2+} is coordinated by the hydroxyl group of Thr 25, an oxygen atom of the β-phosphate of GDP, and four molecules of water [37]. Depending on the nucleotide-loading state of EF-Tu, i.e. GDP or GTP-bound, the protein traverses between an open and a closed conformation. Hereby, in its GTP-bound form, domain I rotates by approximately 90° relative to domains II and III compared to the GDP-bound protein. An extensive rearrangement of the switch I (residues 40-62) and switch II regions (80-100) in the G-domain of *E. coli* EF-Tu is essential to facilitate this change in conformation. A part of the switch I region (residues 52-59) changes from a helical hairpin in the EF-Tu·GDP structure to an α-helix in the EF-Tu·GDPNP structure, while the position of β helix of the switch II region is shifted [34]. Crystal structures of different ternary complexes show that EF-Tu has a closed conformation similar to the free EF-Tu·GDPNP configuration, when bound onto aa-tRNA [38][39]. The changing between GTP-bound active and GDP-bound inactive was regulated by guanine-nucleotide exchange factor (GEFs) and (GAPs) GTPase activation protein [40].

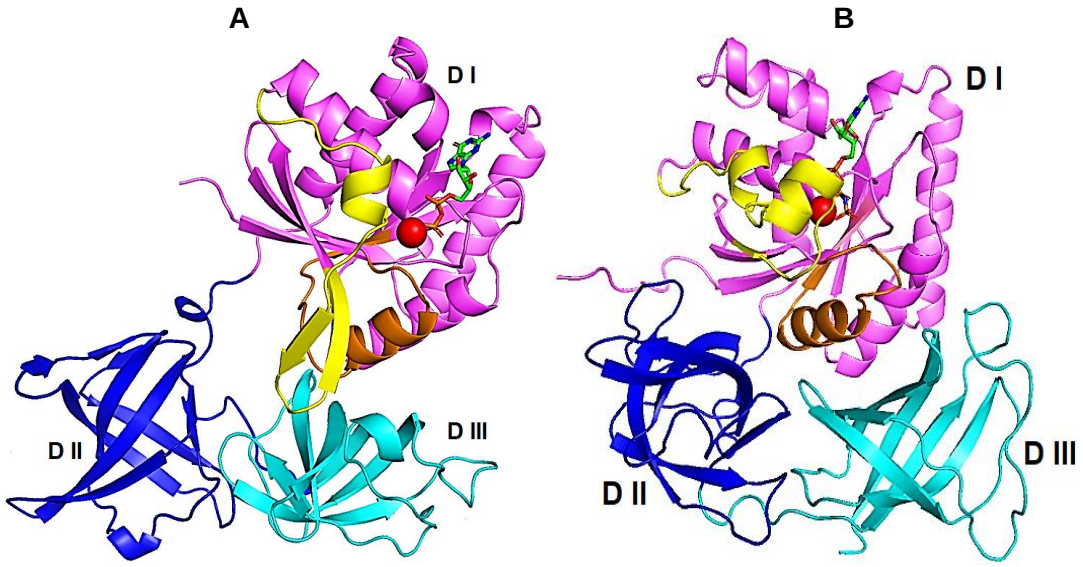

Figure 5. Structure of EF-Tu**.** (A) *Ec*EF-Tu-GDP; (B) EF-Tu-GTP from *T. aquaticus*. The switch I region is shown in yellow and the switch II region in brown. The rest of the polypeptide backbone is shown in violet, blue and cyan for domain I (residues 8-204), domain II (residues 205-298) and domain III (299-393), respectively. GDP or GDPNP molecules are shown in ball and stick models, and Mg^{2+} is shown as a red sphere. The structures were generated by PyMOL.

1.2.3.2.3 The ternary complex

The ternary complex of EF-Tu, GTP and aminoacyl tRNA (aa-tRNA) is a central component in the translation of genetic information during the biosynthesis of proteins, serving as a carrier of aa-tRNA to the A site of translating ribosome. It was known that active elongation factor Tu is not able to differentiate between different aminoacylated elongator tRNAs, however, it has the ability to recognize the sequence to all and it distinguishes between the peptidyl tRNA and uncharged tRNA [41].

It was solved the crystal structure of ternary complex of yeast (Phe-tRNA), EF-Tu from *Thermus aquaticus* and the guanosine triphosphate (GTP) analogue GDPNP to a resolution of 2.7Å. The structure appeared as an asymmetric unit containing three ternary complexes. EF-Tu, the helix of the acceptor and the helix of anticodon are protuberant from the complex as screw. The structure is elongated and resembles a bone-handled corkscrew (115×40×64 Å) [42]. The recognition between aa-tRNA and EF-Tu/GTP occurs in three regions [42]: *(i)* The binding of domain II with CCA Phe end

and the binding of the CCA interface to domain I. *(ii)* The binding of GTPase switch regions with 5'-end which binds to a part of the acceptor stem at the intersection of the three domain interfaces. *(iii)* The binding of the surface of domain III to one side of the T-stem [42].

The recognition between EF-Tu-GDPNP and tRNA includes the specified recognition of the aminoacyl bond and of the fold of the RNA A-helix formed by the T-stem and acceptor stem. For accurate positioning of the whole helix, steric surveillance and electrostatic clash are important characteristic [42]. It was found in *E. coli* that by the mutation of the 3-CCA terminus of tRNAs, EF-Tu/GTP prefers to recognize purines on tRNA more than pyrimidine, mostly cytosine and according to the K_D values of the interaction between of the EF-Tu/GTP ternary complexes with mutated valine tRNAs at the 3'-CCA end, it would prefer this priority: adenine then guanine then uracil. Taken all together, it exhibits the important role of the 3'-CCA end for recognition between EF-Tu and tRNA during the translation [41]. Upon the interaction between codon and anticodon is achieved, ternary complex accommodates in the A site of ribosome via GTP hydrolysis, afterwards, the extension of polypeptide chain is performed by forming a peptide bond between the amino acid of the tRNA in the P site of ribosome and the amino acid of the tRNA in the A site of ribosome. This translocation or movement is mediated by the elongation factor EF-G which binds onto the ribosome, inducing the hydrolysis of its GTP. The deacylated tRNA of the P-site is released after short-term binding to an exit site. The A-site peptidyl tRNA is translocated to the P-site along with the codon-anticodon-linked mRNA. The uncharged tRNA of E-site will be released from ribosome leading to triggering a new cycle of formation of ternary complex or termination of biosynthesis of protein [43].

1.2.3.2.4 Elongation factor Ts

Elongation factor Ts (EF-Ts) is the guanosine nucleotide exchange factor of EF-Tu. Its function is the reactivation of EF-Tu after hydrolysis of GTP, leading to the removal of the GDP from EF-Tu, which allows for faster rebinding of GTP [44].

The crystal structure of EF-Ts in complex with EF-Tu was determined in 1996 by Kawashima *et al.* at 2.5 Å resolution. The structure of EF-Tu/EF-Ts reveals that the complex contains two subunits of both elongation factors. The principle of the

reactivation of EF-Tu is that the interaction between EF-Tu and EF-Ts leads to the disruption of the binding of the magnesium with EF-Tu, and consequently a decrease in the affinity of elongation factor Tu to GDP. The disruption of the binding of magnesium with GDP was achieved by the insertion of conserved peptide 'TDFV' of elongation factor Ts into the elongation factor Tu [45].

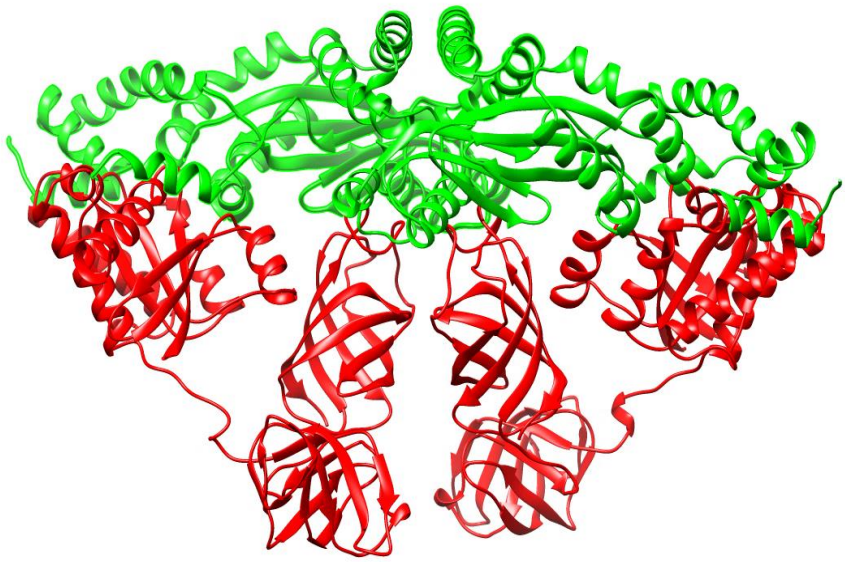

Figure 6. The structure of *E. coli* EF-Tu/EF-Ts complex. EF-Tu is colored in red, EF-Ts in green. The structure was generated by PyMOL.

1.2.3.3 Termination

Critical to the termination of translation are the release factors (RF) RF1, RF2 and RF3 [46]. RF1 and RF2 bind onto the ribosome with the support of a complex of RF3/GTP. RF1 is involved in the detection of the UAA and UAG stop codons at the A site, while RF2 has a preference in terminating translation upon recognition of UAA and UGA stop codons. After recognition, the hydrolysis of the ester bond between the aminoacyl tRNA of the P site and the polypeptide released the nascent chain [47][48]. The hydrolysis of GTP by RF3 serves in the dissociation of RF1 and RF2. Elongation factor EF-G and ribosome recycling Factor (RRF) are able to entirely dissociate the ribosome by removing mRNA and uncharged tRNA [49][50].

1.2.4 The bacterial stringent response

The microorganism's ability to adapt to the changing in environmental conditions is one of their hallmark features. Bacteria have developed many mechanisms for surviving under different stress conditions that it faces during its life. For instance, the concentrations of nutrients such as carbon, nitrogen, phosphate or sulfur and the growth conditions such as pH, temperature, oxygen availability, oxidative stress, osmotic stress or the presence of antimicrobial active substances. All those conditions affect bacterial growth and must be dealt with. Most regulatory mechanisms take place at a genetic level, which allows the bacteria to keep their cell compositions stable and balanced [51][52][53].

The stringent response (SR) or stringent control is an adaptive response in bacteria during unfavorable environmental conditions. It was initially discovered in *Escherichia coli* by Cashel & Gallant in 1969 as an accumulation of hyperphosphorylated nucleotides in response to amino acid starvation concomitant with its important consequences on the pattern of gene expression [54]. The stringent response has been studied for many years and substantiated its important role in growth and control of the expression of genes [55]. The hyperphosphorylated nucleotides accumulating in *E. coli* after amino acid exhaustion were initially dubbed 'magic spots' and only later identified as derivatives of GDP and GTP nucleotides, harboring an additional pyrophosphate moieties at their 3' hydroxyl position at the ribose (see figure (8) [55]. They were called ppGpp and pppGpp, respectively, and are commonly together abbreviated as (p)ppGpp. The synthesis of the (p)ppGpp alarmones marks the onset of the stringent response in the bacteria. Alarmone-dependent regulation is widespread depending on nutrient availability and also interconnects to specialized bacterial traits such as sporulation, biofilm formation and virulence [56].

Albeit historically identified as an adaptive mechanism in *Escherichia coli* during the reaction to amino acid limitation [57], stringent response mechanism mediated by (p)ppGpp were found in many bacterial species [51][53] and plant chloroplasts/plastids [58][59], but not yet identified in archaea or eukaryotes [60]. Furthermore, (p)ppGpp is also synthesized other stress conditions such as limitations of carbon, nitrogen, phosphate, sulfur, ion, or other adverse conditions of growth such as high or low pH values, temperature, availability of oxygen or oxidative stress, osmotic stress, or the presence of antibacterial drugs [56][51][58].

Upon amino acid limitation, the stringent response is triggered by a protein initially called stringent factor (SF) and later identified as Rel/RelA. Rel/RelA binds to ribosomes that contains an unacylated tRNA in the A-site during amino acids starvation [55][61][62], which leads to enhanced (p)ppGpp synthetic activity of Rel/RelA. Among other targets including GTPases [63], so-produced (p)ppGpp will interact with RNAP, which causes a down-regulation of stable RNA biosynthesis and an up-regulation of mRNA encoding for enzymes involved in amino acid biogenesis [64][65].

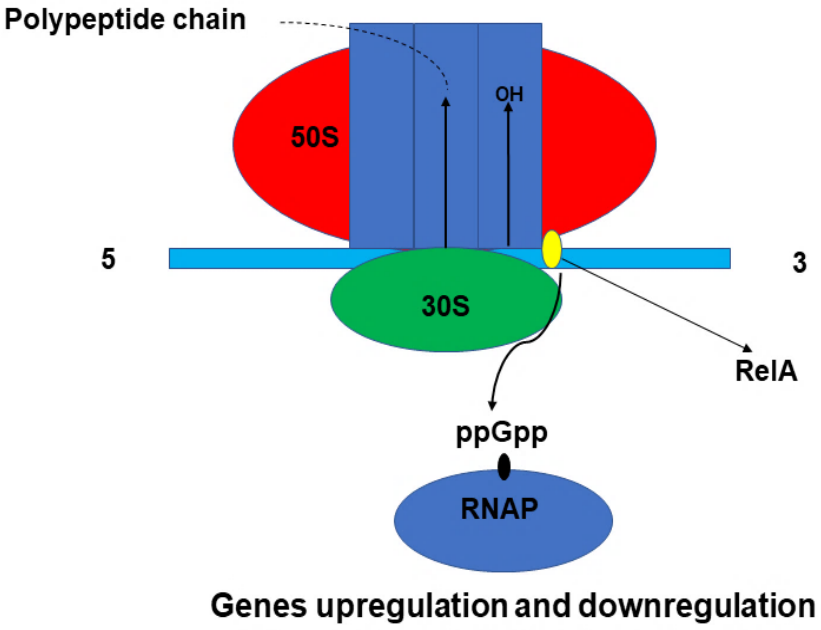

Figure 7. The activation of stringent response by the binding of stringent factor (SF, RelA) onto A site of ribosome.

1.2.4.1 Metabolism of (p)ppGpp

Given the pleiotropic regulation mediated by the (p)ppGpp alarmones, its synthesis and degradation requires specific enzymes that can balance its cellular levels. Furthermore, through differential regulation of these enzymes' activities, environmental and physiological cues may be translated into (p)ppGpp intracellular levels. Enzymes involved in synthesis and degradation appear in different organizations, which are further described in the following chapters. Additionally to these, GppA enzymes are able to interconvert the alarmones, i.e., degrade pppGpp into ppGpp leading to the believe that both alarmones might exhibit different functional outputs in the cell [66].

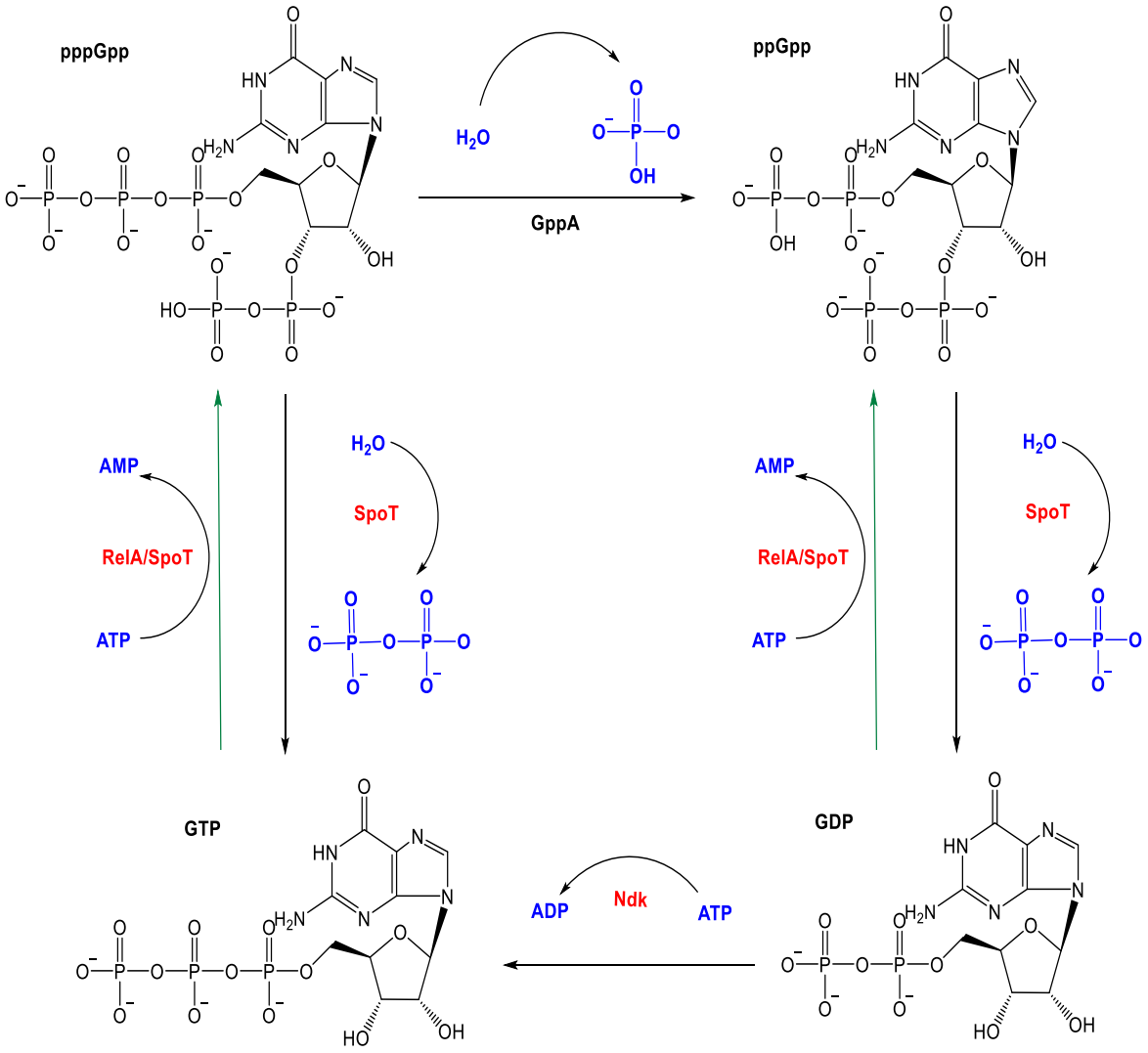

Figure 8. The biosynthesis and degradation of (p)ppGpp.

1.2.4.2 RelA/SpoT Homologue (RSH)

RelA /SpoT Homologue (RSH) enzymes appear in different topologies and may contain domains responsible for (p)ppGpp hydrolysis and/or degradation [63]. Their designation as RSH enzymes originates from their similarity to the RelA and SpoT enzymes found in *Escherichia coli*. However, bacterial species differ in their subset of RSH enzymes, which may contain long RSH homologues (Rel, RelA and SpoT enzymes), small alarmone hydrolases (SAH) that contain only a (p)ppGpp hydrolase domain, or small alarmone synthetases (SAS), which are characterized by the sole presence of a (p)ppGpp synthetase domain [67].

Gram-positive and gram-negative bacteria differ greatly in their RSH enzyme repertoire. Most gram-negatives, like *E. coli*, harbour the two long RSH enzymes RelA and SpoT (see above). In gram-positive microbes, such as *B. subtilis*, two small alarmone synthases (SAS) are present that consist only of a synthase domain and lack obvious regulatory parts. Furthermore, the Rel enzyme found in gram-positives is a bifunctional (p)ppGpp synthase/hydrolase as opposed to e.g., *E. coli* RelA [68].

1.2.4.2.1 Long RSH enzymes (Rel/RelA/SpoT)

The RelA enzyme from *E. coli* was the first enzyme exhibiting (p)ppGpp synthetase activity discovered. It is composed of an N-terminal portion (NTD) that contains a (p)ppGpp hydrolase domain, which is inactive though due to the absence of catalytically essential amino acid residues, and a (p)ppGpp synthetase domain, and a C-terminal portion (CTD) containing a TGS domain (abbreviated for ThrRS, GTPase, and SpoT), an α-helical domain, a zinc-finger domain, and an ACT domain (for aspartate kinase, chorismate mutase, and TyrA) [69]. The CTD of RelA was demonstrated to be responsible for mediating the binding of RelA to ribosomes that are stalled in translation through the presence of an uncharged tRNA in the A site of ribosome, thus elevating (p)ppGpp synthesis by RelA [58][70][71][72]. It was suggested by Agirrezabala and colleagues that the mechanism of activation of RelA critically relies on the inability of deacylated tRNA to continue to the P-site of the ribosome. This A/T-like conformation of the tRNA is important to encourage the interaction between L11 and the NTD of RelA to promote its activation [70][69][72]. It is still unclear though, how exactly the (p)ppGpp synthetase activity is triggered at the ribosome and concomitantly, how it is diminished in the absence of stalled ribosomes.

Regulation of the Rel enzyme possessing both (p)ppGpp hydrolytic and synthetic activities at the ribosome most likely proceeds similarly to its RelA counterpart [73]. However, as those Rel proteins are bifunctional, the their reciprocal enzymatic activities of the hydrolase and synthase domains require tight regulation to avoid futile cycles of (p)ppGpp synthesis and degradation in the absence of ribosomes too. Hogg and his colleagues solved the crystal structure of the NTD of Rel from *Streptococcus equisimilis,* providing some insights into regulation of the opposing activities [74]. Recently, it was furthermore demonstrated for the Rel protein from *B. subtilis* by Pausch and his colleagues that off the ribosome the (p)ppGpp synthetase domain

interacts with the TGS domain, thus holding the former in an inactive state. When bacteria faces nutrient starvation causing ribosome stalling, Rel will bind to those stalled ribosomes, concomitantly leading to a disruption of the synthetase/TGS interaction, which relieves the autoinhibition of the Rel synthetase domain by the TGS [75]. Rel/RelA proteins are additionally subject to allosteric regulation by their products itself. In a study on Rel from *Mycobacterium smegmatis*, an increased pppGpp synthesis was attributable to binding of (p)ppGpp to an unknown allosteric site, while at the same time the hydrolase activity was reduced. This indicates a positive feedback that allows Rel to sense and adjust the alarmone levels in the cell [76]. The relevance of Rel/RelA proteins for (p)ppGpp metabolism and the bacterial cell is underlined by the essentiality of the (p)ppGpp hydrolase domain in particular [76].

Besides the RelA proteins, the activity of which is triggered by stalled ribosomes, *E. coli* harbors a second RSH enzyme, SpoT. The domain architecture of SpoT is highly similar to that of RelA although subtle differences do exist. Specifically, SpoT harbors an active (p)ppGpp hydrolase domain as opposed to the inactive (p)ppGpp hydrolase domain found in RelA. Conversely, SpoT does not bind to stalled ribosomes but its functionality is implicated to be connected to stress conditions such as carbon starvation, and fatty acid or iron limitation [77][78][79][80].

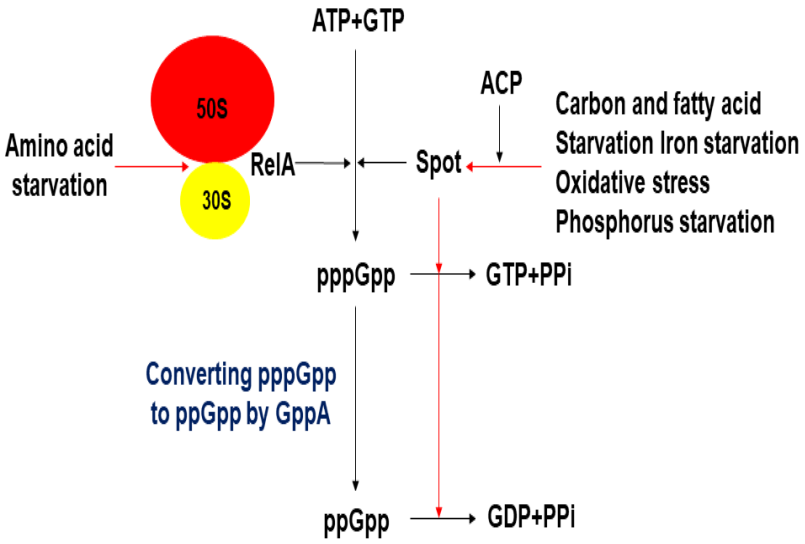

Figure 9. The schematic diagram of the pathway of synthesis and degradation (p)ppGpp by RelA or Spot, relying on the kind of stress [81].

1.2.4.2.2 Small alarmone synthetases (SAS)

Deletion of the genes encoding for RelA and SpoT in Gram-negative organisms results in no detectable amounts of (p)ppGpp. In contrast, upon deletion of the Rel-encoding gene in Gram-positive like *Firmicutes* (p)ppGpp synthesis was still apparent implying that other enzymes may be possess of (p)ppGpp synthetic activity [82][83]. These enzymes could be identified and were designated as small alarmone synthetases (SAS). There is some confusion in literature about the names of those enzymes; Lemos and colleagues named them as RelP and RelQ. However, Nanamiya and colleagues designated the two paralogues of *B. subtilis* SAS1 (gene locus: *yjbM*) and SAS2 (gene locus: *ywaC*), respectivley (SAS1 = RelQ; SAS2 = RelP) [82][84][67].

It was found that SAS1 and SAS2 are able to be transcribed in the different stages of growing curves, however, the transcription SAS1 peaks in the logarithmic phase, while SAS2 is mainly transcribed in the early stationary phase of *B. subtilis* [84]. Further regulation of SAS2 transcription is mediated by extracytoplasmic function (ECF) sigma factors, which are able to boost SAS2 transcription upon cell envelope stress caused by superoxide stress, acid stress, heat stress, ethanol and antibiotics [84][85].

Studies on *Staphylococcus aureus* support the notion that the two SAS enzymes confer elevated resistance to stress conditions in response to cell envelope stress [86]. However, the precise triggers and the ECF sigma factors through which they are mediated are still under debate, mainly because their activation signals and regulated genes do often overlap [87][88][89]. Beside regulation on the transcriptional level, SAS1 enzymes are targets of allosteric stimulation of their (p)ppGpp synthase activity by the (p)ppGpp products [90]. The activity of SAS2 from *S. aureus* was demonstrated to be elevated by zinc ions, however, the cellular role of this regulation remains elusive [91].

1.2.4.2.3 Small alarmone hydrolases (SAH)

Small alarmone hydrolases are the enzymes that are capable of converting (p)ppGpp to GTP or GDP. (p)ppGpp is not generally thought to be found in eukaryotes with the exception of plants and green algae. However, the first SAH enzymes reported were those of Mesh1 from *Homo sapiens* and *Drosophila melanogaster* [92][93]. Despite of

the functional role of Mesh1 enzymes being unclear, deletion of the gene encoding Mesh induces defects in the development of *D. melanogaster.* Besides, the presence of (p)ppGpp-degrading enzymes like Mesh raises the question about a potential functional role of (p)ppGpp in metazoan compounded by the fact that no (p)ppGpp synthases were identified in their genomes until now [67]. Recently, it was demonstrated that *Pseudomonas aeruginosa* harbors a SAH enzyme named *Pa*SAH that is able to hydrolyze (p)ppGpp, but also the closely-related (p)ppApp molecule. *Pa*SAH is in *P. aeruginosa* able to counteract the toxicity of (p)ppApp, which is synthesized by a secreted toxin, Tas1, during interbacterial competition, which imposes another role of SAH enzymes besides their activity on (p)ppGpp, and eventually (p)ppApp, for their native host's regular metabolism [94].

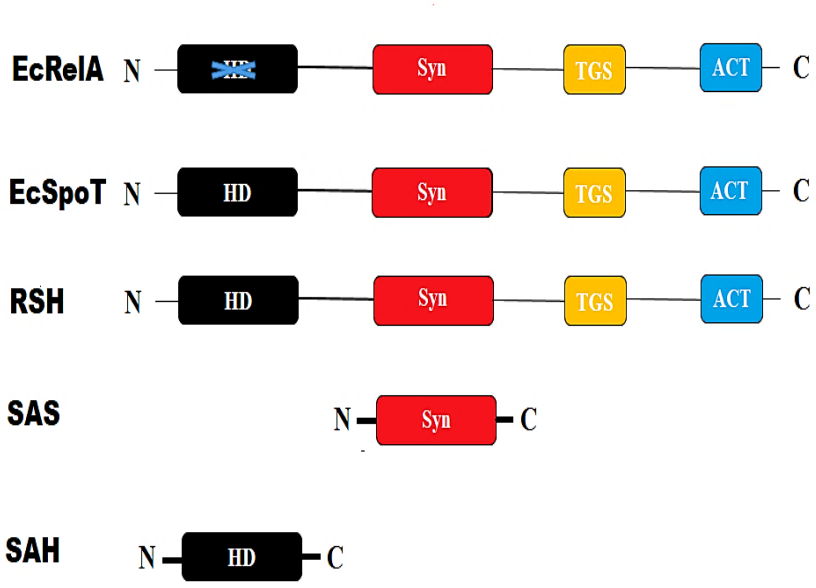

Figure 10. The domain architectures of RSH enzymes.

1.2.4.3 GTPases are affected by (p)ppGpp

1.2.4.3.1 Translational GTPases

Translational GTPases such EF-Tu, EF-G, IF2 and RF3 are the proteins that serve an important role in facilitating, controlling and regulating the biosynthesis of protein on the ribosome [95]. Given the similarities in the molecular structures between pppGpp and GTP, and ppGpp and GDP, it was suggested that pppGpp and ppGpp might interact with proteins that are involved in protein synthesis such IF2, EF-Tu and EF-G

[81][11][96]. This notion is supported in the case of IF-2, the activity of which, i.e. the formation of the initiation complex, is inhibited by ppGpp leading to downregulation of protein biosynthesis [96]. For EF-G and EF-Tu in absence of EF-Ts, inhibitory constants (K_i) for ppGpp of 3.10^{-5} M and 7.10^{-7} M, respectively, are reported [37]. Furthermore, the crystal structure and biochemical studies on RF3 evidence an interaction with ppGpp impairing the function of the release factor [97].

1.2.4.3.2 Ribosome biogenesis GTPases

The biogenesis of ribosomes in prokaryotic cells is a complex process that involves, e.g., the synthesis, cleavage, post-transcriptional modification and refolding of the rRNA. The assembly of a functional ribosome is highly costly and takes approximately [98][99]. A lot of factors aid in the assembly process of ribosomes such as GTPases, rRNA modification enzymes, helicases and other factors [100].

Assembly factors play a fundamental role for speeding up the maturating process of the 30S and 50S subunit of ribosome in the bacteria. Many of those assembly factors are ribosomal GTPases proteins. Their main role is the modification and correct refolding of the ribosomal components [81][11].

In 2016, Rebecca M. Corrigan and colleagues demonstrated that (p)ppGpp interferes with high affinity and specificity with five ribosomal assembly GTPases from *S. aureus*: RsgA, RbgA, Era, HflX, and ObgE. All of those bound (p)ppGpp with affinities comparable to those of GTP/GDP, and their *in vitro* GTPase activity was robustly inhibited by (p)ppGpp, thus implying a decreased ribosome maturation rate under stringent response conditions *in vivo* [11]. Another example, which explains the effect of (p)ppGpp on ribosome-associated GTPases, is CgtA. It binds GDP, GTP and ppGpp. It was found that CgtA interacts with ribosome as an assembly factor of 50S in the normal conditions, however, it interacts with the ribosome as anti-assembly of 50S in the stress conditions in the presence of (p)ppGpp [101].

2 Aim of the work

The overarching goal of the study was to provide a comprehensive description of the abilities of GTPases involved in maturation of the prokaryotic ribosome or translation to interact with (p)ppGpp and the functional consequences of these interactions.

2.1 Objectives of the study

The particular objectives of the study were as follows:

- Establishment of purification strategies for ribosomal and translational GTPases to allow for further structural and functional studies.
- Determination of binding of (p)ppGpp ribosomal and translational GTPases and comparison to binding of the natural ligands GDP and GTP.
- Structural basis of (p)ppGpp coordination and action of ribosomal and translational GTPases.
- Functional implications of (p)ppGpp coordination by ribosomal and translational GTPases.

3 Results

3.1 Purification of EF-Tu

Elongation factor EF-Tu from *E. coli* was cloned encoding an N-terminal hexa-histidine tag and overproduced in *E. coli* BL21(DE3). Hence, the purification of EF-Tu was conducted by a two-step protocol, employing Ni-NTA affinity chromatography and size-exclusion chromatography (SEC) as explained in materials and methods. After Ni-NTA and SEC, *Ec*EF-Tu could be obtained in good amount and purity (figures 11 and 12).

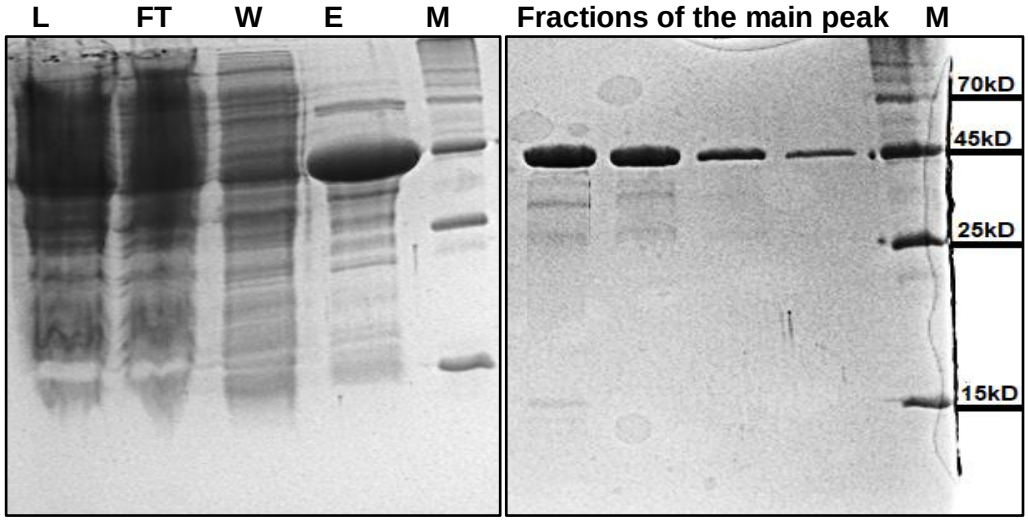

Figure 11. The SDS-PAGE of purification of *Ec*EF-Tu after Ni-NTA. Ladder (M), Load (L), flow-through (FT), wash (W), elution (E).

Figure 12. The SDS-PAGE of purification of *Ec*EF-Tu after SEC. Ladder (M).

Nevertheless, these initial purifications of *Ec*EF-Tu contained high amounts of GDP as evidenced from elevated absorbance ratios of A_{260} to A_{280}. EF-Tu proteins are well known to co-purify with GDP bound because of the nucleotides high affinity to the protein. Hence, an additional step was integrated between Ni-NTA and SEC, i.e., the eluted *Ec*EF-Tu after Ni-NTA was supplemented with 50 mM of EDTA. EDTA complexes the Mg^{2+} cofactor required for coordination of the GDP nucleotide by EF-Tu. Successful expulsion of GDP from EF-Tu was evidenced on SEC by an additional peak absorbing mainly at 260 nm eluting after the *Ec*EF-Tu protein at approximately 290 ml (figure 13).

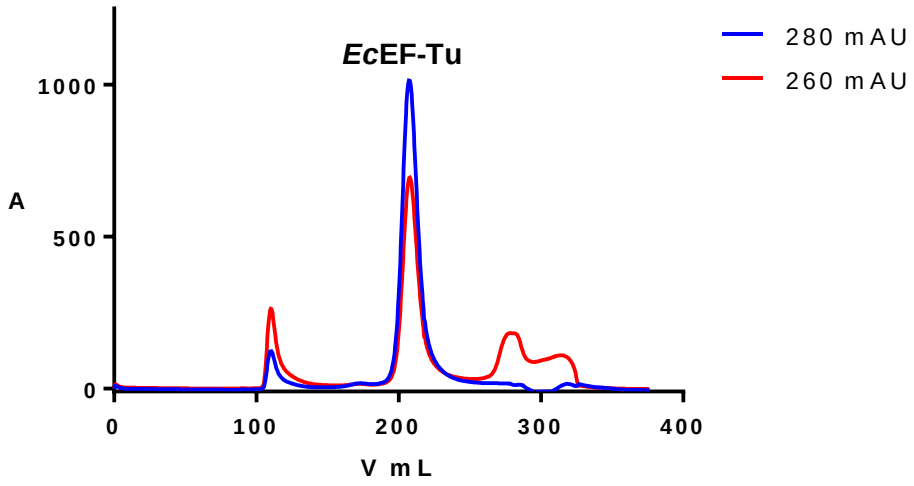

Figure 13. The SEC chromatogram of purification of *Ec*EF-Tu.

In order to substantiate that the released product was GDP, and that the EDTA-treated EF-Tu preparation was free of the nucleotide, high-performance liquid chromatography was conducted with denaturated EF-Tu prepared in either fashion. Comparison of the retention time with that of pure GDP suggested that the GDP was efficiently removed by EDTA treatment (figure 14).

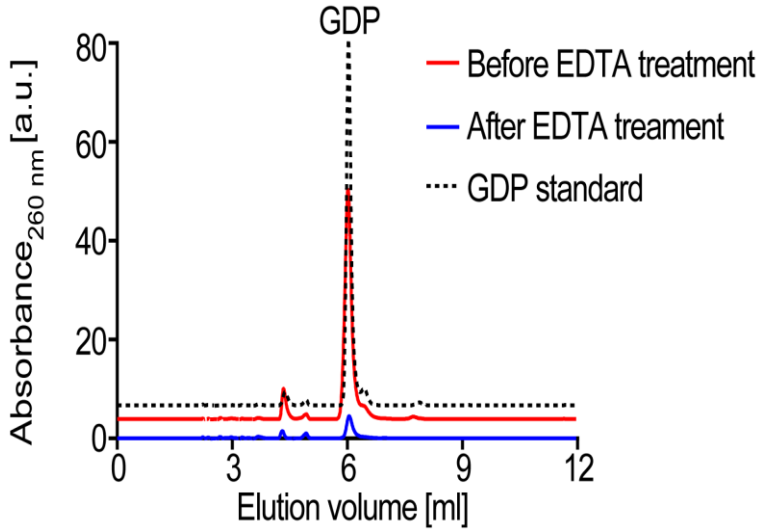

Figure 14. The removal of GDP during purification of EF-Tu. UV traces of *Ec*EF-Tu before (red) and after treatment with EDTA (blue). GDP (black points) was used as a standard.

3.1.1 Purification of EF-Ts

Elongation factor EF-Ts from *E. coli* with an N-terminal hexa-histidine tag was overproduced in *E. coli* BL21(DE3). The purification of EF-Ts was carried out by a two-steps protocol, employing Ni-NTA affinity chromatography and size-exclusion chromatography (SEC) as explained in materials and methods. In SEC chromatogram, *Ec*EF-Ts from *E. coli* was eluted at roughly 200 ml, as seen in figure (17). EF-Ts exhibited an elevated A_{260} to A_{280}. owing to the protein possessing no tryptophan residues.

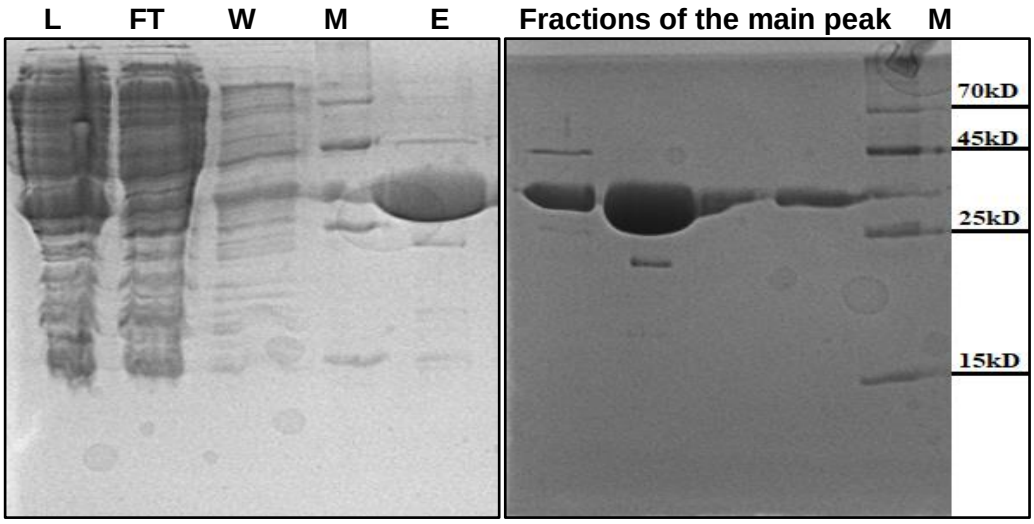

Figure 15. The SDS-PAGE of purification of *Ec*EF-Ts after Ni- NTA. Ladder (M), Load (L), flow-through (FT), wash (W), elution (E).

Figure 16. The SDS-PAGE of purification of *Ec*EF-Ts after SEC. Ladder (M).

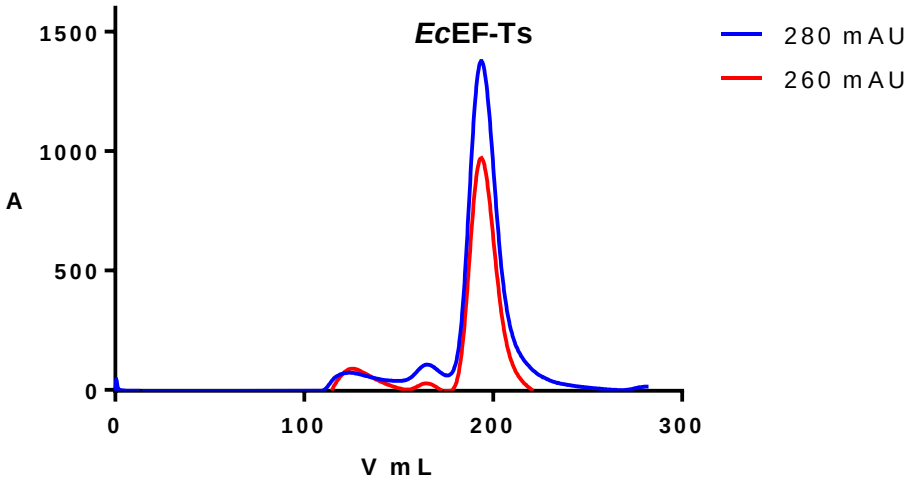

Figure 17. The SEC chromatogram of purification of *Ec*EF-Ts.

3.1.2 Studying the interaction of *Ec*EF-Tu with ppGpp and GDPs by ITC

With the almost nucleotide-free *Ec*EF-Tu at hand, its interaction with ppGpp, and GDP as a control, was studied by isothermal titration calorimetry (ITC). Due to the protein preparation being carried out in the absence of Mg^{2+}, magnesium chloride was supplemented again in these assays. ITC revealed a high binding affinity of GDP to EF-Tu of approximately 120 nM at a molar ratio of roughly one, consistent with one nucleotide-binding site present per EF-Tu monomer (figure 18). The alarmone ppGpp exhibited an even higher affinity to EF-Tu of 14 nM (figure 18). Due to unclear reasons, no binding affinity could be obtained with ITC for GTP and pppGpp.

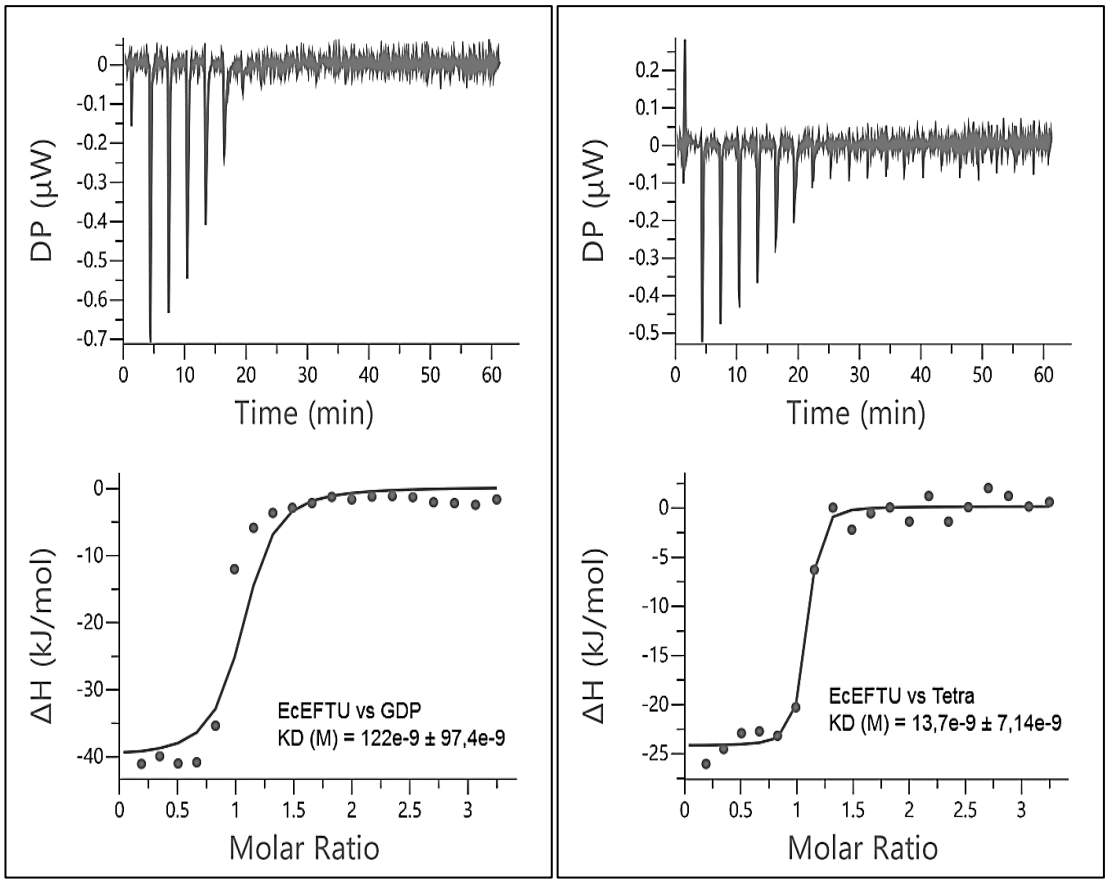

***Ec*EF-Tu vs GDP K_D (M) = 122e^{-9} ± 97.4 e^{-9}** ***Ec*EF-Tu vs ppGpp K_D (M) = 13.7e^{-9} ± 7.14 e^{-9}**

Figure 18. The ITC titration curves (upper panels) and binding isotherms (lower panels) of *Ec*EF-Tu interaction with GDP left, ppGpp right. The processing of data was done by Pietro Giammarinaro.

3.1.3 Studying the interaction between *Ec*EF-Tu and GDP, GTP, GMPPNP, ppGpp, pppGpp and pNppGpp by MST

In order to consolidate ppGpp-binding to *Ec*EF-Tu and to study the potential binding of pppGpp as well, microscale thermophoresis (MST) was employed as another technique. In these experiments, the binding affinities of GDP and ppGpp, and those of GTP and pppGpp were probed. Additionally, to avoid artificial results caused by e.g. GTP hydrolysis by EF-Tu, a β/γ non-hydrolysable GTP derivative (GMPPNP) and a similar pNppGpp compound were utilized (figure 19). In MST, GDP exhibited a higher affinity of 23±8 nM than in ITC (120 nM, see above). The affinity of GDP exceeded that of GTP (157±79nM) approximately 5-fold. A discrepancy in the affinities of ppGpp and pppGpp to *Ec*EF-Tu, i.e., 85 ±36 nM and 159±67nM respectively, was in agreement with the notion that binding of the diphosphate nucleotides (GDP, ppGpp) proceeded

with higher affinity than that of their triphosphate nucleotide counterparts (GTP, pppGpp). GMPPNP and pNppGpp bound with similar affinities of approximately 150 nM to *Ec*EF-Tu suggesting that they rely on the same binding site and similar binding modes (figure 19). Collectively, these data suggest that the alarmones bind to EF-Tu with high affinity similar to their GDP and GTP counterparts.

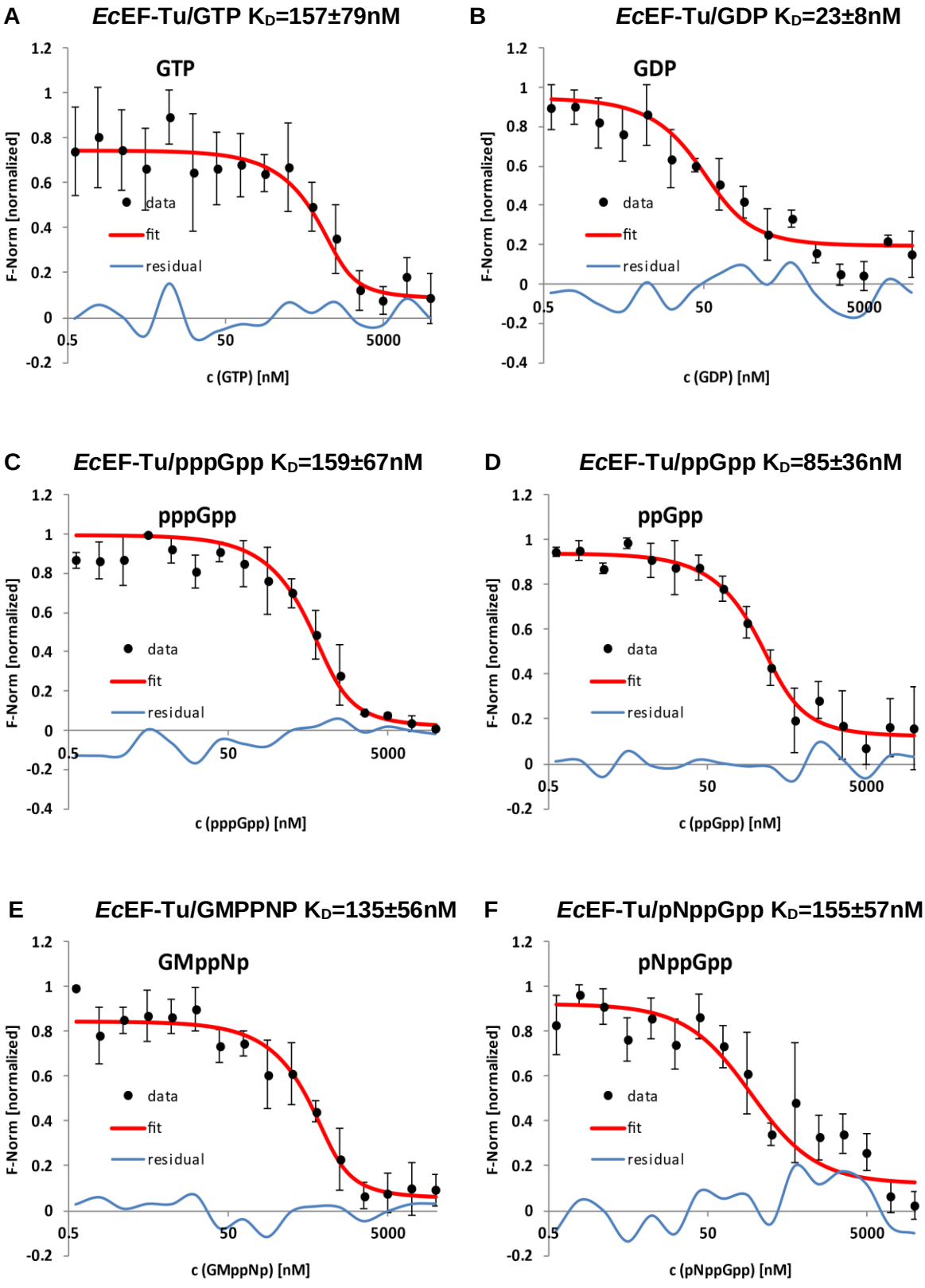

Figure 19 A-F. Binding of GTP (A), GDP (B), pppGpp (C), ppGpp (D), GMPPNP (E) and pNppGpp (F) to *Ec*EF-Tu determined by MST. Data processing was done by Dr. Sven Andreas Freibert.

3.1.4 Studying the interaction between *Ec*EF-Tu and nucleotides in presence and Absence of EF-Ts by pull-down

The interaction between *Ec*EF-Tu and nucleotides (GDP, GTP, ppGpp, pppGpp) was further studied with a pull-down approach. Hereby, the impact of the presence of EF-Ts on EF-Tu's nucleotide binding was evaluated as well. EF-Tu was incubated in absence or with 1 mM nucleotides and afterwards via its His_6-tag immobilized on Ni-NTA beads. After washing and elution of the protein (figure 20), the absorbance at 280 and 260 nm was quantified. Binding of guanosine nucleotides to EF-Tu is evidenced by an elevated A_{260}/A_{280} ratio caused by the guanosine nucleotides' absorbance maximum at 254 nm (table 3.1). This result is in agreement with the nanomolar affinity of nucleotide binding to EF-Tu (see above). In presence of EF-Ts, however, no change in the A_{260}/A_{280} ratio was apparent, compared to the sample not containing any nucleotide (table 3.1). This suggests that EF-Ts does either prevent nucleotide binding to EF-Tu or that it removes any nucleotide bound by the latter.

Table 3-1. The organization of pull-down interaction

Sample	**1**	**2**	**3**	**4**	**5**	**6**	**7**	**8**	**9**	**10**
EF-Tu	+	+	+	+	+	+	+	+	+	+
EF-Ts	-	-	-	-	-	+	+	+	+	+
Nucleotide	-	GDP	GTP	G4P	G5P	-	GDP	GTP	G4P	G5P
A_{260}/A_{280}	0.76	0.91	1.00	0.91	0.92	0.71	0.72	0.71	0.71	0.72

*G4P and G5P denote ppGpp and pppGpp, respectively. The absorbance ratio A260/A280 was determined spectrophotometrically from the eluted protein (see figure 20).

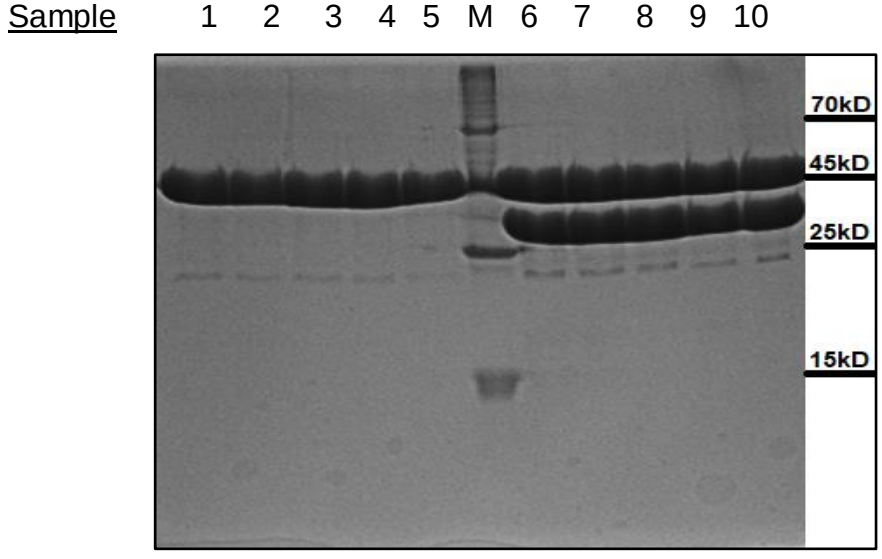

Figure 20. The SDS-PAGE of the interaction between EF-Tu, nucleotides and EF-Ts.

3.1.5 Assay the content of nucleotides of EF-Tu after pull-down by HPLC

To further corroborate the ability of nucleotides to interact with EF-Tu and its dependence on EF-Ts, the eluted proteins from the pull-down experiment (see above, figure 20) were further analyzed by high-performance liquid chromatography. To do so, the proteins were denaturated by treatment with chloroform and short heating to 95°C and the aqueous phases containing the nucleotides subjected to HPLC analysis. The identities of the bound nucleotides were validated by comparison of their retention times with that of a standard mixture containing all investigated guanosine nucleotides. These assays substantiate the notion that EF-Tu is able to interact with GDP, ppGpp and pppGpp in absence of EF-Ts (figure 21, blue traces). Upon incubation of EF-Tu with nucleotides in presence of EF-Ts no nucleotides bound to EF-Tu are retrieved (figure 21, red traces) indicating that EF-Ts dimishes the interaction of EF-Tu with guanosine nucleotides.

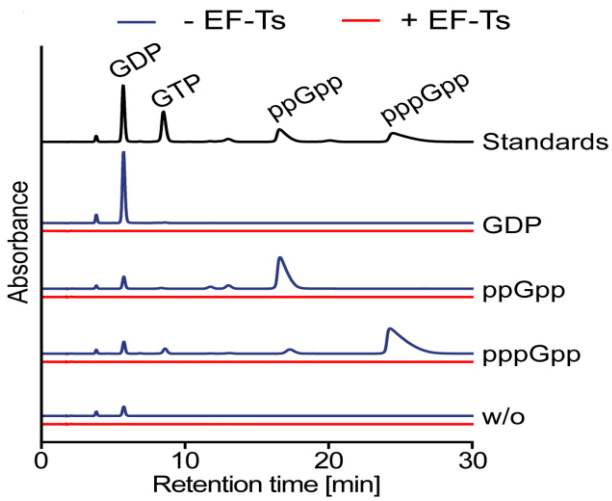

Figure 21. HPLC chromatograms of pull-down samples shown in figure 20, measured at 260 nm wavelength. EF-Tu with or without the indicated nucleotides was subjected to pull-down in absence (blue trace) or presence (red trace) of EF-Ts, and the eluted protein denaturated to set free the bound nucleotides. The black trace represents the UV chromatogram of a standard mixture containing GDP, GTP, ppGpp, and pppGpp.

3.1.6 Confirmation of Tu and TS interaction by SEC

The interaction between *Ec*EF-Tu and nucleotides (GDP, GTP, ppGpp, pppGpp), and its dependence on EF-Ts, was further studied by analytical size-exclusion chromatography as describe in material and methods. Hereby, the impact of the presence of EF-Ts on EF-Tu's nucleotide binding was evaluated as well. The data demonstrated the formation of EF-Tu.EFTs complex in the presence and absence of the nucleotides. It was evidenced the formation of EF-Tu.EFTs complex by the shift of EF-Tu peak to the front by EF-Ts.

According to SEC-chromatograms, the ratio A_{254}/A_{280} which was directly quantified from chromatograms and nanodrop, as seen in the table (3-2), thus, the binding of guanosine nucleotides onto EF-Tu was confirmed. Those results are in agreement with the results of nucleotide binding to EF-Tu (see above).

In the presence of EF-Ts, however, no change in the A_{254}/A_{280} ratio is apparent, compared to the sample not containing any nucleotide. This suggests that EF-Ts does either prevent nucleotide binding to EF-Tu or that it removes any nucleotide bound by the latter.

Table 3-2. The ratio 254/280 of the interaction EF-Tu, nucleotides and Ts

Sample	A254/280
TU	**0.74**
TU-GDP	0.79
TU-GTP	0.79
TU-Tetra	0.79
TU-Penta	0.79
TU-TS	**0.45**
TU-GDP-TS	0.45
TU-GTP-TS	0.45
TU-Tetra-TS	0.45
TU-Penta-TS	0.45

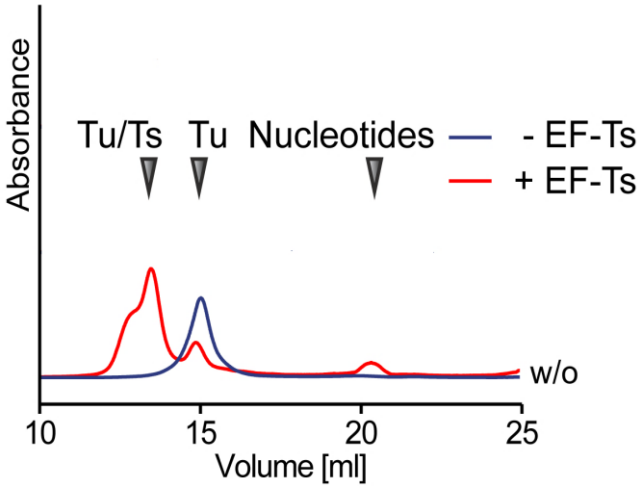

Figure 22. The analytical SEC of the interaction of Tu and Ts without nucleotides. Blue is in the absence of EF-Ts, red is in the presence of EF-Ts.

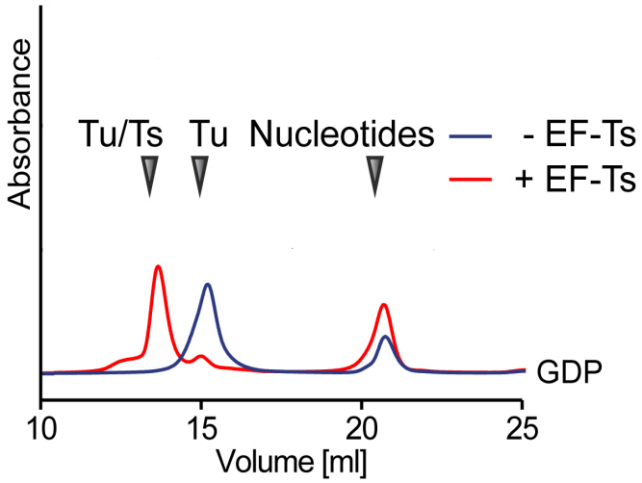

Figure 23. The analytical SEC of the interaction of Tu and GDP in the presence of EF-Ts (red) and in the absence of EF-Ts (blue).

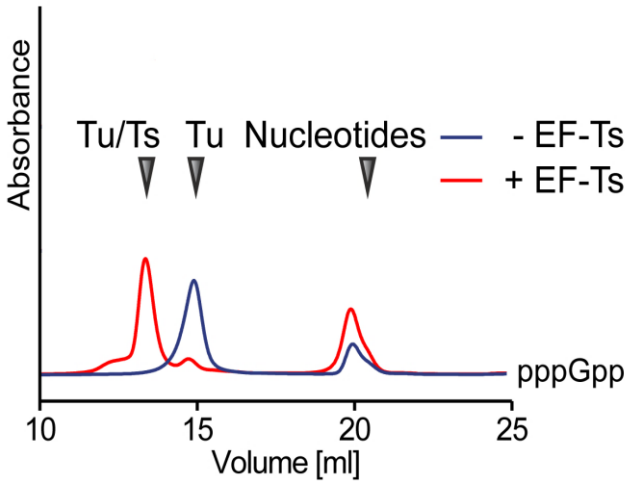

Figure 24. The analytical SEC of the interaction of Tu and pppGpp in the presence of EF-Ts (red) and in the absence of EF-Ts (blue).

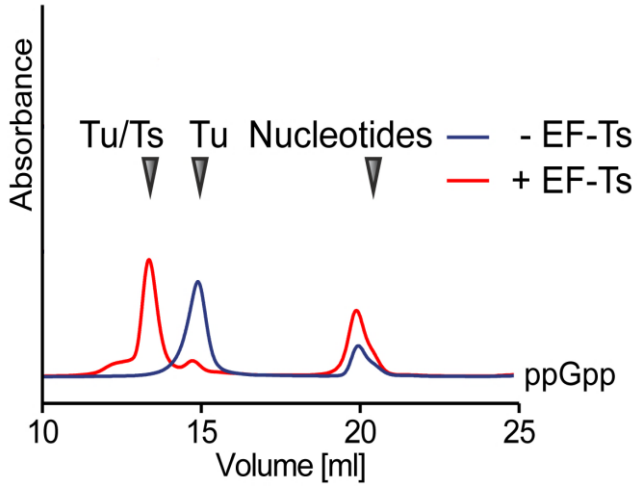

Figure 25. The analytical SEC of the interaction of Tu and ppGpp in the presence of EF-Ts (red) and in the absence of EF-Ts (blue).

3.1.7 Determination of the crystal structure of EF-Tu bound to ppGpp/Mg^{2+}

In order to get structural insights about the binding mode of (p)ppGpp and conformational changes of EF-Tu that may accompany their coordination, crystallization trials were conducted with *Ec*EF-Tu with either ppGpp or pppGpp. *Ec*EF-Tu was purified as described above in the absence of magnesium ions and EDTA treatment to remove residually bound GDP. These EF-Tu preparations were

concentrated to 1 mM and supplemented again with 10 mM $MgCl_2$ and either ppGpp or pppGpp added at 10 mM final concentration.

Crystals appeared after approximately two days in different conditions, however, the best shapes or qualities of the crystals were obtained from the following conditions: *(i)* 1 M lithium chloride, 0.1 M HEPES pH 7.0, 10% (w/v) PEG 6000, *(ii)* 0.15 M ammonium sulfate, 0.1 M MES pH 6.0, 15% (w/v) PEG4000, and *(iii)* 0.1 M magnesium chloride, 0.1 M HEPES pH 6.5, 15% (w/v) PEG4000. These conditions, besides promoting growth of crystals with good shape (figure 26), appeared most promising as they were of near-neutral pH, which is of importance because extremely acidic or basic pH values may render EF-Tu incapable of nucleotide interaction or cause elevated chemical degradation of the nucleotides.

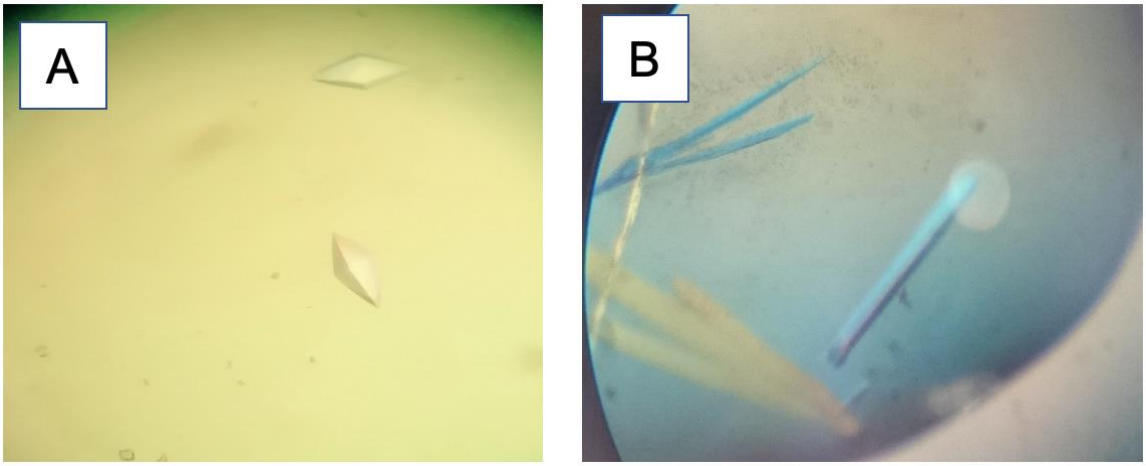

Figure 26. A-B. Representative crystals of *Ec*EF-Tu co-crystallized with pppGpp.

Crystals could be obtained for both ppGpp and pppGpp ligands. However, crystallographic datasets of high quality affording determination of the structure of *Ec*EF-Tu could only be obtained in presence of pppGpp. The crystal diffracted to a resolution of 2.0 Å, and the final model was refined to R_{work} and R_{free} values of 0.21 and 0.26, respectively (Table 3-3).

Notably, although EF-Tu was crystallized in presence of pppGpp, the alarmone ppGpp was found in the final structure. Hence, this dataset is from here on denoted as EF-Tu/ppGpp.

Table 3-3. The crystallographic data collection and refinement statistics

***E. coli* EF-Tu ppGpp/Mg^{2+}**	
Data collection	
Space group	$P4_32_12$
Resolution (Å)	48.78 - 2.0 (2.072-2.0)
Unit cell parameters	
***a*, *b*, *c* (Å)**	68.991, 68.991, 158.853
***α*, *β*, *γ* (°)**	90, 90, 90
R_{merge}	0.02123 (0.2664)
Average $I/\sigma(I)$	12.64 (2.09)
No. of total reflections	53564 (5224)
No. of unique reflections	26782 (2612)
Redundancy	2.0 (2.0)
Completeness (%)	99.99 (100.00)
CC1/2	0.999 (0.833)
Refinement	
R_{work}	0.2021 (0.2823)
R_{free}	0.2500 (0.3075)
No. of atoms	
Overall	2983
Protein **Ligand**	2835 37
Water	111
Average *B*-factors ($Å^2$)	
Overall	39.34
Protein **Ligand**	39.46 33.63
Water	38.37
Root-mean-square deviation	
Bond lengths (Å)	0.014
Bond angles (°)	1.93
Ramachandran plot (%)	
Favored	94.49
Allowed	4.41

*Values in parenthesis denote data for the highest-resolution shell.

The crystal structure of *Ec*EF-Tu-ppGpp encompassed almost the entire protein except for amino acid residues 40-60. The overall topology of *Ec*EF-Tu-ppGpp was very similar to that of *Ec*EF-Tu bound to GDP (PDB 1EFG, [102]). The N-terminal domain I, or G-domain encompassed amino acid residues 1-200 and contained the

ppGpp/Mg^{2+} ligands (figure 27). Residues approximately 201-300 and 301-393 arrange in β-barrel structures, denoted as domains II and III.

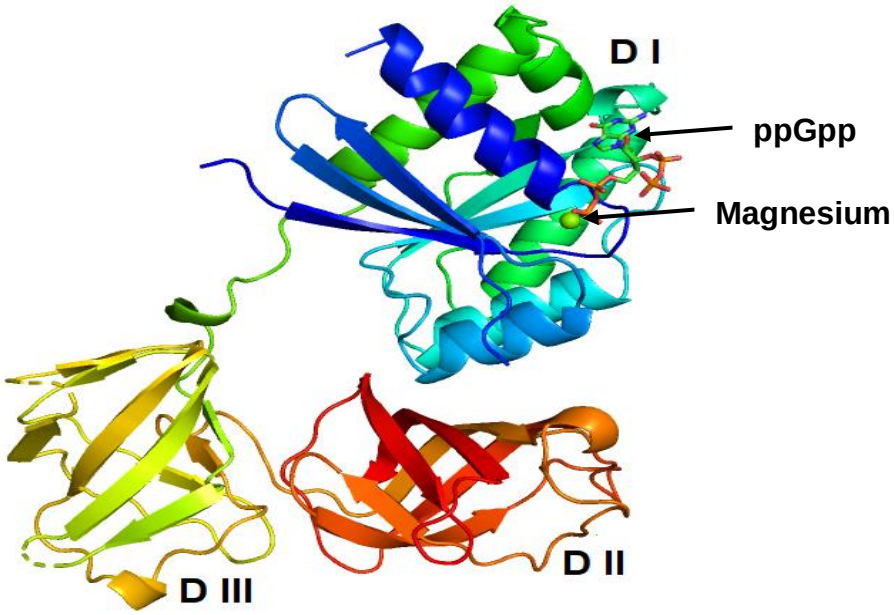

Figure 27. The structure of *Ec*EF-Tu-ppGpp with Mg^{2+}. Roman numbers denote the domains I-III of EF-Tu. The magnesium ion appears as a green sphere. The figure was generated by PyMOL.

The structure of *Ec*EF-Tu bound to ppGpp superimposes very well with that of the GDP-bound state of the protein with a root mean square deviation (r.m.s.d.) of 0.474 Å over 2011 atoms (figure 28). It, however, shows marked differences to the crystal structure of *Ec*EF-Tu solved in presence of the GTP analogue GMPPNP as shown in figure (28).

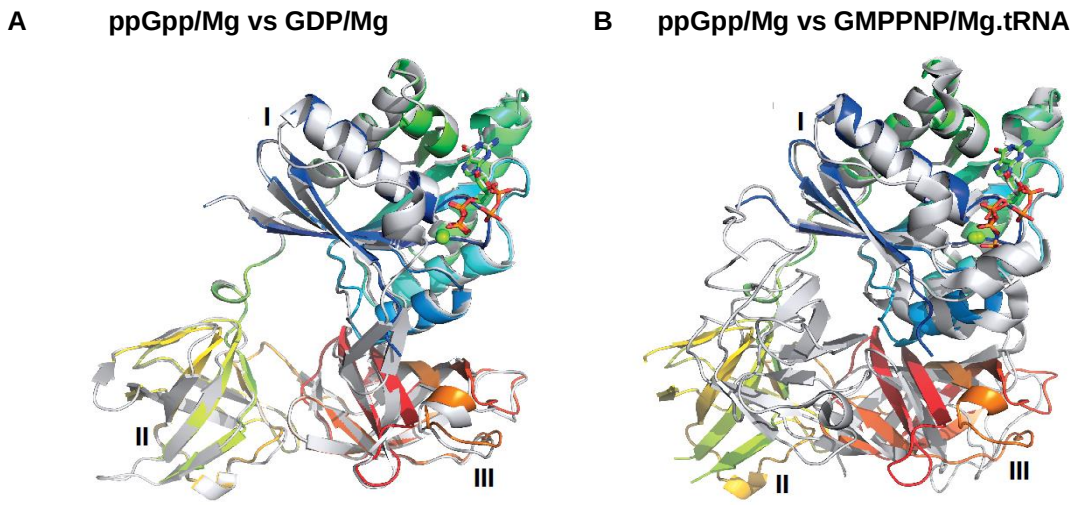

Figure 28. Comparison of the ppGpp-bound state of EF-Tu with other nucleotide-bound states. Roman numbers denote the domains I-III of EF-Tu.

Closer examination of the catalytic site in our structure of EF-Tu.ppGpp shows clear electron density for the guanosine moiety, the 5' α- and β-phosphates, the magnesium ion and the 3' δ– and ε-phosphates (figure 29). There is no further electron density present at the 5' end of ppGpp that would be in agreement with the presence of pppGpp with which EF-Tu was initially crystallized.

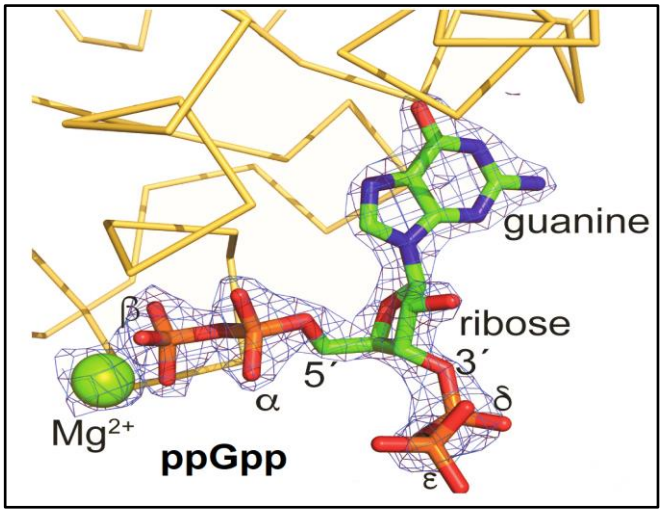

Figure 29. The electron density of ppGpp (sticks) and magnesium (green sphere) after final refinement. Yellow ribbons indicate the backbone of *Ec*EF-Tu. The figure was generated with PyMOL.

3.1.8 Coordination of ppGpp and Mg^{2+}

Deep examination in the catalytic site points out that the location of guanine base is between the side chains of K136 and L175 as a sandwich. It was found that ε-amino group of K136 interacts with O1 of the ribose, moreover, hydrogen-bonds are established between guanine base, 6'-oxo group and the N1 and 2'-amino group of the base and the side chains of N135, D138 and S173. The α-and β-phosphates at the 5' end of the ribose are coordinated primarily by the backbone amides of D21, G23, K24, T25 and T26, and furthermore by the side chains of K24 and T25. The β–phosphate specifically interacts with the side chain hydroxyl group of T25, four water molecules, and the magnesium ion. No specific interactions are established with the δ- and ε-phosphates at the 3' end. In the crystal structure of GDP-bound *Ec*EF-Tu, the position occupied by these two phosphates in presence of ppGpp would be that of residues 40-60, the switch I region, which are disordered in ppGpp-bound *Ec*EF-Tu (figure (30).

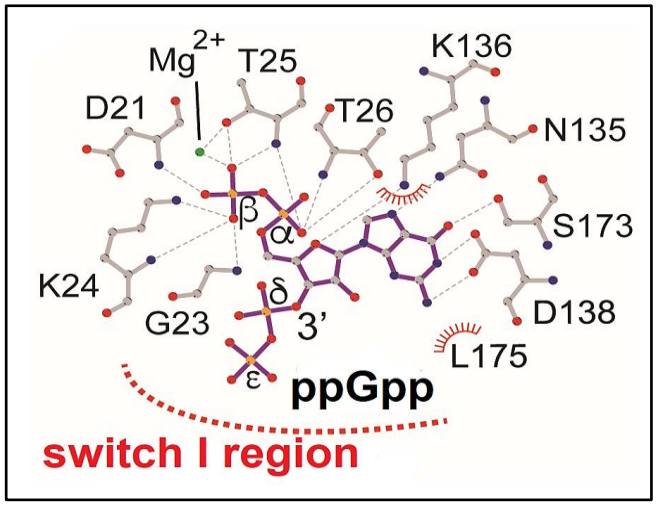

Figure 30. The coordination of ppGpp/Mg by *Ec*EF-Tu. Atoms are colored in grey (carbon), orange (phosphor), blue (nitrogen) and red (oxygen). Hydrogen-bonding interactions are indicated by black dotted lines.

A superimposition of the ppGpp and GDP-bound structures of EF-Tu highlights the incompatibility between the position of the δ- and ε-phosphate moieties of ppGpp and the switch I region, because of electrostatic clashes of the pyrophosphate with the residues F46 and D50 (figure 31 A and B). It may be suggested that this potential clash

is the reason for the switch I region in presence of ppGpp ligand being disordered. Similar steric hinderance between ppGpp and the switch I region would also be present in the GMPPNP-induced closed conformation of EF-Tu (figure 31C). Consequently, ppGpp should inhibit the function of EF-Tu by rearrangement of the switch I region of the elongation factor.

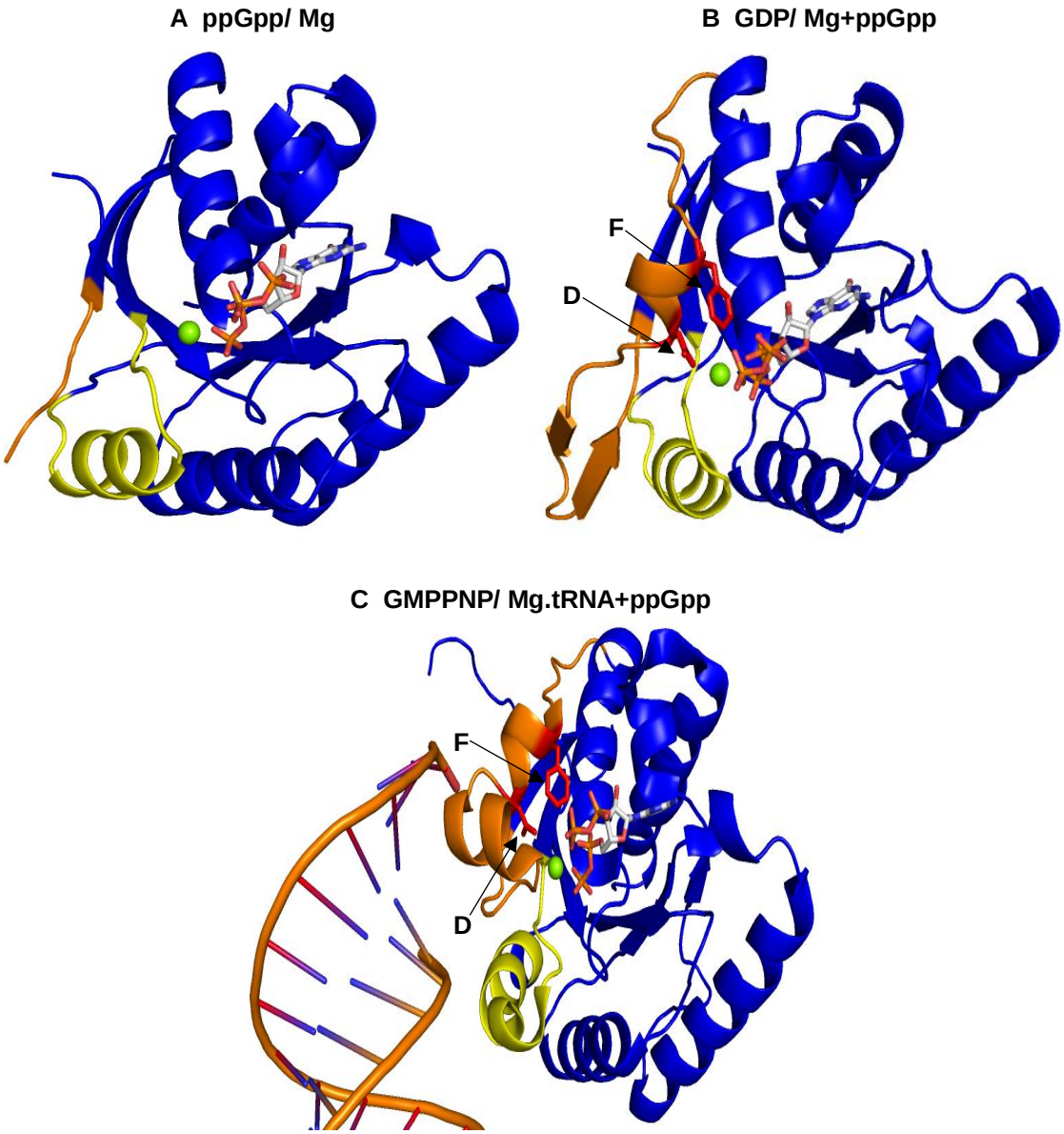

Figure 31 A-C. Cartoon representation of the catalytic domains of EF-Tu in complex with ppGpp/Mg (A), GDP/Mg (B, PDB: 1EFC) and GMPPNP/Mg, Phe-tRNA^{Phe} and kirromycin (C, PDB: 1OB2). The switch I and II regions are colored in orange and yellow, respectively. The rest of the catalytic domain was colored by blue. The F46 and D50 residues are colored in red. The ligand ppGpp was placed into all structures based on superpositions with ppGpp/Mg-bound EF-Tu.

3.1.9 Inhibition of translation by (p)ppGpp

To elucidate the role of (p)ppGpp in the inhibition of protein biosynthesis, the (p)ppGpp-dependent inhibition of translation was assayed *in vitro*. Hereby, a plasmid encoding for eGFP was used as template for transcription and translation, utilizing the RTS kit (Biozym), which contains all components for both processes. The assay was carried out in presence of rising concentrations of ppGpp or pppGpp to study their effect on translation. A weakness of this setup is that the (p)ppGpp present in the reaction might act on other proteins besides EF-Tu, e.g. RNAP [103][104]. The experiment demonstrated that pppGpp and ppGpp inhibit the translation activity, depending on the dose of pppGpp and ppGpp, as seen in figure (32).

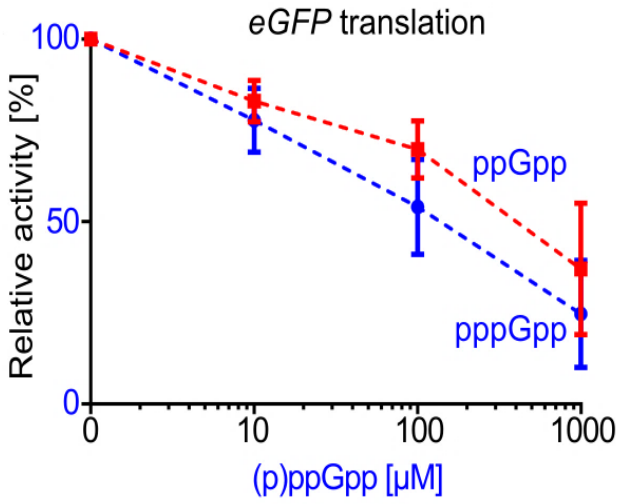

Figure 32. The *in vitro* Inhibition of translation by ppGpp and pppGpp. The activity in absence of (p)ppGpp was set to be 100%. Blue is the inhibition of translation by pppGpp and red is the inhibition of translation by ppGpp. The experiment was conducted by Anita Dornes.

3.1.10 The ability of EF-Tu to convert pppGpp to ppGpp

Although EF-Tu was crystallized in the presence of pppGpp, the crystal structure evidenced ppGpp bound to the protein. This might be caused by the higher affinity of ppGpp to EF-Tu rather than pppGpp leading a residual ppGpp contamination in our pppGpp preparation to bind to the protein. However, this finding might also suggest that EF-Tu would be able to convert pppGpp to ppGpp by the removal of the 5' γ-

phosphate. This reaction would be reminiscent of the canonical hydrolysis of GTP to GDP by EF-Tu. To probe EF-Tu's ability to hydrolyze pppGpp, the protein together with the nucleotide was incubated and determined the identity and quantity of the nucleotides by analytical HPLC. Indeed, incubation of pppGpp together with EF-Tu results in an increase of the ppGpp peak area, suggesting enzymatic hydrolysis as in figure (33).

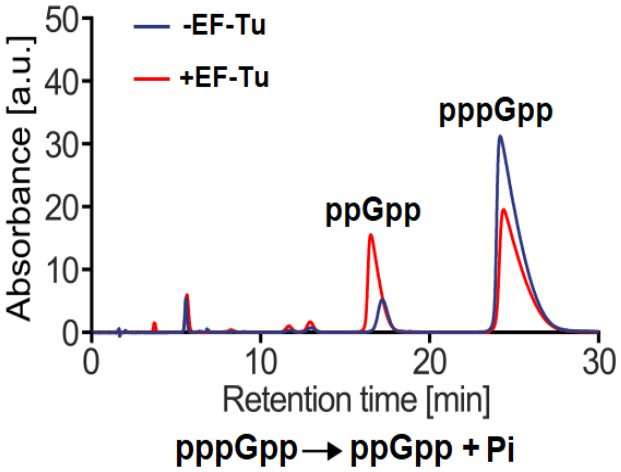

Figure 33. The representative chromatogram depicting the ability of *Ec*EF-Tu to degrade pppGpp into ppGpp through removal of the 5' γ-phosphate. Blue is the amount of nucleotides in absence of EF-Tu and red in the presence EF-Tu.

To further substantiate this observation, the hydrolysis of pppGpp was assayed in presence of increasing amounts of EF-Tu in a time-dependent fashion. These assays revealed production of ppGpp with increasing incubation time and enzyme concentration as in figure (34). Hence, EF-Tu appears to possess hydrolytic activity towards pppGpp.

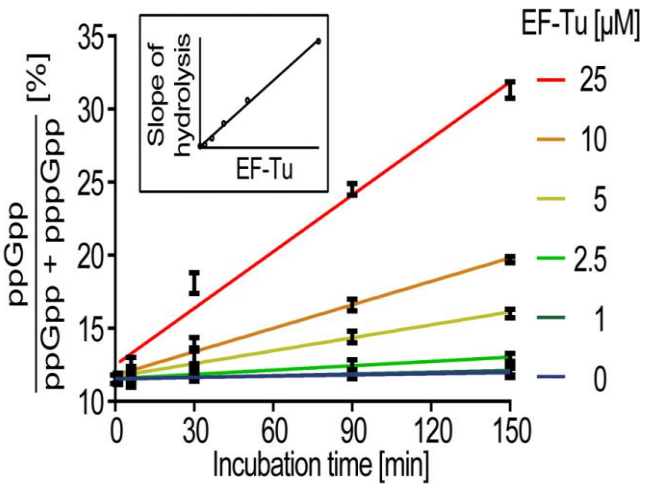

Figure 34. The slope of the linear regressions versus the concentration of *Ec*EF-Tu. The different colors point out to different concentrations of EF-Tu.

3.2 Purification of ribosomal proteins

3.2.1 GTP-binding protein EngA

EngA, also known as GTPase Der, exhibits an archetypical topology. It contains two GTPase domains, GTPase domain 1 (also GD1) and GTPase domain 2 (also GD2) of approximately 170 amino acid residues size, which are followed by a KH domain of roughly 100 amino acids [105]. Although GTP may bind to either of the GTPase domains, the activity of the GD2 is approximately 100-fold less than that of the GD1 [106].

The GTPase activity of EngA is critically involved in the maturation of 50S ribosomal subunits [107]. It is presumed that depending on the nucleotide bound within GD1 domain, either GTP or its hydrolysis product GDP, it rotates and by that exposes the positively-charged surface of the KH domain for binding of 23S rRNA [108][105].

3.2.1.1 Purification of EngA

To study a potential binding of (p)ppGpp to EngA and its influence on EngA conformation, the homologs from *E. coli* and *B. subtilis* fused with an N-terminal hexa-histidine tag were overproduced in *E. coli* BL21(DE3). The purification of EngA was done by a two-step protocol, employing Ni-NTA affinity chromatography and size-

exclusion chromatography (SEC), as explained in materials and methods. In SEC chromatogram, EngA from *B. subtilis* (*Bs*) or *E. coli* (*Ec*) eluted at 200 ml as shown in figures (37) and (38), respectively. The next peak, which was eluted after EngA with maximum absorbance 260 nm wavelength, represents the GDP that was set free during the purification of both EngA proteins by EDTA treatment.

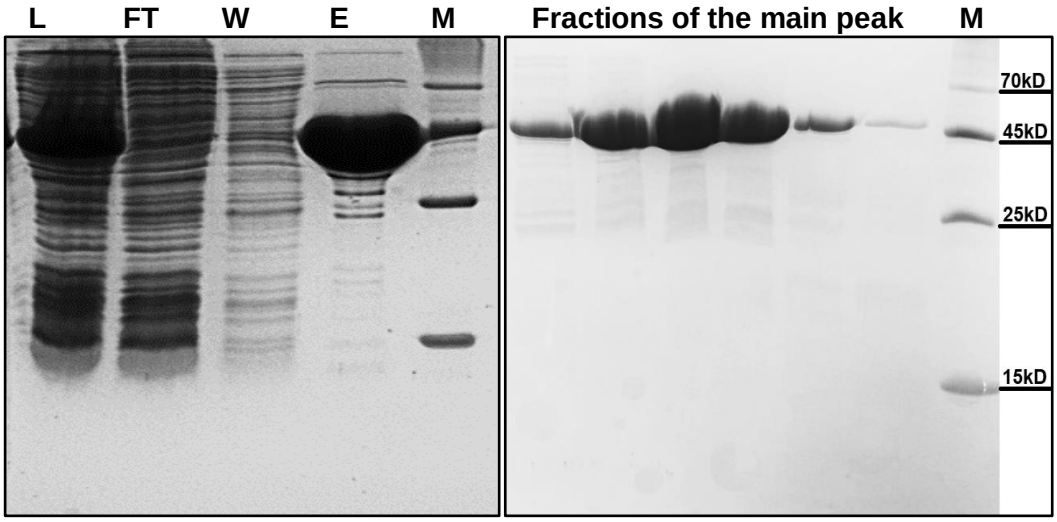

Figure 35. The SDS-PAGE of purification of *Bs*EngA after Ni-NTA. Ladder (M), Load (L), flow-through (FT), wash (W), elution (E).

Figure 36. The SDS-PAGE of purification of *Bs*EngA after SEC. Ladder (M). Similar quality and quantity were achieved for the purification of *Ec*EngA.

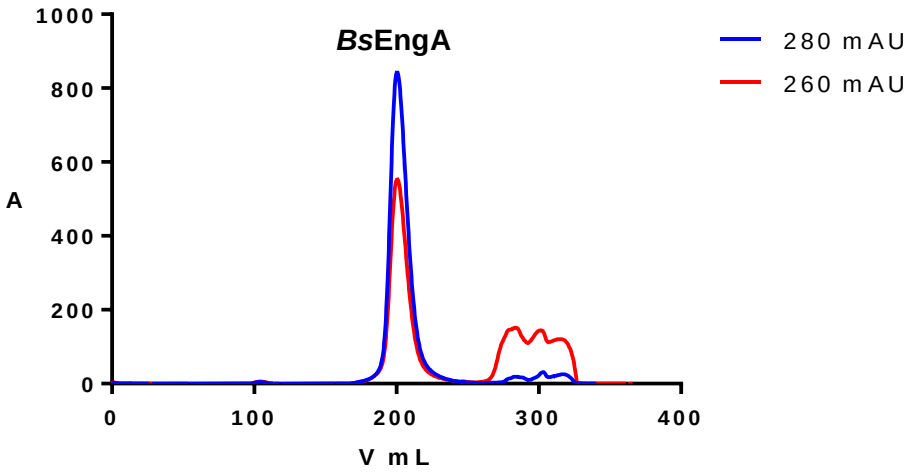

Figure 37. The SEC chromatogram of purification of *Bs*EngA.

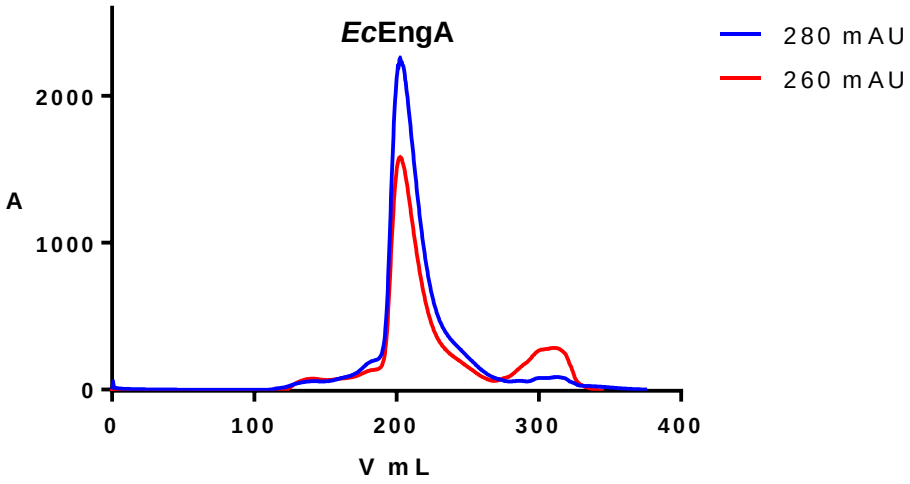

Figure 38. The SEC chromatogram of purification of *Ec*EngA.

3.2.1.2 Binding of GDP and ppGpp to *E. coli* EngA

The interaction of EngA with ppGpp, and as control with GDP, was studied for the homolog from *E. coli* by isothermal titration calorimetry. *Ec*EngA bound both nucleotides with comparable affinities, i.e. K_D values of 3.25 ± 1.39 and 4.54 ± 1.44 µM for GDP and ppGpp, respectively (figure 39). This suggests EngA as a high-affinity target protein for ppGpp.

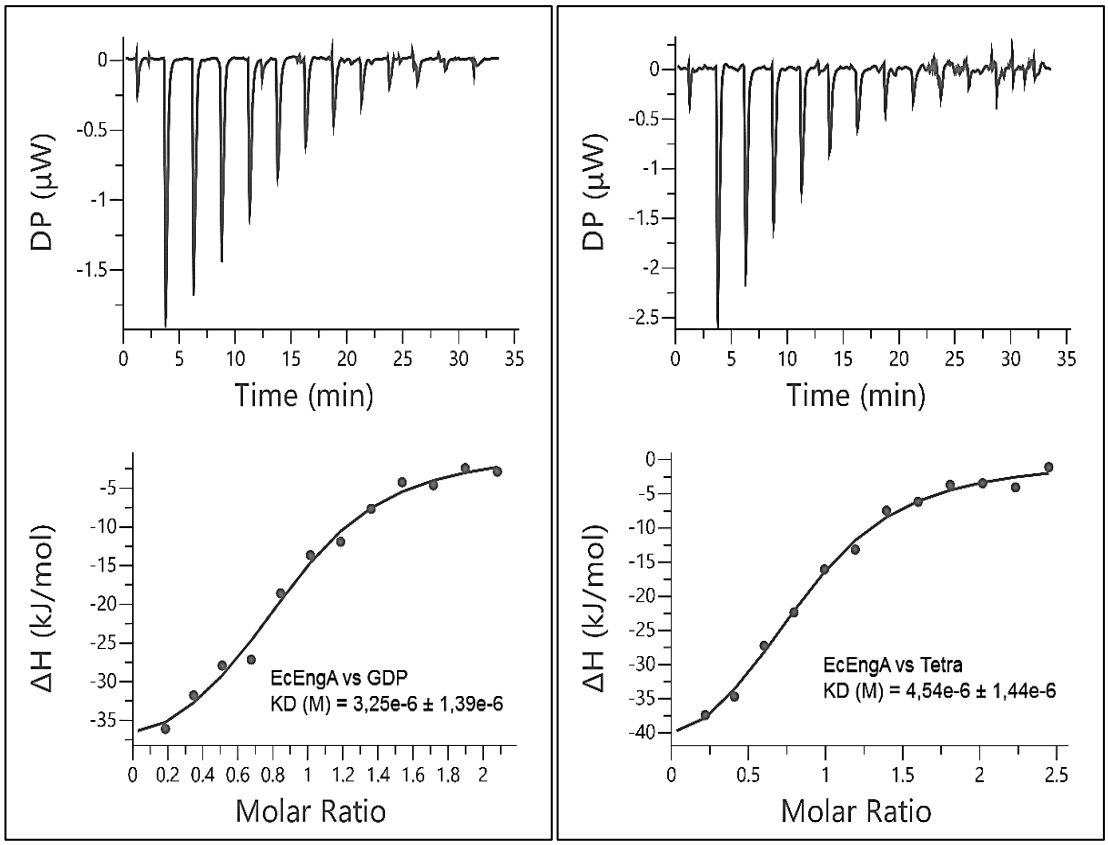

***Ec*EngA vs GDP K_D (M) = $3.25e^{-6} \pm 1.39\ e^{-6}$** **_Ec_EngA vs ppGpp K_D (M) = $4.54e^{-6} \pm 1.44\ e^{-6}$**

Figure 39. The titration curves (upper panels) and binding isotherms (lower panels) of the interaction of *Ec*EngA with GDP (left) or ppGpp (right). The processing of the data was done by Pietro Giammarinaro.

3.2.1.3 Conformational dynamics of EngA

To further investigate the influence of guanosine nucleotide-binding on the conformational dynamics of EngA, hydrogen–deuterium exchange mass spectrometry (HDX-MS) was performed in the presence of GDP, GMPPNP, ppGpp, and pNppGpp. The non-hydrolyzable GTP analog GMPPNP was before used in crystallographic studies [106] and represents a suitable proxy for the natural ligand GTP. For direct comparison, a similarly substituted (i.e. β-/γ- methylene bridged phosphates) analog of pppGpp, i.e. pNppGpp, was employed.

Reduction in deuterium incorporation of EngA was apparent for all investigated nucleotides in representative peptides of the GD1 and GD2 domains (figure 40). Hereby, the diphosphate nucleotides GDP and ppGpp evoked higher protection against HDX than their triphosphate counterparts. This may either suggest different

binding affinities of the diphosphate and triphiosphate compounds or reflect different conformational changes induced by the nucleotides.

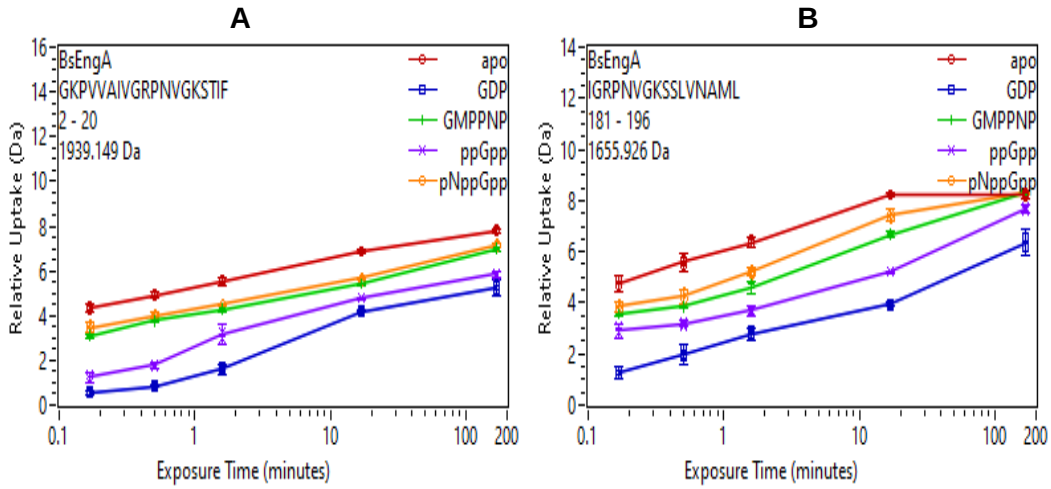

Figure 40 A, B. The time courses of deuterium uptake of representative peptides of the GD1 and GD2 of *Bs*EngA in the apo state and different nucleotide-bound states. The processing of the data was done by Dr. Wieland Steinchen.

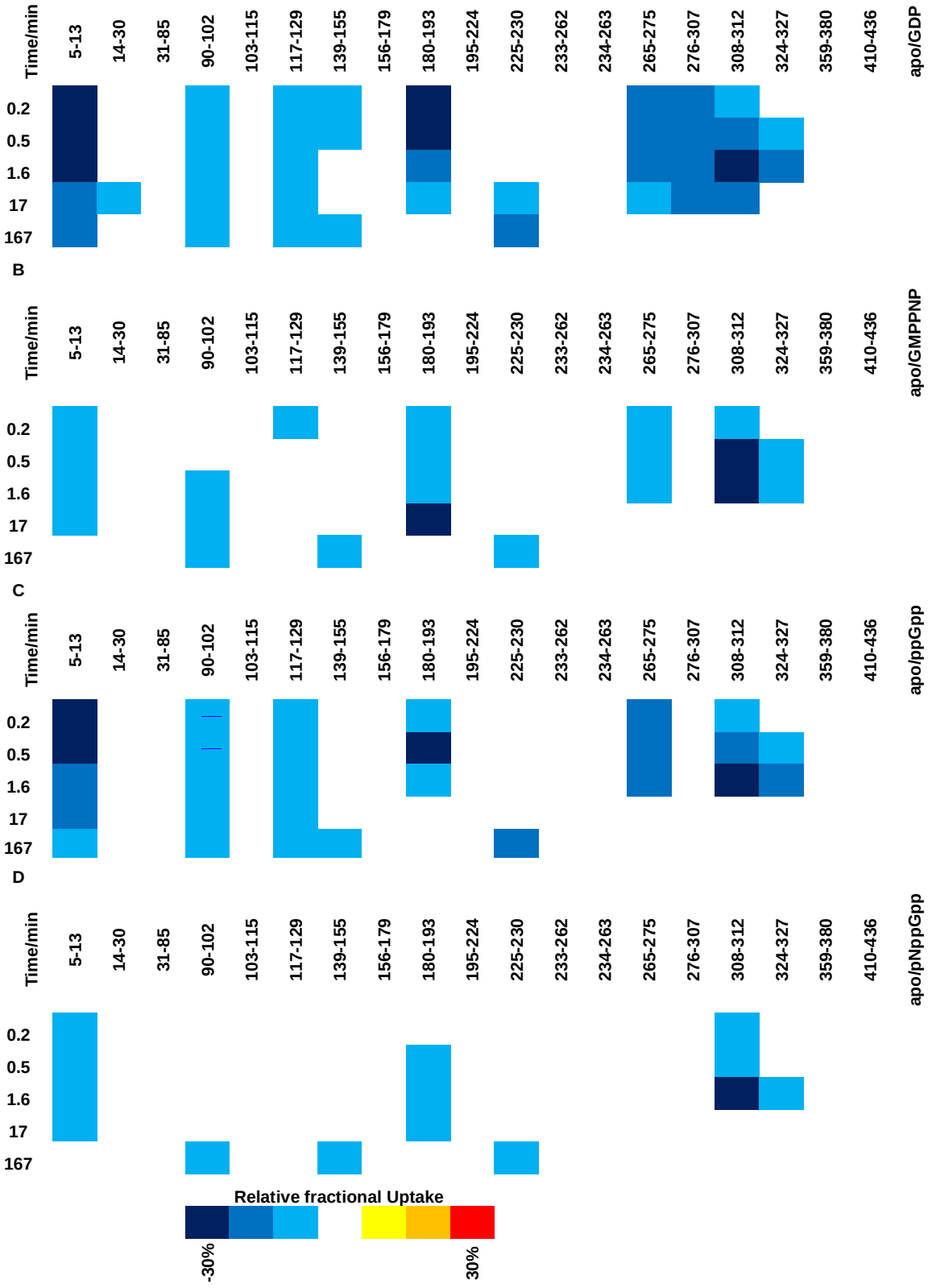

Figure 41. The differences in HDX between the apo state of *Bs*EngA and different ligand-bound states. Blue regions mark lower HDX and red regions mark higher D-incorporation. The processing of data was done by Dr. Wieland Steinchen.

On the whole *Bs*EngA protein, multiple areas with reduced deuterium incorporation in presence of the tested ligands was apparent on amino acid sequence level (figure 41). Projection of these affected areas onto the crystal structure of BsEngA however shows that these differences only occur in the GD1 and GD2 domains (figure 42).

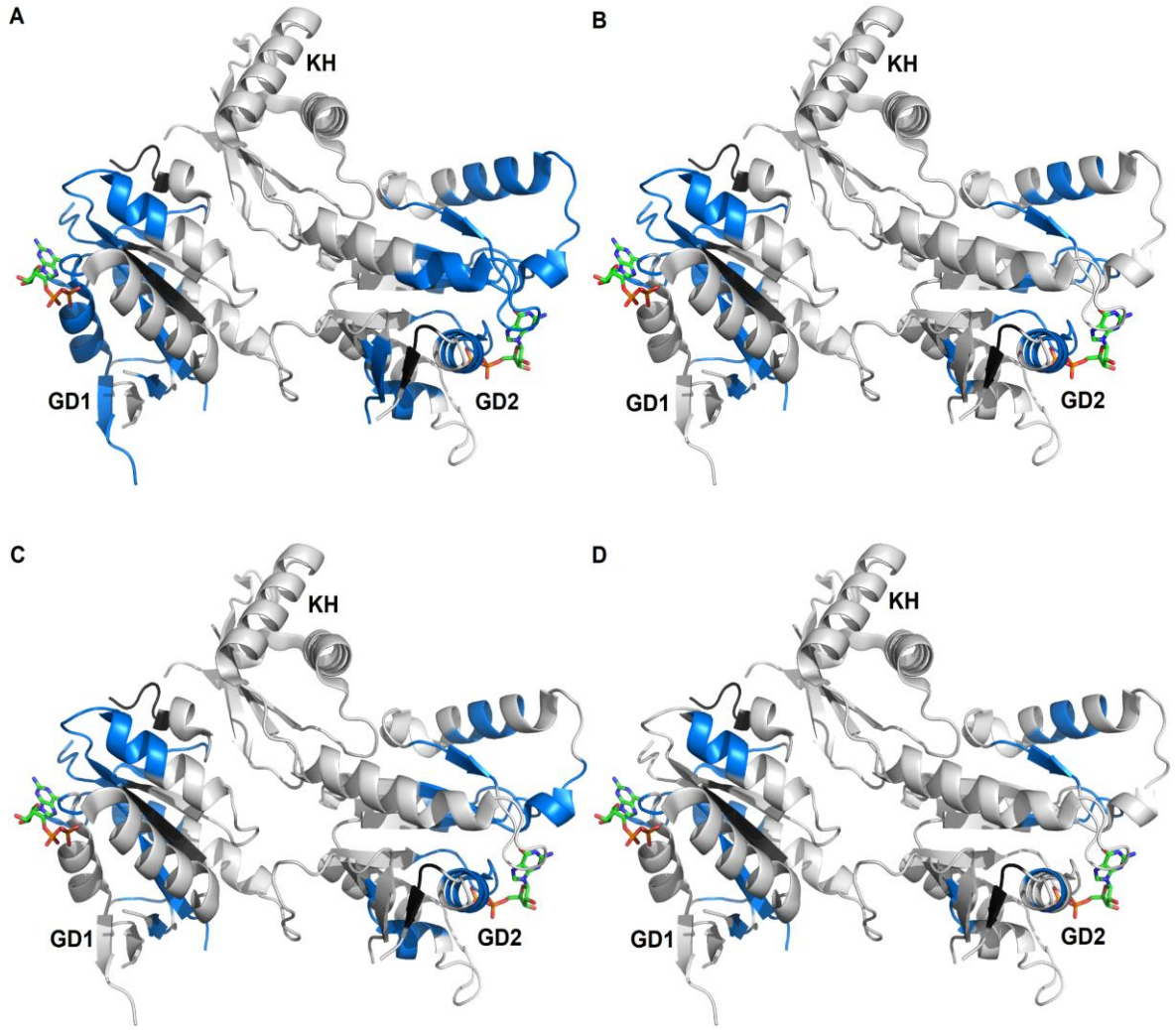

Figure 42 A- D. The differences in HDX on structural model of *Bs*EngA in the presence of GDP, GMPPNP, ppGpp and pNppGpp. The structures were generated by PyMOL.

These results are inconsistent with the reported conformational changes that were thought to accompany GTP binding to EngA, through which the KH domains should undergo a movement relative to the GD1 and GD2 domains, as suggested by Münch and colleagues [105].

3.2.2 GTPase Era

Era is a GTPase implicated to partake in the assembly of the 30S ribosomal subunit [109]. Era is composed of an N-terminal GTPase and a C-terminal RNA-binding domain. Structural and biochemical evidence suggests that Era binds to the 3' end of 16S rRNA and by that serves as an important checkpoint in the assembly of the 30S ribosomal subunit [110][111].

3.2.2.1 Purification of Era

The Era proteins from *E. coli*, *B. subtilis* and *Geobacillus thermodenitrificans* with a C-terminal hexa-histidine tag was overproduced in *E. coli* BL21(DE3). The purification of Era from all three organisms was done by a two-step protocol, employing Ni-NTA affinity chromatography and size-exclusion chromatography (SEC), as explained in materials and methods. In SEC chromatogram, Era was eluted at roughly 235 ml as in figures (44-45-46). The next peak, which was eluted after Era with maximum absorbance 260 nm wavelength, represents the GDP that was set free during the purification of Era proteins by EDTA treatment.

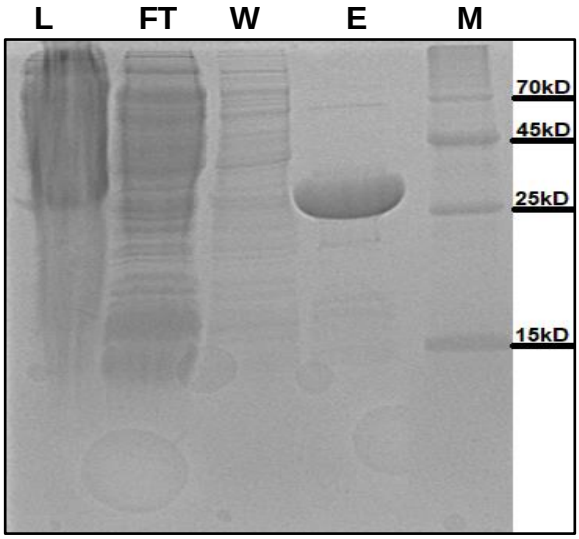

Figure 43. The SDS-PAGE of purification of *Gth*Era after Ni-NTA chromatography. Similar quality and quantity were achieved for the purifications of *Bs*Era and *Ec*Era. Ladder (M), Load (L), flow-through (FT), wash (W), elution (E).

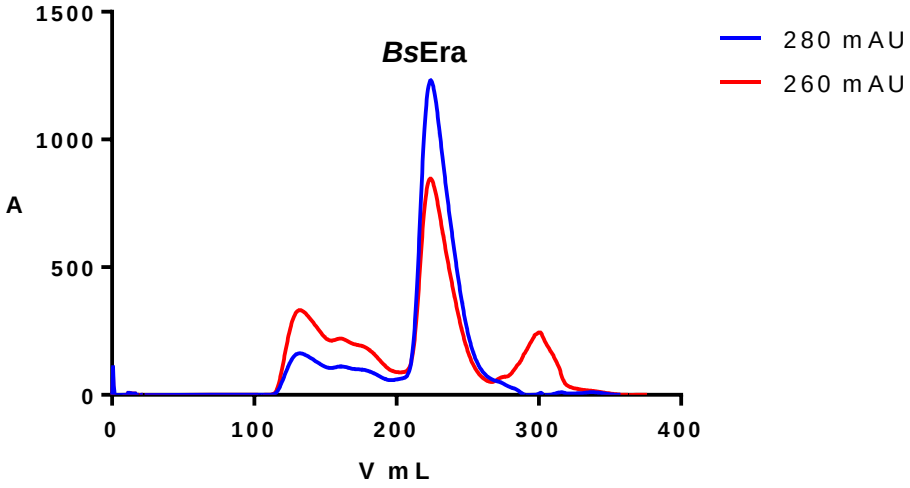

Figure 44. The SEC chromatogram of purification of *Bs*Era.

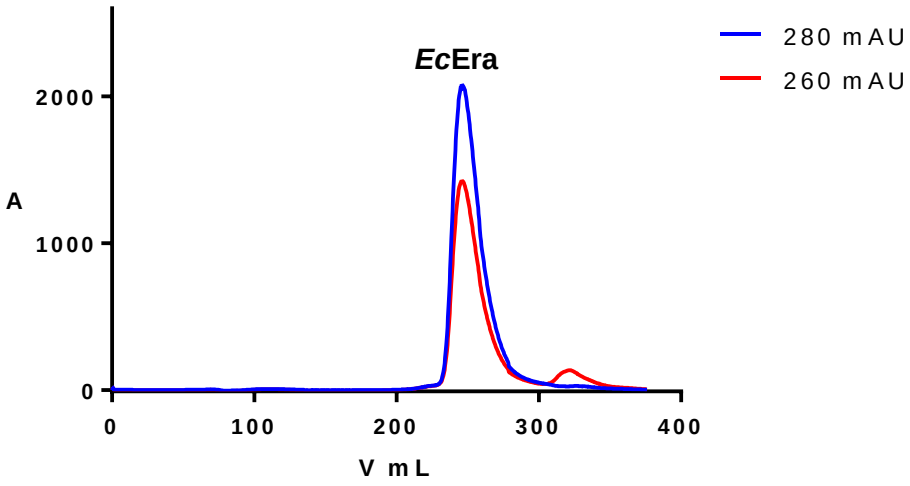

Figure 45. The SEC chromatogram of purification of *Ec*Era.

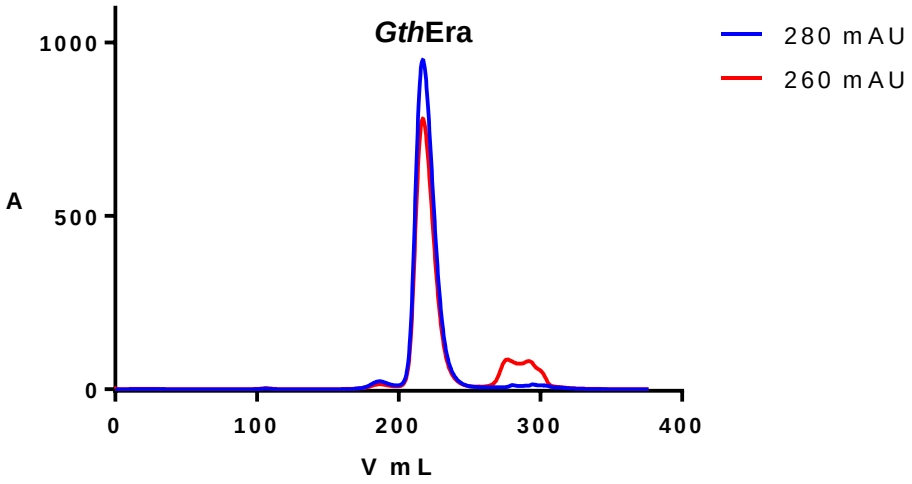

Figure 46. The SEC chromatogram of purification of *Gth*Era.

3.2.2.2 Interaction of *E. coli* Era with GDP and pppGpp

The interaction of *Ec*Era and nucleotides ppGpp and GDP was studied by isothermal titration calorimetry (ITC). *Ec*Era exhibited a very strong and comparable binding of GDP and ppGpp, reflected by K_D values of 341 ± 57.9 and 587 ± 158 nM for GDP and ppGpp, respectively (figure 47).

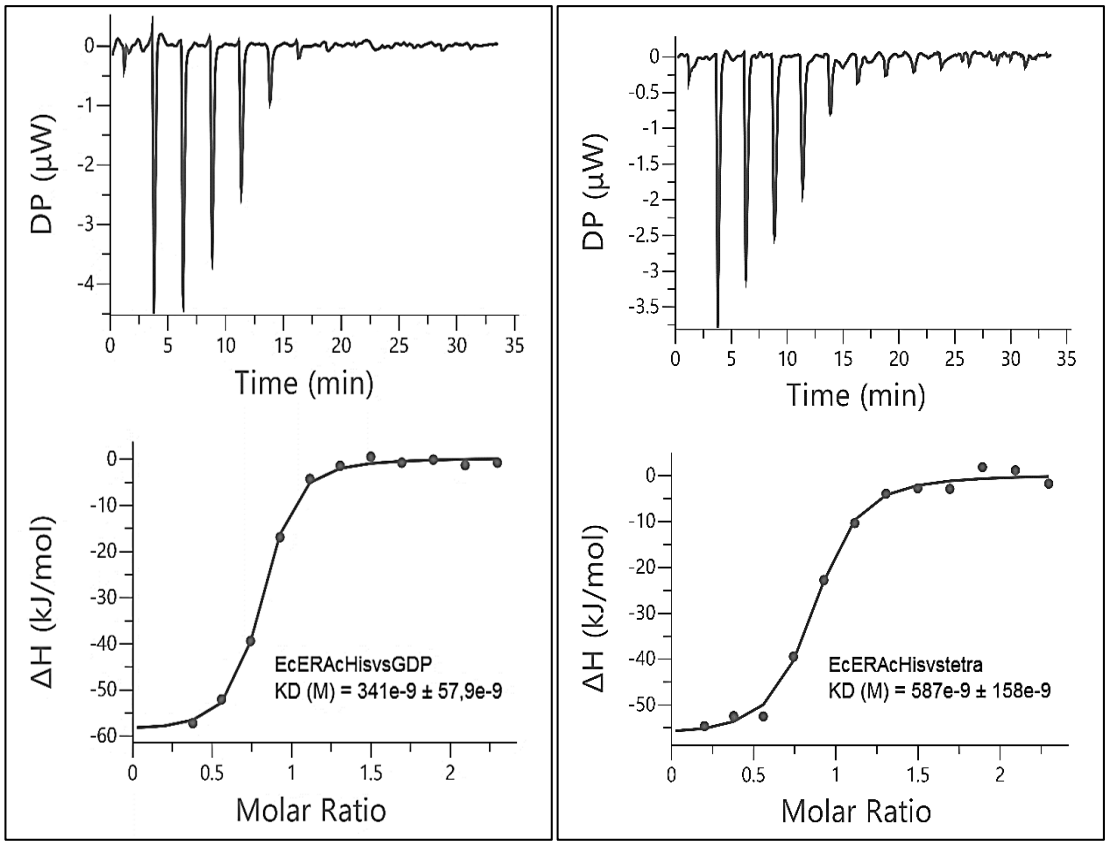

***Ec*Era vs GDP K_D (M) = 341e^{-9}±57.9 e^{-9}** ***Ec*Era vs ppGpp K_D (M) = 587e^{-9}±158 e^{-9}**

Figure 47. The ITC titration curves (upper panels) and binding isotherms (lower panels) of *Ec*Era interaction with GDP (left) or ppGpp (right). The processing of the data was done by Pietro Giammarinaro.

3.2.2.3 Conformational dynamics of Era

To study the role of GDP, GMPPNP, ppGpp, and pNppGpp on the conformational dynamics of Era, hydrogen–deuterium exchange MS (HDX-MS) was performed in the presence of GDP, GMPPNP, ppGpp, and pNppGpp. A representative peptide spanning the G1 element, which is indispensable for nucleotide-binding to GTPases, of Era corroborated binding of the investigated nucleotides to Era (figure 48).

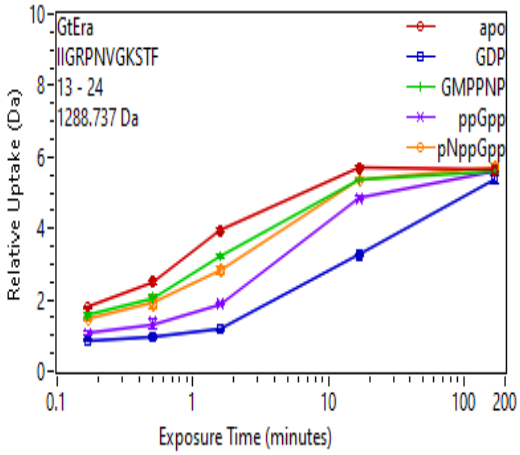

Figure 48. The time courses of deuterium uptake of catalytic peptide of *Gth*Era in the apo- and different nucleotide-bound states. The processing of the data was done by Dr. Wieland Steinchen.

The HDX-MS profiles on the whole amino acid sequence of *Gth*Era reveal differential deuterium incorporation in presence of ligands only for the N-terminal portion of the protein (figure 49). Projecting the ligand-induced HDX protection onto a structural model of *Gth*Era shows that these protected areas line the GTP-binding site within the N-terminal GTPase domain (figure 50).

It may thus be hypothesized that major (p)ppGpp-dependent conformational changes of Era require the presence of the 16S rRNA. Also plausible would be that (p)ppGpp acts on Era solely through steric clashes between the 3' pyrophosphate moiety present in (p)ppGpp, a similar phenomenon as described above for EF-Tu (compare to figures 30 and 31).

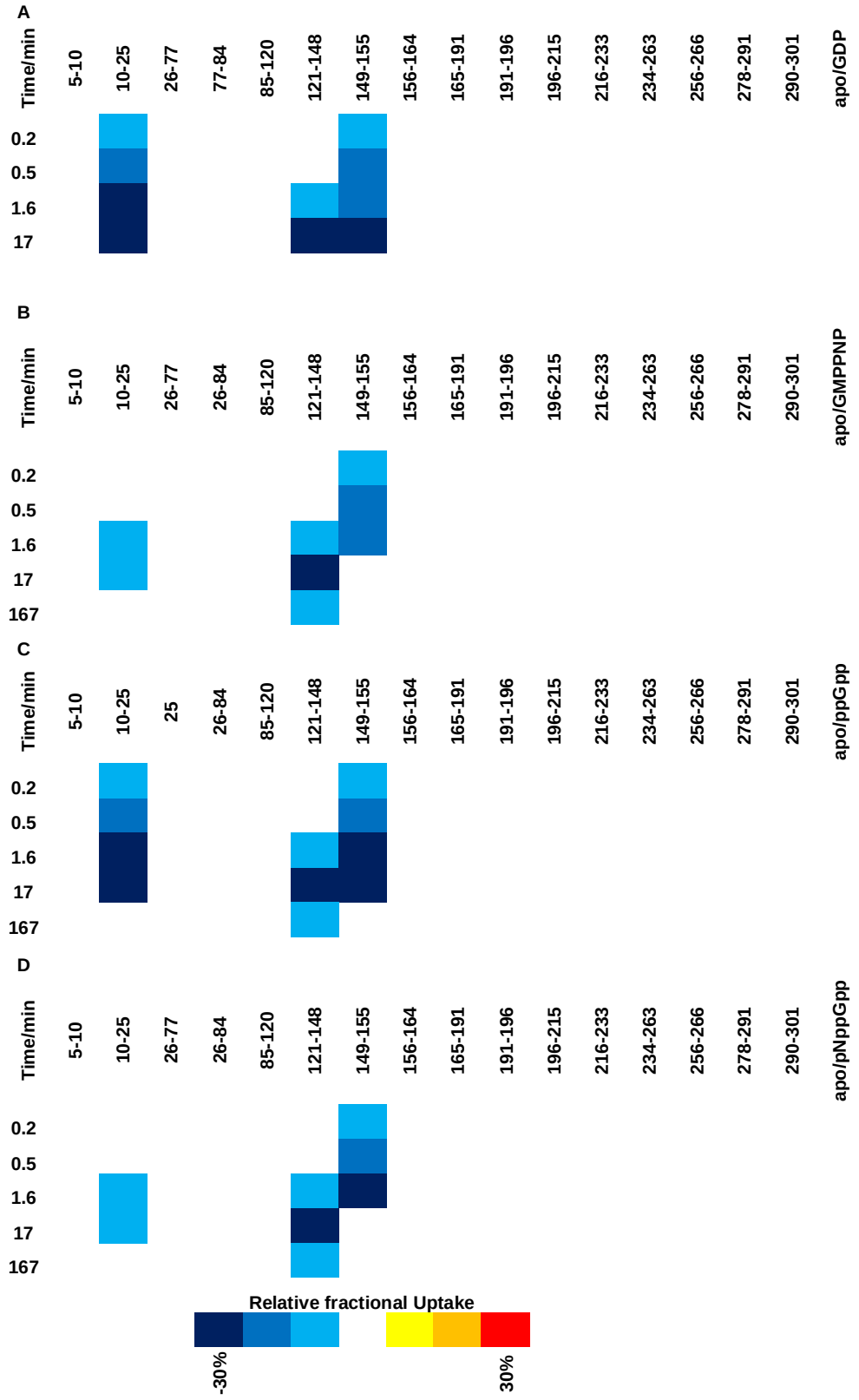

Figure 49. The differences in HDX between GDP, GMPNPP, ppGpp, pNppGpp and apo of *Gth*Era. Blue regions mark lower D-incorporation and red regions mark higher D-incorporation. The processing of the data was done by Dr. Wieland Steinchen.

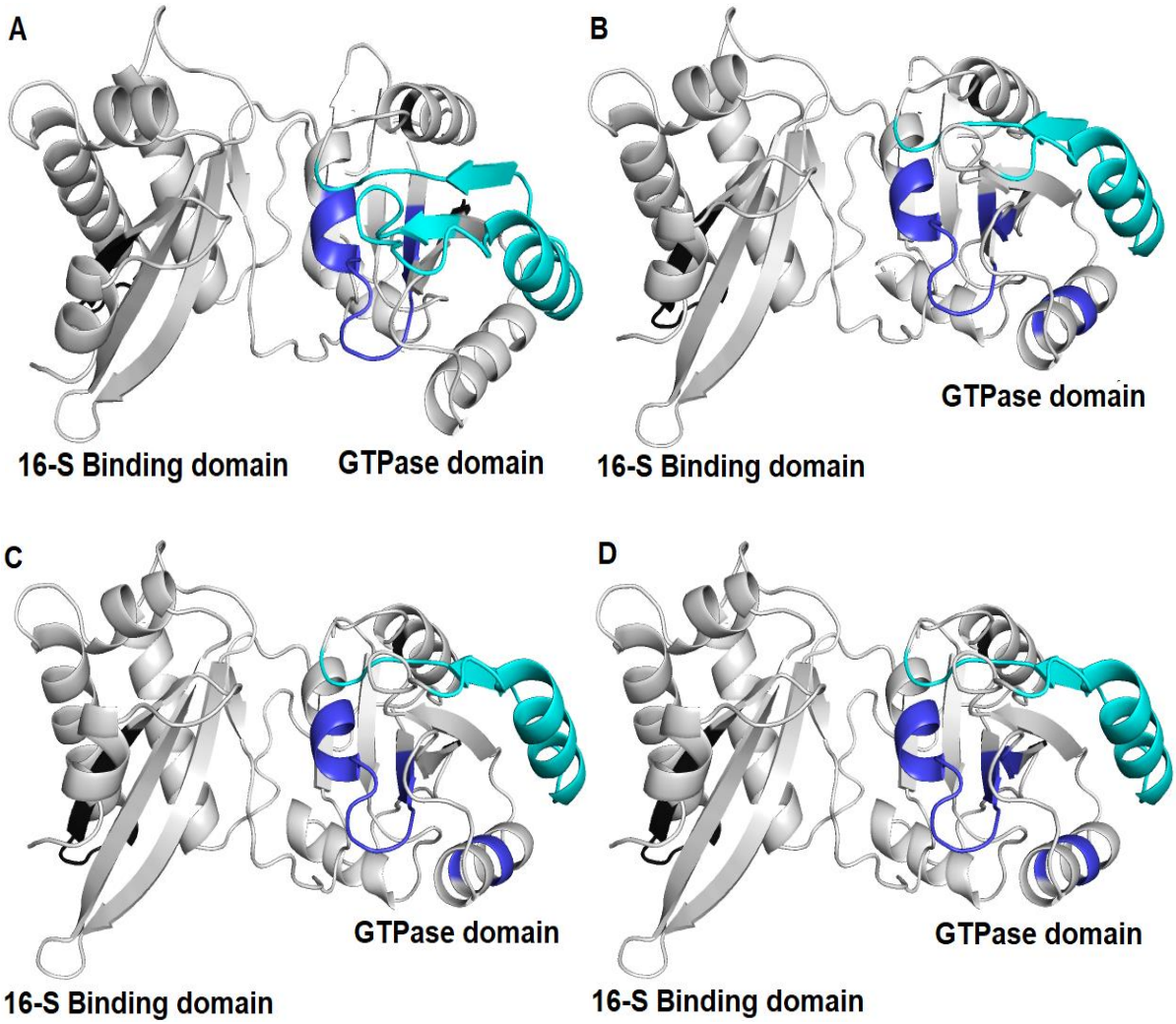

Figure 50 A- D. The differences in HDX in presence of GDP, GMPPNP, ppGpp and pNppGpp plotted on structural model of *Gth*Era. The structures were generated by PyMOL.

3.2.3 Elongation factor G

Elongation factor G (EF-G) is a G-Protein, which bears close similarity in its topology to EF-Tu. Like the latter, it is composed of an N-terminal GTPase domain that is followed by two β-barrel domains. However, and unlike EF-Tu, EF-G harbors two additional C-terminal domains essential for its binding to the ribosome and structurally occupying a similar place at the protein as tRNA at EF-Tu [112]. EF-G and EF-Tu do also occupy similar positions at the ribosome, however, the function of EF-G is to translocate the $tRNA^2$ (A site/P site)-mRNA complex by one codon to free the A site for the next aa-tRNA [113][114]. The translocation motion is accompanied by GTP hydrolysis through EF-G followed by its release from the ribosome [115].

The crystal structures of EF-G from *T. thermophilus* bound to GDP [102] and EF-G from *Thermus thermophilus* with GDPNP [116] illustrate the major conformational differences between the GDP and GTP-bound states of EF-G. It was demonstrated though that there is no major difference between the GTP, GDP and apo structures of EF-G off the ribosome. Instead, the nucleotide-dependent rearrangement in EF-G conformation between active state with GTP and inactive state with GDP comes from its binding onto ribosome [116].

3.2.3.1 Purification of Elongation factor EF-G

Elongation factor G from *E. coli* with a C- or N-terminal hexa-histidine tag was overproduced in *E. coli* BL21(DE3). The purification of EF-G was done by a two-step protocol, employing Ni-NTA affinity chromatography and size-exclusion chromatography (SEC), as explained in materials and methods. In SEC, *Ec*EF-G has been eluted at 200 ml, as seen in figure (52). Moreover, the next peak, which was eluted after EF-G with maximum absorbance 260 nm wavelength, represents the GDP that was set free during the purification of EF-G protein by EDTA treatment.

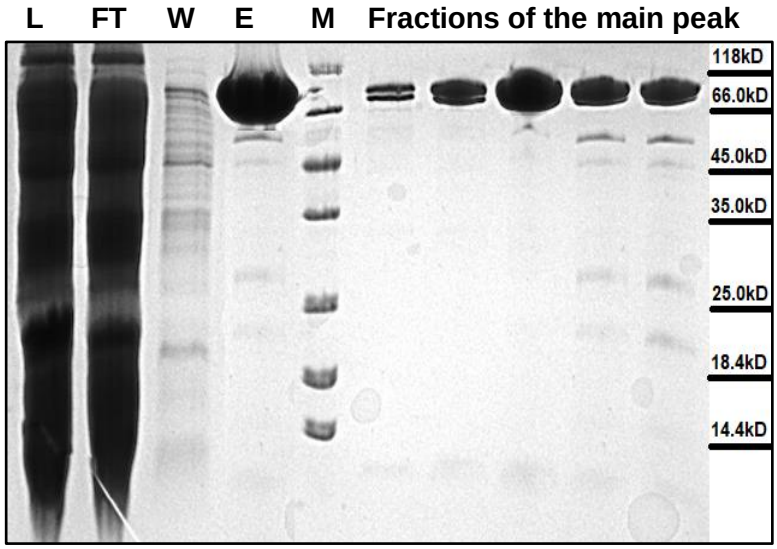

Figure 51. The SDS-PAGE of purification of *Ec*EF-G after Ni-NTA chromatography and the main peak after SEC. Ladder (M), Load (L), flow-through (FT), wash (W), elution (E).

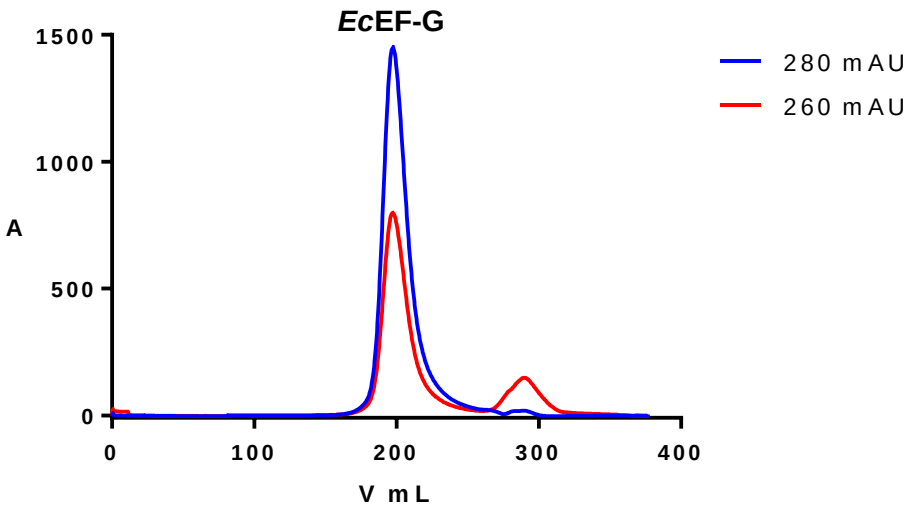

Figure 52. The SEC chromatogram of purification of *Ec*EF-G**.**

3.2.3.2 The interaction of EF-G with ppGpp and GDP

The interaction of EF-G from *E. coli* with GDP and ppGpp was probed by isothermal titration calorimetry. Both nucleotides exhibited comparable binding characteristics reflected by K_D values of 54.1 ± 7.2 and 66.8 ± 8.0 µM for GDP and ppGpp, respectively (figure 53).

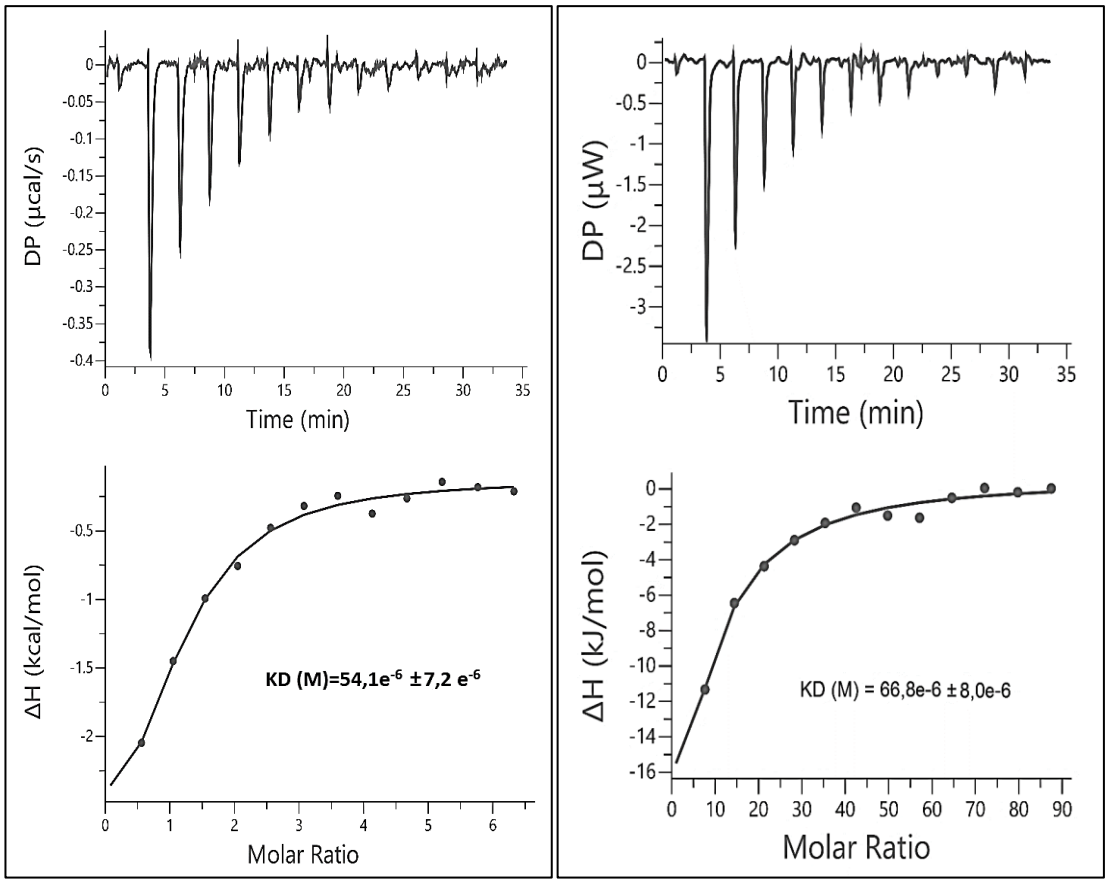

***Ec*EF-G vs GDP K_D (M) = 54.1e^{-6} ± 7.2 e^{-6}** **_Ec_EF-G vs ppGpp K_D (M) = 66.8e^{-6} ± 8.0 e^{-6}**

Figure 53. The ITC titration curves (upper panels) and binding isotherms (lower panels) of *Ec*EF-G interaction with GDP (left), ppGpp (right). The processing of the data was done by Pietro Giammarinaro.

4 Discussion

4.1 Efficient and rapid technique for purifying EF-Tu and G-proteins

The conclusive study of nucleotide-binding properties of GTPases necessitates that the proteins in question are available in their nucleotide-free forms. However, owing to their high affinity for GDP also evidenced in the ITC experiments presented here, the GTPases typically retain their GDP during protein purification under standard conditions.

To circumvent this issue, a protocol was conceived for the purification of EF-Tu from *E. coli*. The protein was initially purified by two steps, i.e., Ni-NTA and size-exclusion chromatography (SEC), in the absence of magnesium ions. However, only the inclusion of an additional EDTA treatment in between Ni-NTA and SEC, which was conducted to strip-off residual Mg^{2+} and by that the bound nucleotide, afforded purification of GDP-free EF-Tu. Similar protocols were applied to the purification of the ribosomal maturation GTPases EngA and Era, and the translational GTPase EF-G. ITC, MST, and HDX-MS studies revealed good binding properties of all tested nucleotides demonstrating the feasibility of the method.

4.2 New conformation of EF-Tu induced by ppGpp

Due to the similarity in the structure between pppGpp, ppGpp, GTP, GDP, it was suggested that (p)ppGpp may interact with proteins that are involved in protein biosynthesis such IF2, EF-Tu, EF-G, Era and EngA [81][11][96].

In 1972, it was demonstrated by Miller *et al.* through functional assays that ppGpp binds EF-Tu 50 time tighter than GTP with a K_D of 8 nM and that ppGpp interacts competitively towards GDP and GTP [117].

Similar results were found for EF-Tu interacting with ppGpp proceeding with an inhibitory constant (K_i) of 70 nM when ppGpp is in two-fold excess over GTP in the absence of EF-Ts, however, in the presence of EF-Ts, the interaction between EF-Tu and ppGpp became weaker. It was thus suggested that ppGpp may be capable of inhibiting the cycle of elongation factor EF-Tu in an indirect manner through depleting free EF-Ts by formation of a EF-Tu/ppGpp/EF-Ts complex [37]. In Both hypotheses,

the mechanism of the interaction of ppGpp with EF-Tu still elusive. As no ternary complex between EF-Tu/(p)ppGpp/EF-Ts could be substantiated in this work, a direct mode of action of (p)ppGpp on EF-Tu functionality appears more plausible currently.

As we know, the stringent response is a mechanism, in which microorganisms can response to the amino acids starvation by producing the unusual nucleotides (p)ppGpp. When less aminoacylated tRNAs are available for translation [118][119], the synthesis of (p)ppGpp is triggered by the binding of complex stringent factor RelA and uncharged tRNAs loading into the A-site of ribosome to produce (p)ppGpp [69][120]. This mechanism leads to the increase in the concentration of (p)ppGpp up to 1 mM, which leads to a rapid shut down of the cell to a persistent state and encouraging drug tolerance [121][73].

The binding of ppGpp and pppGpp for EF-Tu determined in this work suggest similar affinities for (p)ppGpp and the natural GTP and GDP nucleotides. Hence, both ppGpp and pppGpp act on EF-Tu as competitive inhibitors. As intracellular GTP levels decline with the raise in (p)ppGpp [122], this competitive mode of inhibition already impedes EF-Tu function. Nevertheless, it was also demonstrated that ppGpp binding to EF-Tu leads to a previously unknown conformation that is remiscent to EF-Tu bound to GDP but not identical. Mainly, probably due to electrostatic clashing between 3’-phosphate of ppGpp with residues of the switch I region of EF-Tu, this switch I became disordered and thus untraceable in our crystal structure. Consequently, this ppGpp-bound EF-Tu should be unable to coordinate aa-tRNA, for which a structural rearrangement of the switch I region is essential (figure 54).

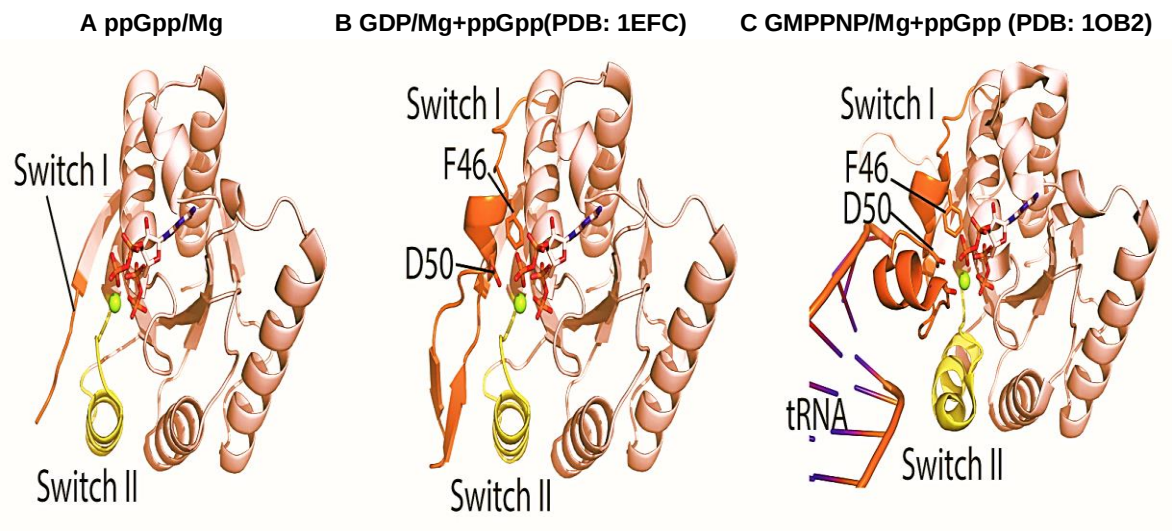

Figure 54 A-C. Comparison of the *Ec*EF-Tu catalytic domains in the different bound states.

4.3 Contribution between stringent response and phosphorylation to inhibit protein biosynthesis

The pronounced disordering of the switch I region of EF-Tu upon binding of ppGpp raises the question whether this only impedes aa-tRNA coordination or if other properties of EF-Tu may be affected. EF-Tu is well known to be subject to posttranslational modification by phosphorylation. It was demonstrated that the phosphorylation of EF-Tu protein on serine, threonine, and tyrosine (Ser/Thr/Tyr) residues control EF-Tu protein activity in prokaryotic cells [123][124]. For instance, upon exposure of *B. subtilis* to nutrient limiting conditions that trigger its sporulation, EF-Tu is phosphorylated at Thr63 and Thr385 residues through the phosphotransferase YabT [125]. Phosphorylation of the switch I-contained threonine was evidenced for *E. coli* (Thr61), *B. subtilis* (Thr63, see above) and *M. tuberculosis* (Thr64) [126]. It was also for *E. coli* shown by Talavera *et al*. that phosphorylation occurs at Thr382 (corresponding to Thr385 in *B. subtilis* EF-Tu) through the enzyme Doc, which leads to an entrapment of the topology of this phosphorylated EF-Tu in an open inactive conformation state, making it unable to interact with aa-tRNA [126].

Inspection of the accessibility of Thr61 of *E. coli* EF-Tu in dependence of the bound nucleotide shows that it is surface-exposed in presence of ppGpp, but partially covered by the ordered switch I region in presence of GDP (figure 55). In EF-Tu/GMPPNP/tRNA, Thr61 is entirely buried and should not be subject to phosphorylation. This collectively suggests that ppGpp-binding to EF-Tu may promote

Thr61 phosphorylation, which may interfere with EF-Tu function beyond the presence of ppGpp even after overcoming of a cellular stress condition. This model is in particular tempting for the entrance of some microbial species like *B. subtilis* during entry in dormant state, e.g. sporulation [125][127].

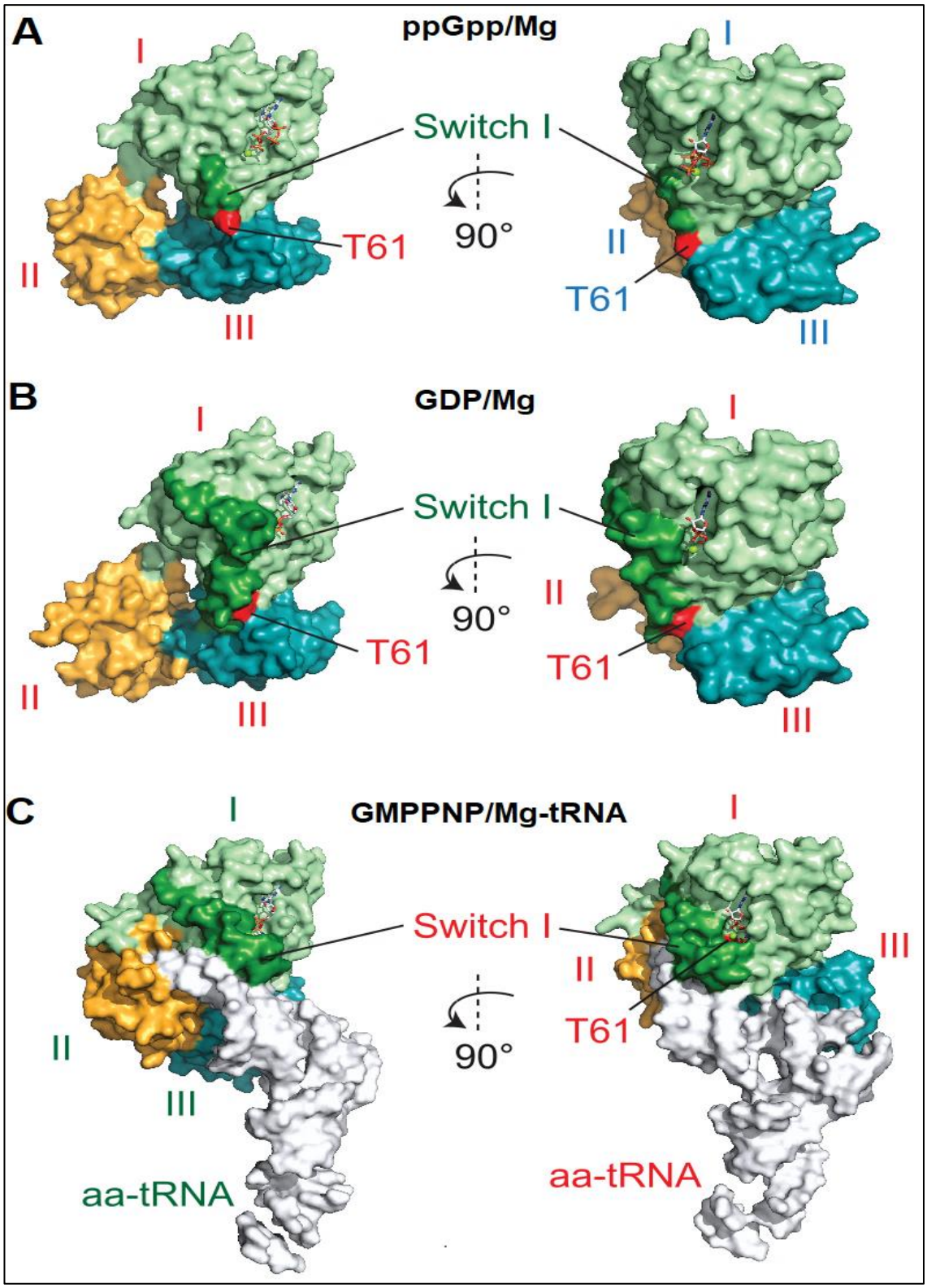

Figure 55. A-C. The crystal structure of *Ec*EF-Tu in presence of ppGpp (A), GDP (B, PDB: 1EFC [34] (Song, Parson. et at. 1999) GMPPNP/Mg/Phe-tRNA^{Phe} (C, PDB: 1OB2) is shown on surface representation with the EF-Tu domains colored in pale green (DI), orange (DII), teal (DIII) and the tRNA in white. The threonine T61 and the SI region are colored in red and forest, respectively.

4.4 Role of EF-Ts for (p)ppGpp recycling

During conventional translation elongation, recycling of the EF-Tu/GDP complex is achieved by the action of the guanosine nucleotide exchange factor EF-Ts. EF-Ts binds to EF-Tu/GDP and enforces the release of the nucleotide allowing for faster rebinding of GTP. Our pull-down and analytical SEC experiments suggested that EF-Ts has the ability to remove all nucleotides that bind onto EF-Tu, even ppGpp and pppGpp. This ability of removing ppGpp and pppGpp could be essential to control the activity of elongation factor EF-Tu during a (p)ppGpp-mediated stress scenario or during resuscitation from this stress. Interestingly, Benjamin and his colleagues found evidence for the presence of a quaternary complex of EF-Tu/GTP/tRNA/EF-Ts, which may expand the possibilities of EF-Ts action beyond its role as a dedicated guanosine exchange factor for EF-Tu [128]. The implications of EF-Ts-mediated nucleotide removal from individual EF-Tu as exemplified in the assays of this work are still beyond comprehension.

4.5 Dual role of EF-Tu as GTPase and pppGpp hydrolase

It was known that the GppA protein from *E. coli* is able to convert pppGpp to ppGpp, the latter of which is the primary alarmone interacting with RNAP in *E. coli* [66]. It was discovered by surprise that elongation factor EF-Tu may also degrade pppGpp to ppGpp by removing the γ-phosphate moiety from pppGpp, as seen in figure (56).

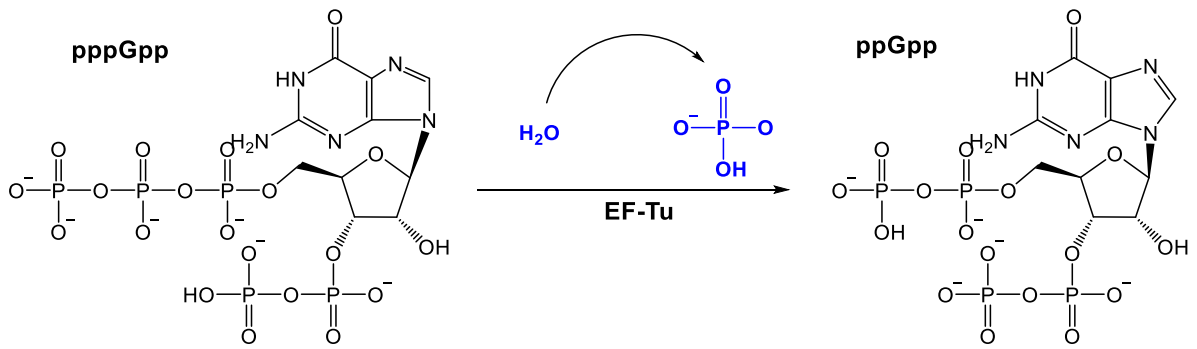

Figure 56. The reaction of converting pppGpp to ppGpp by EF-Tu and GppA.

The ability of EF-Tu to degrade pppGpp might suggest that other GTPases such EF-G, Era or EngA might also have the capacity to contribute in degradation of pppGpp to ppGpp. Hereby, further enzymes besides GppA could be involved in the homeostasis of ppGpp and pppGpp in the cell. Divergent functions and potencies between both alarmones are just starting to be addressed, on the one hand, as shown by Yang J and his colleagues who identified NahA, which can degrade (p)ppGpp to pGpp. He could prove that pGpp in not able to bind onto GTPase, however, it regulates the biosynthesis of purine [129]. On the other hand, Pausch and colleagues showed that RbgA from *B. subtilis* is not able to convert pppGpp to ppGpp [130].

4.6 Competitive inhibition of translational GTPases by (p)ppGpp

In this work, it was attempted to study the interaction between Era, EngA and the nucleotides GDP, GMPPNP, ppGpp and pNppGpp by HDX to observe the effect of nucleotides on the conformation of those ribosomal proteins.

From HDX and ITC data, it was demonstrated that ppGpp and pppGpp has the ability to interact with Era and EngA with almost the same binding strength of GDP, thus, alarmones inhibit GTPases competitively by competing with the GTP/GDP for the binding site. According to HDX data, however, no clear difference in the overall conformation could be seen, thus, it was suggested that the rearrangement of the Era conformation and EngA between the on state with GTP and the off state with GDP may rely on the presence of ribosome or rRNA. This conclusion is in contrast with Münch *et al*. [105] who suggested that the binding of GTP on the first catalytic domain of *Bs*EngA could induce a shift in its switch II region, and by thus promotes exposure of the RNA-binding surface of the KH domain that would otherwise be buried in between the GD1 and GD2 domains, which had stipulated the belief that this rearrangement of conformation aided the recognition between EngA and ribosome, and that is crucial for the function of this family of enzymes [105].

4.7 Role of (p)ppGpp for persister cell formation

Due to the far-reaching adaptational program initiated by (p)ppGpp, an implication of the alarmones in the resistance of bacteria to antibiotic treatment is not only

conceivable but documented in some studies. For example, in one case study, an infant leukemia patient developed a vancomyin-resistant *Enterococcus faecium* (VRE) bacteremia that persisted treatment with appropriate antibiotics [131]. Sequencing of multiple of these VRE isolates consistently carried a mutation in the *relA* gene that resulted in elevated (p)ppGpp synthetase activity of the protein, and hence increased cellular alarmone levels in the VRE. In this regard, the resistance of the VRE was presumably conferred by enhanced biofilm formation of the organism due to (p)ppGpp, instead of (p)ppGpp promoting a selective resistance against the antibiotics linezolid and daptomycine employed for treatment, for both of which no geneticically encoded resistance mechanisms are known so far [131]. Similar observations were made for infections with *S. aureus* [132] and *P. aeruginosa* [133]. The major problem in such cases is that, after treatment of bacterial infections with antibiotics, some bacteria remain alive. When the effect of the antibiotic is over, these bacteria will grow again, leading to an entire bacterial population of persisters [134].

Besides these general actions of (p)ppGpp, they may also interference with antiobiotic treatment due to functional overlap of targets. Alarmones are known to affect a plethora of cellular processes [63], and for example, also partake in regulation of cell wall remodeling for which reason they may interfere with the action of cell wall-targeting antiobiotics [135]. Another example is microcin J25, a 21 amino acid-containing peptide that binds to RNAP and prevents the access of NTP substrates to the enzyme [136]. The binding site of (p)ppGpp at RNAP is in proximity of the microcin J25 binding site, therefore (p)ppGpp, together with the RNAP accessory protein DksA, are able to nullify the effect of microcin J25 on RNAP activity [137]. Furthermore, in *M. tuberculosis* cells during carbon starvation, the Rel protein appeared to be essential for the development of chronic persistence [138][139][140].

These complications gave rise to the idea of interfering with (p)ppGpp metabolism as a potential therapeutic strategy for future antibiotics [56][141]. In this regard, Wexselblatt *et al.* synthesized a chemical compound named Relacin inspired by the structure of (p)ppGpp. In Relacin, the 3’ and 5’ phosphate moieties of (p)ppGpp are replaced by glycyl-glycine dipeptides, and additionally functionalized at the guanine base (figure 57). Albeit exhibiting some inhibitory activity on *E. coli* RelA *in vitro*, the required doses to fully inhibit the enzyme render an *in vivo* application questionable [142][143]. This weakness of Relacin may in parts be evoked by its substitutions,

mainly the replacement of the phosphate moieties, that due to their conformational flexibility and ability to engage in salt bridging interactions or coordinate with metal ions, should be critical to (p)ppGpp's magic. Certainly, more efforts need to be made in order to establish the bacterial stringent response system as a druggable therapeutic target process in bacteria.

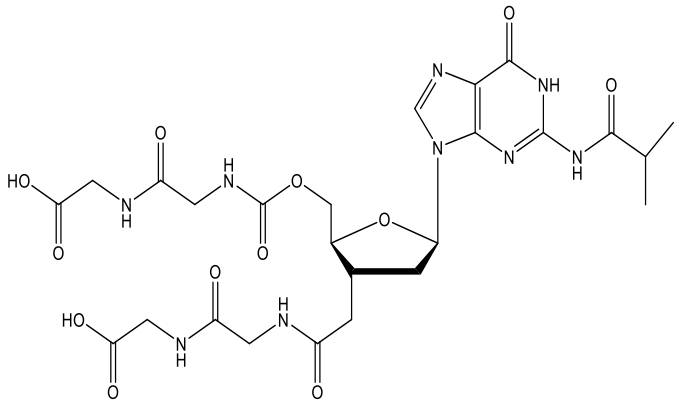

Figure 57. The chemical structure of Relacin.

5 Materials and Methods

5.1 Materials

5.1.1 Chemicals and consumables

Martials	Supplier
Acrylamide/Bisacrylamide (37.5:1)	Roth
Acetonitrile	Roth
Acetic acid	VWR
Agar-Agar	Roth
Agarose	Roth
Ammonium persulfate	Merck
Coomassie Brilliant Blue R 250	Roth
K_2HPO_4	Merck
Dithiothreitol	Roth
Desoxynucleoside triphosphates	Thermo Fisher
EDTA	Panreac
Ethanol 96%	Merck
Imidazole	Roth
Isopropanol	Merck
HEPES	Roth
JCSG Core Suite I-IV	Qiagen
Tris	Roth
Kanamycin sulfate	Roth
Ampicillin	Roth
NaCl	Thermo Fisher
$MgCl_2$	Roth
Na_2HPO_4	Merck
KCl	Merck
NaH_2PO_4	Merck
NaOH	Grüssing
KOH	Chemsolute
Sodium dodecyl sulfate	Roth
β-Mercaptoethanol	Roth
TEMED	Roth
PEG400	Merck
PEG600	Merck
PEG1000	Merck
PEG3350	Merck
PEG4000	Merck
PEG6000	Merck
PEG8000	Merck
Lactose	Roth

LB medium	Roth
Boric acid	Roth
Glycine	Roth
Hydrochloric acid	VWR
1 kb DNA Ladder	NEB
10X CutSmart® Buffer	NEB

5.1.2 Enzymes and cloning equipment

Restriction enzymes, Q5 High-Fidelity DNA polymerase, T4 DNA Ligase and their respective reaction buffers were purchased from New England Biolabs (NEB). DNA ladder 1kb was used as standard for agarose gel electrophoresis.

5.1.3 Bacterial strains and plasmids

5.1.3.1 Oligonucleotides

For amplification of genes, DNA oligonucleotides were purchased from Sigma Aldrich in the purity ‘salt free’. Oligonucleotides used in this study are listed in **Table S1**.

5.1.3.2 Vectors

For overproduction of target proteins in *E. coli* BL21(DE3), the vectors pET24d(+), pET16b, pET28a(+) (all Novagen) or pGAT2 (EMBL Heidelberg) were employed.

Table 5-1. All used vectors

Plasmid	Remark	Origin
pET24d	lacZ, kanmaycin-resistant	Novagen
pET16b	lacZ, ampicillin-resistant	Novagen
pGAT2	lacZ, ampicillin-resistant	(EMBL Heidelberg)
pET28a	lacZ, kanamycin-resistant	Novagen

All plasmids were used in this study are listed in **Table S2**. Plasmids were obtained using standard cloning techniques described in chapter **5.2**.

5.1.3.3 Bacterial strains

Chemical competent *E. coli* DH5α cells (Thermo Fisher) were used for plasmid amplification. Chemical competent *E. coli* BL21(DE3) (Thermo Fisher) cells were used for protein production.

5.1.4 Growth media and buffers

5.1.4.1 Growth media

Lysogeny broth (LB) medium (composition stated in **table 5-3**) was purchased as a premixed powder and, after dissolving in deionized waters, sterilized (121°C, 20 min) before use. SOC medium has the following component as in the **table 5-2**.

Table 5-2. Components of SOC medium

Components	Final concentration mM
Tryptone	2% (w/v)
Yeast extract	0.5% (w/v)
NaCl	10
KCl	2.5
$MgCl_2$	10
Glucose monohydrate	20

Components were dissolved in desalted water and the pH of the solution adjusted to 7.0 with NaOH.

Table 5-3. Components of LB medium

Components	Final concentration g/l
Tryptone	10
Yeast extract	5
NaCl	10

5.1.4.2 Antibiotics

Ampicillin and kanamycin were purchased from Roth. The stock solutions of antibiotics were prepared by dissolving the antibiotic in double-distilled water and filtrated through

a 0.2 µM filter under sterile conditions. Antibiotic stock solutions were kept at -20°C until use. Final concentrations of antibiotics are given in **table 5-4**.

Table 5-4. Concentrations of antibiotics

Antibiotics	Stock concentration mg/ml	Working concentration µg/ml
Ampicillin	100	100
Kanamycin	50	50

5.1.4.3 Buffers for preparing chemical competent *E. coli* cells

Table 5-5. Components of CC Buffer

Components of CC buffer	Final concentration mM
HEPES	10 mM
$CaCl_2$	15 mM
KCl	250 mM
$MnCl_2$	55 mM

Components were dissolved in double-distilled water and the pH of the solution was adjusted to 6.7 with KOH. After filtration through a 0.2 µM filter under sterile conditions, the buffer was kept at 4°C until usage.

5.1.4.4 Buffers for protein purification

Proteins were purified by a two-step protocol employing Ni-NTA affinity or GST affinity purification followed by size-exclusion chromatography (SEC). The buffers used were of the following composition:

Table 5-6. Components of lysis and washing buffer for all proteins

Ni-NTA-lysis and washing buffer	Final concentration mM
HEPES	20
NaCl	250
KCl	20
Imidazole	40

Adjustment of pH to 8.0 with NaOH.

Table 5-7. Components of lysis and washing buffer for EngA

Ni-NTA-lysis and washing buffer	Final concentration mM
HEPES	20
NaCl	250
KCl	20
Imidazole	5

Adjustment of pH to 8.0 with NaOH.

Table 5-8. Components of elution buffer

Ni-NTA-elution buffer	Final concentration mM
HEPES	20
NaCl	250
KCl	20
Imidazole	500

Adjustment of pH to 8.0 with NaOH.

Table 5-9. Components GST elution buffer

GST-elution buffer	Final concentration mM
HEPES	20
NaCl	250
KCl	20
Glutathione	20

Adjustment of pH to 7.5 with NaOH.

Table 5-10. Components of SEC buffer

SEC-buffer	Final concentration mM
HEPES	20
NaCl	250
KCl	20

Adjustment of pH to 7.5 with NaOH followed by filtration through a 0.2 µM filter.

5.1.4.5 Buffers for HDX

D_2O-containing SEC buffers for deuteration during HDX experiments were prepared by dissolving the solid components in deuterium oxide 99.9% (Sigma Aldrich). The pD value of the solution was adjusted to 7.5 using 10 M NaOD (obtained by dissolving NaOH pellets in deuterium oxide 99.9%). During the establishment of the pD value of deuterated SEC buffer with a pH electrode calibrated for H_2O, the differing dissociation constants of H_2O and D_2O were taken into account [144]. Peptides were separated during HDX employing HDX buffer A and B. The quench buffer for stopping the HDX reaction and the wash solution for cleaning the columns used in the HDX setup had the following composition:

HDX quench buffer		**HDX column wash solution**	
KH_2PO_4/H_3PO_4	400 mM	Guanidine-HCl	500 mM
		Acetonitrile	4% (v/v)
pH 2.2 with H_3PO_4		pH 2.2 with H_3PO_4	

HDX buffer A		**HDX buffer B**	
Double-distilled water		Acetonitrile	
Formic acid	0.1% (v/v)	Formic acid	0.1% (v/v)

5.1.4.6 Buffers for agarose gel electrophoresis

Agarose gels were prepared by dissolving agarose in TBE buffer. For visualization of nucleic acids, one drop of Midori Green Direct (Nippon Genetics) solution was added directly to the molten agarose resulting in a final concentration of approximately 0.00005% (w/v). The following buffers were used for agarose gel electrophoresis:

Table 5-11. Components of TBE buffer

TBE buffer components	Final concentration
Tris	90 mM
Boric acid	90 mM
EDTA	2 mM

Table 5-12. Components of 6x DNA loading dye

6x DNA loading dye components	Final concentration
TBE buffer	1x concentrated
Glycerol	20% (v/v)
Bromophenol blue	0.25% (w/v)

The pH was adjusted to 8.3 with NaOH.

5.1.4.7 Buffers for SDS-PAGE

For separating and visualizing proteins, sodium dodecyl sulfate polyacrylamide gel electrophoresis (SDS-PAGE) was used. Gels for SDS-PAGE were prepared by using a Mini-PROTEAN 3 Multi-Casting Chamber (Biorad) and had the composition detailed in **table 5-13**. Gels were stored at 4 °C until usage.

Table 5-13. Components of combination and separation gel

Material	Stacking gel	Separation gel
Acrylamide	4.5% (v/v)	15% (v/v)
Tris	125 mM	375 mM
SDS	0.1% (w/v)	0.1% (w/v)
APS	0.1% (w/v)	0.1% (w/v)
TEMED	0.1% (v/v)	0.1% (v/v)
pH adjusted with HCl	6.8	8.8

In order to use SDS-PAGE and visualize the proteins on gel, the following buffers must be prepared and used.

Table 5-14. Components of SDS running buffer

SDS running buffer components	Final concentration
Tris	25 mM
Glycine	192 mM
SDS	0.1% (w/v)

Table 5-15. Components 5x SDS loading dye

5x SDS loading dye components	Final concentration
Tris-HCl pH 6.8	300 mM
SDS	10% (w/v)
β –mercaptoethanol	25% (v/v)
Glycerin	25% (v/v)
Bromophenol blue	0.05% (w/v)

Table 5-16. Components of SDS staining solution

SDS staining solution components	Final concentration
Comassie blue R250	0.36% (w/v)
Ethanol 99%	45.5% (v/v)
Acetic acid 99%	9% (v/v)

Table 5-17. Components of SDS destaining solution

SDS destaining solution components	Final concentration
Ethanol 99%	30% (v/v)
Acetic acid 99%	10% (v/v)
ddH_2O	40%(v/v)

5.1.4.8 Nucleotides

In order to calculate the concentrations of guanosine nucleotides, the absorbance of an approximately 1 mM concentrated dilution was determined at 260 nm wavelength and its concentration was determined by using an extinction coefficients of ε = 13,700 $M^{-1} * cm^{-1}$ and guanosine nucleoside (GDP, GTP, ppGpp and pppGpp) [145].

5.1.5 Protein biochemistry

Prepacked columns (HisTrap FF, 1 ml or 5 ml bed volume) for purification of hexa-histidine tagged proteins were purchased from GE Healthcare. Purified proteins were concentrated using Amicon Ultra-15 centrifugal filter units (Merck) with molecular weight cut-offs of 10 kDa. PageRuler unstained protein ladder (Thermo Fisher) and Pierce unstained protein MW marker (Thermo Fisher) served as standards for molecular weight estimation on SDS-PAGE gels.

5.1.6 Crystallization and data collection

Crystallization screens were carried out by the sitting-drop method in SWISSCI MRC 2-well or SWISSCI MRC 3-well plates (Jena Bioscience) using the JCSG Core Suites (Qiagen) with 96 conditions on each plate. Data sets at the Europe Synchrotron Radiation Facility (ESRF, Grenoble) were collected. The crystal-containing loop is automatically installed onto the goniometer in a 100 K, and cooled by nitrogen gas flow. The data was collected with a DECTRIS PILATUS 6M detector at the ID29 beamline.

5.1.7 Laboratory equipment

Name of equipment	Supplier
Agarose gel equipment (casting stand and combs)	Cleaver Scientific
Autoclave	Ibs Tecnomara
Centrifuge 5418 R	Eppendorf
Centrifugation cup (1,000 ml)	Thermo
Centrifugation tube (50 ml)	Eppendorf
Cryo loops	Hampton Research
Columns (HisTrap FF, 1 ml or 5 ml) for purification of hexa-histidine tagged proteins	GE Healthcare
Columns (HisTrap FF, 5 ml) for purification of GST-tagged proteins	GE Healthcare
Dewar div	Isotherm KGW
Dialysis-membrane MWCO 3500	Spectrum labs
Electrophoresis chamber	neoLab
Erlenmeyer flasks (50-2000 ml)	Schott
Examination gloves LATEX	VWR
Falcon (15 ml, 50 ml)	Sarstedt
Freezer -80 °C	divers manufacturer
Frenchpress	SLM AMINCO
Incubator Incuce II	MMM Group
Measuring cylinders (10-50 -1000-2000 ml)	VWR
Microwave D450W Inverter	Panasonic
Mixer (D-6010)	neoLab
M-110L Microfluidizer	Microfluidics
Microscope	Olympus
Nanodrop Lite (Spectrophotometer Peqlab)	Thermo Scientifc
NeoBlock1 (2-2503)	neoLab
NeoBlock HeizerDuo (2-2504)	neoLab
Pipettes (10 µl, 20 µl, 200 µl, 1000 µl)	neoLab

Parafilm (4 ln x 250ft)	Parafilm
Peristaltic pump	Gilson
PCR cycler 5332	Eppendorf
pH-meter	Mettler Toledo
Petri dish (92x16 mm) with cams	Sarstedt
Pipette Tip (10 µl, 200 µl, 1000 µl)	Sarstedt
Crystallization robot	ArtRobbins
Shaker Dos-10L	neoLab
Sealing foil for crystallization trays	Duck Tape
SWISSCI MRC 2-well/3-well crystallization plates	SWISSCI
SDS-PAGE equipment	Biorad
Sterile syringe filter, 0.2 µm/0.45 µm	VWR International
Thermo mixer	eppendorf
Vortexer (D-6012)	neoLab
Vortex	IKA England Ltd.
Weight S-203, d = 0.001 g	Denver Instrument
Weight SI-203, d = 0.1 mg	Denver Instrument
Protein purification accessories	
Äkta purifier	GE Healthcare
Äkta prime	GE Healthcare
His-Trap FF 1-5ml	GE Healthcare
Hi Load 10/300 Superdex S200 pg	GE Healthcare
Hi Load 16/600 Superdex S200 pg	GE Healthcare
Hi Load 26/600 Superdex S200 pg	GE Healthcare
HPLC Equipment	
Agilent 1100 Series	Agilent Technologies
G1311A Quaternary Pump	Agilent Technologies
G1313A Autosampler	Agilent Technologies
G1314A Variable wavelength detector (VWD)	Agilent Technologies
G1316A Column Compartment	Agilent Technologies
G1379A Degasser	Agilent Technologies
EC 250/4.6 NUCLEODUR C18 HTec, 3 µm	Macherey-Nagel
Agilent ChemStation B.04.03	Agilent Technologies
HDX Equipment	
ACQUITY UPLC M-class system	Waters
Two-arm robotic autosampler	LEAP Technologies
Enzymate BEH Pepsin column 2.1 x 30 mm	Waters
ACQUITY UPLC BEH C18 1.7 µm 1.0 x 100 mm column	Waters
AQUITY UPLC BEH C18 1.7 µm 2.1 x 5 mm VanGuard	Waters
SYNAPT G2-Si HDMS mass spectrometer ESI	Waters

5.2 Methods

5.2.1 Molecular cloning

5.2.1.1 DNA amplification by PCR (polymerase chain reaction)

Purified vector DNA or chromosomal DNA of the respective genes of interest or microbial organism were used as a template to amplify the DNA. PCR reactions were carried out according to the instructions of NEB and continued primers in concentration of 50 pM and 50 U/ml Phusion DNA polymerase (NEB). PCR conditions were typically performed as described as in **table 5-18** for 30 amplification cycles (steps 2-4) [146].

Table 5-18. Thermo cycler-program for the colony PCR

Stepps	Colony PCR
Initial denaturation	95 °C, 360 s
Denaturation	95 °C, 45 s
Annealing	55 °C, 45 s
Elongation	72 °C, 250 s
Final Elongation	72 °C, 480 s

5.2.1.2 Separation of DNA by agarose gel electrophoresis

The separation of DNA molecules was carried out by agarose gel electrophoresis. Agarose gels were typically prepared at 1-1.5% (w/v) depending on the amplified gene of interest by dissolving the appropriate amount of agarose in TBE buffer, aided by heating in a microwave for approximately 5 minutes. DNA fragments were separated for roughly 20-40 min at 130 V. DNA and RNA bands were visualized under UV light at 300 nm.

5.2.1.3 Purification of DNA fragments

DNA was purified from agarose gels with the GeneJET Gel Extraction Kit (Thermo Fisher) according to the manufacturer's instructions. Plasmid DNA was purified with the GeneJET Plasmid Miniprep Kit (Thermo Fisher) according to the manufacturer's instructions.

5.2.1.4 Preparation of chemical competent *E. coli*

Chemical competent *E. coli* BL21(DE3) and DH5α cells were prepared by inoculating the *E. coli* strain in 5 ml of LB medium without antibiotic at 37 °C at 200 rpm overnight. The overnight culture was used to inoculate 500 ml of LB medium without antibiotic and incubated at 30 °C and 200 rpm until the optical density at 600 nm wavelength reached approximately 0.5. Subsequently, the cultures were chilled on ice for 15 minutes before the harvest of the cells through centrifugation at 4 °C and 4,000 x g. The supernatant was discarded, the cells were resuspended in 100 ml of CC buffer and again chilled on ice for 15 minutes followed by centrifugation at 4 °C and 4,000 x g for 10 min. Again, the supernatant was discarded, cells were resuspended in 18.6 ml CC-Buffer and 1.4 ml DMSO and chilled in ice for 15 minutes. afterwards, the cell suspension was aliquoted (150 µl), flash-frozen in liquid nitrogen and stored at -80 °C.

5.2.1.5 Transformation of chemical competent *E. coli*

Transformation of *E. coli* BL21(DE3) and DH5α was performed by incubating one aliquot of chemical-competent cells with 1 µl of plasmid solution (typically 50-100 ng/µl) for 5 min on ice. Subsequently, the cells were heat-shocked at 42 °C for 60 s and kept on ice for 2 min before the addition of 300 µl SOC medium. Cells were regenerated for 60 min at 37 °C and 200 rpm and plated on agar containing the antibiotic at 37 °C overnight.

5.2.2 Purification of overproduced proteins

5.2.2.1 Overproduction of proteins

The proteins were expressed as follows: Sterilized LB medium was supplemented with 12.5 g D-Lactose monohydrate per litre and the respective antibiotic and inoculated with *E. coli* BL21(DE3) transformed with the respective plasmids. Cultures were incubated at 30°C for approximately 16 h.

5.2.2.2 Protein purification

The bacteria that contained the overexpressed protein were harvested by centrifugation at 4 °C and 4,000 x g for 20 min. The cell pellet was resuspended in 30 ml of resuspension buffer per liter of bacterial culture and cells lysed by a Microuidizer or French press. The lysate was centrifuged (47,000 x g, 4 °C, 30 min) and the clear supernatant loaded onto a HisTrap FF-column or GST column equilibrated with 10 CV (column volume) binding buffer. After washing with 20 CV of binding buffer, the target protein was eluted by using 20 ml of elution buffer which contained 500 mM imidazole for His-tag and 20 mM glutathione for GST-tagged target proteins. The elution was concentrated with an Amicon Ultra-15 Centrifugal Filter Unit at 4,000 x g and 4 °C until a final volume of 500 to 1,000 µl. The concentrated protein was then loaded onto a Superdex 26/60 S200 column equilibrated with SEC buffer and eluted at 2.5 ml/min flow rate of SEC buffer. Protein-containing fractions, as judged from the absorbance readings at 280 and 260 nm were collected and concentrated with Amicon Ultra-15 Centrifugal Filter Unit at 4,000 x g and 4 °C according to the experimental requirements. In the case of crystallization, the protein was used immediately. For biochemical studies, the protein was flash-frozen in liquid nitrogen and stored at -80 °C until use.

5.2.2.3 Determination of protein concentration

The concentration of the purified protein was determined with a NanoDrop Lite Spectrophotometer by measuring the absorbance of the protein solution at a wavelength of 280 nm. To calculate the protein concentration, the law of Lambert-Beer was used [147].

5.2.2.4 Release of GDP from G-protein

To trigger the release of GDP from proteins, the eluate of the Ni-NTA affinity purification was treated with 50 mM of EDTA (pH 8.0, dissolved in double-distilled water) for 30 min, followed by concentration and injection onto SEC. The ratio of the absorbance at 280 and 260 nm was employed as a measure for the GDP content of the protein and validated by analytical HPLC.

5.2.2.5 SDS-PAGE

According to their molecular weight, the separation of proteins was carried out by SDS-PAGE (Sodium dodecyl sulfate polyacrylamide gel electrophoresis) for 40 mins at 270 V. By default, 12.5% (v/v) gels were used. For size determination, Broad Range Protein Marker (New England Biolabs, P7702S) was used. Proteins were stained with Coomassie Brilliant Blue R250.

5.2.3 Interaction of GTPases with nucleotides

5.2.3.1 Isothermal titration calorimetry (ITC)

ITC experiments were performed in SEC buffer containing 20 mM HEPES-Na, pH 7.5, 20 mM $MgCl_2$, 20 mM KCl and 200 mM NaCl at 25 °C with a MicroCal PEAQ-ITC instrument (Malvern Panalytical). For ITC experiments on the EF-Tu, EF-G, Era and EngA, 25 µM of each protein was utilized. The concentration of nucleotides was 250 µM. In all measurements, a first injection of 0.4 µl of nucleotide solution was followed by 12 injections at 3 µl each. I performed the experiments under supervision of Pietro Giammarinaro. Data processing was done by Pietro Giammarinaro with the MicroCal PEAQ-ITC Analysis software (Malvern Panalytical).

5.2.3.2 Microscale thermophoresis (MST)

In order to determine the binding affinity of EF-Tu with nucleotides (GDP, GTP, GMPPNP, pppGpp, ppGpp and pNppGpp), a MicroScale Thermophoresis was carried out in cooperation with Dr. Sven-Andreas Freibert (AG Lill, University of Marburg, Department of Medicine). MST was carried out on a Monolith NT.115 (NanoTemper Technologies GmbH, Munich, Germany) at room temperature. A protein stock solution (concentration of 800 µM) was labeled with the dye NT 647 according to the supplier's protocol (NanoTemper Technologies). For MST measurements, 400 nM of labeled protein were mixed with different concentrations of nucleotides ranging from 0.6 nM to 20 µM final concentration of nucleotide interaction partners. MST experiments were conducted in a buffer containing 20 mM HEPES-Na, pH 7.5, 20 mM KCl, 200 mM NaCl and 20mM $MgCl_2$). Tween20 (Sigma) was present at a final concentration of 0.05 mM.

When an infrared laser is switched on, the protein moves in a directed manner. Thus, a decrease in fluorescence. By increasing the concentration of nucleotides lead to a change in the movement in the event of binding. These changes as a function of the nucleotide's concentration ultimately lead to a sigmoidal curve from the turning point of which the dissociation constant K_D or affinity of the protein to nucleotides can be determined. The analysis of the data and evaluation was performed by Dr. Sven-Andreas Freibert (University of Marburg).

5.2.4 Interaction of EF-Tu and EF-Ts

5.2.4.1 Pull-down assays

100 µM EF-Tu was incubated in SEC buffer with 1 mM $MgCl_2$ and 1 mM of nucleotides in absence or presence of EF-Ts (100 µM) for 5 min at room temperature. Afterwards, 100 µl of Ni-NTA beads were added, transferred into spin columns and washed five times with 500 µl SEC buffer containing 40 mM imidazole. The protein was eluted by SEC buffer containing 500 mM imidazole. The absorbance of protein at 280 and 260 nm was measured spectrophotometrically in the absence and presence of Ts. The nucleotide content of EF-Tu was determined by analytical HPLC after denaturation of the protein by chloroform and heat treatment as described in the assay for the analysis of EF-Tu's nucleotide content.

5.2.4.2 Analytical size-exclusion chromatography (SEC)

100 µM EF-Tu was incubated with 1 mM $MgCl_2$ and nucleotides (200 µM) in absence or presence of EF-Ts in SEC buffer for 5 min at room temperature. 1 ml of this mixture was injected into SEC on a HiLoad 26/600 Superdex 200 pg column (GE Healthcare), which already equilibrated with SEC buffer. The absorbance of protein was calculated directly from SEC and nano drops in the absence or presence of Ts.

5.2.5 In vitro translation assays

The production of green fluorescent protein (GFP) was examined by using a coupled transcription/translation system (RTS 100 E. coli HY Kit, Biotechrabbit). Reactions

were performed in 50 µl, contained 12 µl *E. coli* lysate, 10 µl reaction mix, 12 µl amino acid solution, 1 µl of methionine, 5 µl reconstitution buffer and 1 µg of the control vector GFP. The Addition of ppGpp or pppGpp were at final concentrations of 10, 100 or 1,000 µM. The reaction time was 240 minutes at 30 °C. For maturation of GFP, the mixture of reaction was incubated at 4 °C for 24. The production of GFP was assayed by fluorescence measurement (Excitation/Emission = 395/509 nm) with a spectramax M4 multi-mode microplate reader (Molecular Devices). The experiment was performed by Anita Dornes.

5.2.6 Enzymatic activity of EF-Tu

5.2.6.1 Determination of EF-Tu nucleotide content

5.2.6.1.1 Assay of EF-Tu nucleotide content and activity.

By using high-performance liquid chromatography (HPLC), the amount of the nucleotide of EF-Tu was assayed. By adding two volume parts chloroform followed by 15 s of vigorous mixing, 15 s heat treatment at 95 °C and flash-freezing in liquid nitrogen, denaturation of 200 µM of EF-Tu was performed. After thawing, this mixture was centrifuged (17,300 x g, 30 min, 4 °C) and the aqueous phase was removed. The sample was diluted 1:5 with double-distilled water and analyzed for its nucleotide contents by HPLC. Separation of the nucleotide analytes was conducted with a Metrosep A Supp 5-150/4.0 (Methrom) column at 0.7 ml/min flow rate of 100 mM $(NH_4)_2CO_3$ pH 9.25 and detected at a wavelength of 260 nm.

5.2.6.2 Hydrolytic activity of EF-Tu towards pppGpp

In order to test the activity of *E. coli* EF-Tu towards pppGpp, 1/2.5/5/10/25 µM EF-Tu *E. coli* was incubated with 1 mM pppGpp for 1/6/30/90/150 min at 37 °C in SEC buffer supplemented with 20 mM $MgCl_2$. Reactions were stopped and analyzed as described above (Assay of EF-Tu nucleotide content and activity).

5.2.7 Hydrogen-deuterium exchange mass spectrometry (HDX-MS).

HDX-MS experiments with *B. subtilis* EngA and *G. thermodenitrificans* Era were conducted essentially as described previously [130]. Samples for HDX-MS contained 50 µM of purified *B. subtilis* EngA or *G. thermodenitrificans* Era mixed without nucleotide or with 500 µM GDP, GMPPNP, ppGpp or pNppGpp in SEC buffer (20 mM HEPES-Na pH 7.5, 20 mM KCl, 20 mM $MgCl_2$, 250 mM NaCl). The preparation of HDX reactions was aided by a two-arm robotic autosampler (LEAP technologies). 7.5 µl of protein sample were mixed with 67.5 µl of D_2O-containing SEC buffer to start the exchange reaction and were further incubated at 25 °C for 10, 30, 95, 1,000 or 10,000 seconds , after which 55 µl of the reaction were withdrawn and mixed with an equal volume of quench buffer (400 mM KH_2PO_4/H_3PO_4, 2 M guanidine-HCl, pH 2.2) kept at 1 °C. 95 µl of the resulting quenched reaction were injected into an ACQUITY UPLC M-Class System with HDX Technology (Waters) [148]. Undeuterated HDX samples were prepared similarly by 10-fold dilution with H_2O-containing SEC buffer. The sample was flushed out of the loop (50 µl) with H_2O + 0.1% (v/v) formic acid (100 µl/min) and delivered to a column (2 mm x 2 cm) filled with immobilized porcine pepsin kept at 12 °C. The resulting peptic peptides were collected on a trap column (2 mm x 2 cm) filled with POROS 20 R2 material (Thermo Scientific) kept at 0.5 °C. After 3 min of protein digestion and peptide trapping, the trap column was placed in line with an ACQUITY UPLC BEH C18 1.7 µm 1.0 x 100 mm column (Waters), and the peptides eluted at 0.5 °C using a gradient of H_2O + 0.1% (v/v) formic acid (A) and acetonitrile + 0.1% (v/v) formic acid (B) at a flow rate of 30 µl/min as follows: 0-7 min/95-65% A, 7-8 min/65-15% A, 8-10 min/15% A, 10-11 min/5% A, 11-16 min/95% A. The eluting peptides were guided to a G2-Si HDMS mass spectrometer with ion mobility separation (Waters), ionized with an electrospray ionization source (25°C capillary temperature, spray voltage 3.0 kV) and mass spectra acquired in positive ion mode over a range of 50 to 2,000 m/z in $HDMS^E$ or HDMS mode for undeuterated and deuterated samples, respectively [149][150]. [Glu1]-Fibrinopeptide B standard (Waters) was employed for lock-mass correction. During separation of the peptide mixtures on the C18 column, the pepsin and trap columns were washed three times with 80 µl of 4% (v/v) acetonitrile and 0.5 M guanidine hydrochloride each. Furthermore, blank injections were performed between each sample to reduce peptide carry-over. All measurements were carried out in triplicate. Peptide identification and analysis of deuterium incorporation were carried out with ProteinLynx Global SERVER (PLGS, Waters) and DynamX 3.0

softwares (Waters) as described previously [151]. I provided the samples, the HDX experiment was conducted by Dr. Wieland Steinchen, and HDX data analysis were performed in collaboration with Dr. Wieland Steinchen.

5.2.8 Structural biology

5.2.8.1 Protein crystallization

Crystallization trials were set up aided by a pipetting robot (Gryphon, Art Robbins Instruments). Precipitant solutions of the commercially available screens JCSG cores I-IV (Qiagen) were predispensed into the reservoirs (50 µl for 2-well plates and 30 µl for 3-well plates) and 0.25 or 0.5 µl to the well. Into these, protein solution was dispensed (0.25 or 0.5 µl resulting in 1:1, 1:2 or 2:1 ratios of protein:precipitant), the plates sealed and kept at room temperature. Crystal growth was monitored once daily until crystals were visible through a microscope. The conditions, where crystal growth was apparent, were eventually further optimized in subsequent screens.

5.2.8.2 Harvest of protein crystals

For harvest of the protein crystals, the sealed well was opened and approximately 1 equivalent of precipitant solutions supplemented with 20-30% (v/v) glycerol was added to the drop. Crystals were retrieved with cryo-loops, flash-frozen in liquid nitrogen and kept under nitrogen until data collection.

5.2.8.3 Data collection

Crystallographic datasets were collected at the Europe Synchrotron Radiation Facility (ESRF, Grenoble) or (DESY Hamburg). The crystal-containing loop was automatically installed onto the goniometer in a 100 K and chilled by nitrogen gas flow and data collected with a DECTRIS PILATUS 6M detector at the ID29 beamline. Further details on data collections are provided in **table 3-3**.

5.2.8.4 Processing of collected datasets and structure determination

Crystallographic data were processed with XDS [152][153][154] and the CCP4i2-implemented program AIMLESS [155] applied for scaling and merging of the data. Molecular replacement was performed with CCP4i2-integrated Expert MR-PHASER [156] using the coordinates of a monomer (chain A) of *E. coli* EF-Tu structure (PDB: 1EFC) as input model for molecular replacement. Refinement calculations were carried out with PHENIX refine [157]. If there is no clear change in R work and R free and exploration of the difference map proposed that no more corrections or additions were required, the refinement was terminated.

5.2.8.5 Structural analysis and visualization

In order to visualize and interpret structural models, PyMOL was used [158].

6 References

[1] N. Sonenberg, J. W. B. Hershey, and M. B. Mathews, *Translational Control of Gene Expression. Monograph 39*. Cold Spring Harbor Laboratory Press, 2000.

[2] F. H. CRICK, “On protein synthesis.,” *Symp. Soc. Exp. Biol.*, vol. 12, pp. 138–163, 1958.

[3] A. Liljas, *Structural aspects of protein synthesis*. World Scientific, 2004.

[4] K. H. Nierhaus and D. N. Wilson, *Protein Synthesis and Ribosome Structure*. 2006.

[5] S. Melnikov, A. Ben-Shem, N. Garreau De Loubresse, L. Jenner, G. Yusupova, and M. Yusupov, “One core, two shells: Bacterial and eukaryotic ribosomes,” *Nat. Struct. Mol. Biol.*, vol. 19, no. 6, pp. 560–567, 2012, doi: 10.1038/nsmb.2313.

[6] G. E. PALADE, “A small particulate component of the cytoplasm.,” *J. Biophys. Biochem. Cytol.*, vol. 1, no. 1, pp. 59–68, Jan. 1955, doi: 10.1083/jcb.1.1.59.

[7] H. Stark *et al.*, “The 70S Escherichia coli ribosome at 23 å resolution: fitting the ribosomal RNA,” *Structure*, vol. 3, no. 8, pp. 815–821, 1995, doi: 10.1016/S0969-2126(01)00216-7.

[8] A. McLennan, A. Bates, P. Turner, and M. White, *Bios instant notes in molecular biology*. Taylor & Francis, 2012.

[9] J. D. Puglisi, S. C. Blanchard, and R. Green, “Approaching translation at atomic resolution,” *Nat. Struct. Biol.*, vol. 7, no. 10, pp. 855–861, 2000, doi: 10.1038/79603.

[10] Z. Shajani, M. T. Sykes, and J. R. Williamson, “Assembly of bacterial ribosomes,” *Annu. Rev. Biochem.*, vol. 80, pp. 501–526, 2011, doi: 10.1146/annurev-biochem-062608-160432.

[11] R. M. Corrigan, L. E. Bellows, A. Wood, and A. Gründling, “ppGpp negatively impacts ribosome assembly affecting growth and antimicrobial tolerance in Gram-positive bacteria,” *Proc. Natl. Acad. Sci.*, vol. 113, no. 12, p. E1710 LP-E1719, Mar. 2016, doi: 10.1073/pnas.1522179113.

[12] Y. Watanabe *et al.*, “Primary and higher order structures of nematode (Ascaris suum) mitochondrial tRNAs lacking either the T or D stem.,” *J. Biol. Chem.*, vol. 269, no. 36, pp. 22902–22906, 1994.

[13] S. J. Sharp, J. Schaack, L. Cooley, D. J. Burke, and D. Söll, “Structure and transcription of eukaryotic tRNA genes.,” *CRC Crit. Rev. Biochem.*, vol. 19, no. 2, pp. 107–144, 1985, doi: 10.3109/10409238509082541.

[14] M. B. HOAGLAND, M. L. STEPHENSON, J. F. SCOTT, L. I. HECHT, and P. C. ZAMECNIK, “A soluble ribonucleic acid intermediate in protein synthesis.,” *J. Biol. Chem.*, vol. 231, no. 1, pp. 241–257, 1958, doi: 10.1016/s0021-9258(19)77302-5.

[15] A. Rich and U. L. Rajbhandary, “TRANSFER RNA : MOLECULAR,” 1976.

[16] M. Taiji, S. Yokoyama, and T. Miyazawa, “Slow transacylation of

peptidyladenosine allows analysis of the 2'/3'-isomer specificity of peptidyltransferase," *Biochemistry*, vol. 24, no. 21, pp. 5776–5780, 1985.

[17] T. Awai, N. Ichihashi, and T. Yomo, "Activities of 20 aminoacyl-tRNA synthetases expressed in a reconstituted translation system in Escherichia coli," *Biochem. Biophys. Reports*, vol. 3, pp. 140–143, 2015, doi: 10.1016/j.bbrep.2015.08.006.

[18] N. Krahn, J. T. Fischer, and D. Söll, "Naturally Occurring tRNAs With Non-canonical Structures," *Front. Microbiol.*, vol. 11, no. October, pp. 1–18, 2020, doi: 10.3389/fmicb.2020.596914.

[19] A. Antoun, M. Y. Pavlov, K. Andersson, T. Tenson, and M. Ehrenberg, "The roles of initiation factor 2 and guanosine triphosphate in initiation of protein synthesis," *EMBO J.*, vol. 22, no. 20, pp. 5593–5601, Oct. 2003, doi: 10.1093/emboj/cdg525.

[20] J. Shine and L. Dalgarno, "The 3'-terminal sequence of Escherichia coli 16S ribosomal RNA: complementarity to nonsense triplets and ribosome binding sites," *Proc. Natl. Acad. Sci. U. S. A.*, vol. 71, no. 4, pp. 1342–1346, Apr. 1974, doi: 10.1073/pnas.71.4.1342.

[21] J. E. McCarthy and R. Brimacombe, "Prokaryotic translation: the interactive pathway leading to initiation.," *Trends Genet.*, vol. 10, no. 11, pp. 402–407, Nov. 1994, doi: 10.1016/0168-9525(94)90057-4.

[22] C. O. Gualerzi and C. L. Pon, "Initiation of mRNA translation in prokaryotes," *Biochemistry*, vol. 29, no. 25, pp. 5881–5889, Jun. 1990, doi: 10.1021/bi00477a001.

[23] G. Stahl, G. P. McCarty, and P. J. Farabaugh, "Ribosome structure: revisiting the connection between translational accuracy and unconventional decoding.," *Trends Biochem. Sci.*, vol. 27, no. 4, pp. 178–183, Apr. 2002, doi: 10.1016/s0968-0004(02)02064-9.

[24] K. Scheffzek and M. R. Ahmadian, "GTPase activating proteins: structural and functional insights 18 years after discovery.," *Cell. Mol. Life Sci.*, vol. 62, no. 24, pp. 3014–3038, Dec. 2005, doi: 10.1007/s00018-005-5136-x.

[25] M. Valle *et al.*, "Incorporation of aminoacyl-tRNA into the ribosome as seen by cryo-electron microscopy.," *Nat. Struct. Biol.*, vol. 10, no. 11, pp. 899–906, Nov. 2003, doi: 10.1038/nsb1003.

[26] M. V. Rodnina and W. Wintermeyer, "Peptide bond formation on the ribosome: Structure and mechanism," *Curr. Opin. Struct. Biol.*, vol. 13, no. 3, pp. 334–340, 2003, doi: 10.1016/S0959-440X(03)00065-4.

[27] A. S. Spirin, "The ribosome as an RNA-based molecular machine.," *RNA Biol.*, vol. 1, no. 1, pp. 2–8, 2004, doi: 10.4161/rna.1.1.889.

[28] D. Kavaliauskas, P. Nissen, and C. R. Knudsen, "The busiest of all ribosomal assistants: elongation factor Tu.," *Biochemistry*, vol. 51, no. 13, pp. 2642–2651, Apr. 2012, doi: 10.1021/bi300077s.

[29] I. M. Krab and A. Parmeggiani, "EF-Tu, a GTPase odyssey.," *Biochim. Biophys. Acta*, vol. 1443, no. 1–2, pp. 1–22, Nov. 1998, doi: 10.1016/s0167-4781(98)00169-9.

[30] A. G. Gilman, “G proteins: transducers of receptor-generated signals.,” *Annu. Rev. Biochem.*, vol. 56, pp. 615–649, 1987, doi: 10.1146/annurev.bi.56.070187.003151.

[31] M. Kjeldgaard and J. Nyborg, “Refined structure of elongation factor EF-Tu from Escherichia coli.,” *J. Mol. Biol.*, vol. 223, no. 3, pp. 721–742, Feb. 1992, doi: 10.1016/0022-2836(92)90986-t.

[32] G. Polekhina, S. Thirup, M. Kjeldgaard, P. Nissen, C. Lippmann, and J. Nyborg, “Helix unwinding in the effector region of elongation factor EF-Tu-GDP.,” *Structure*, vol. 4, no. 10, pp. 1141–1151, Oct. 1996, doi: 10.1016/s0969-2126(96)00122-0.

[33] K. Abel, M. D. Yoder, R. Hilgenfeld, and F. Jurnak, “An alpha to beta conformational switch in EF-Tu.,” *Structure*, vol. 4, no. 10, pp. 1153–1159, Oct. 1996, doi: 10.1016/s0969-2126(96)00123-2.

[34] H. Song, M. R. Parsons, S. Rowsell, G. Leonard, and S. E. Phillips, “Crystal structure of intact elongation factor EF-Tu from Escherichia coli in GDP conformation at 2.05 A resolution.,” *J. Mol. Biol.*, vol. 285, no. 3, pp. 1245–1256, Jan. 1999, doi: 10.1006/jmbi.1998.2387.

[35] H. Berchtold, L. Reshetnikova, C. O. A. Reiser, N. K. Schirmer, M. Sprinzl, and R. Hilgenfeld, “Erratum: Crystal structure of active elongation factor Tu reveals major domain rearrangements (Nature (1993) 365 (126-132)),” *Nature*, vol. 365, no. 6444, p. 368, 1993, doi: 10.1038/365368a0.

[36] M. Kjeldgaard, P. Nissen, S. Thirup, and J. Nyborg, “The crystal structure of elongation factor EF-Tu from Thermus aquaticus in the GTP conformation,” *Structure*, vol. 1, no. 1, pp. 35–50, 1993, doi: https://doi.org/10.1016/0969-2126(93)90007-4.

[37] A. M. Rojas, M. Ehrenberg, S. G. Andersson, and C. G. Kurland, “ppGpp inhibition of elongation factors Tu, G and Ts during polypeptide synthesis.,” *Mol. Gen. Genet.*, vol. 197, no. 1, pp. 36–45, 1984, doi: 10.1007/BF00327920.

[38] P. Nissen *et al.*, “Crystal structure of the ternary complex of Phe-tRNAPhe, EF-Tu, and a GTP analog.,” *Science*, vol. 270, no. 5241, pp. 1464–1472, Dec. 1995, doi: 10.1126/science.270.5241.1464.

[39] P. Nissen, S. Thirup, M. Kjeldgaard, and J. Nyborg, “The crystal structure of Cys-tRNACys–EF-Tu–GDPNP reveals general and specific features in the ternary complex and in tRNA,” *Structure*, vol. 7, no. 2, pp. 143–156, 1999, doi: https://doi.org/10.1016/S0969-2126(99)80021-5.

[40] V. Hauryliuk, S. Hansson, and M. Ehrenberg, “Cofactor dependent conformational switching of GTPases,” *Biophys. J.*, vol. 95, no. 4, pp. 1704–1715, Aug. 2008, doi: 10.1529/biophysj.107.127290.

[41] J. C. H. Liu, M. Liu, and J. Horowitz, “Recognition of the universally conserved 3’-CCA end of tRNA by elongation factor EF-Tu,” *Rna*, vol. 4, no. 6, pp. 639–646, 1998, doi: 10.1017/S1355838298980013.

[42] P. Nissen, M. Kjeldgaard, S. Thirup, B. F. C. Clark, and J. Nyborg, “The ternary

complex of aminoacylated tRNA and EF-Tu-GTP. Recognition of a bond and a fold," *Biochimie*, vol. 78, no. 11–12, pp. 921–933, 1996, doi: 10.1016/S0300-9084(97)86714-4.

[43] S. Rudorf and R. Lipowsky, "Protein Synthesis in E. coli: Dependence of Codon-Specific Elongation on tRNA Concentration and Codon Usage," *PLoS One*, vol. 10, no. 8, pp. e0134994–e0134994, Aug. 2015, doi: 10.1371/journal.pone.0134994.

[44] B. J. Burnett *et al.*, "Elongation factor Ts directly facilitates the formation and disassembly of the Escherichia coli elongation factor Tu·GTP·aminoacyl-tRNA ternary complex.," *J. Biol. Chem.*, vol. 288, no. 19, pp. 13917–13928, May 2013, doi: 10.1074/jbc.M113.460014.

[45] T. Kawashima, C. Berthet-Colominas, M. Wulff, S. Cusack, and R. Leberman, "The structure of the Escherichia coli EF-Tu·EF-Ts complex at 2.5 Å resolution," *Nature*, vol. 379, no. 6565, pp. 511–518, 1996, doi: 10.1038/379511a0.

[46] Y. Nakamura and K. Ito, "Making sense of mimic in translation termination," *Trends Biochem. Sci.*, vol. 28, no. 2, p. 99—105, Feb. 2003, doi: 10.1016/s0968-0004(03)00006-9.

[47] E. Scolnick, R. Tompkins, T. Caskey, and M. Nirenberg, "Release factors differing in specificity for terminator codons," *Proc. Natl. Acad. Sci. U. S. A.*, vol. 61, no. 2, pp. 768–774, Oct. 1968, doi: 10.1073/pnas.61.2.768.

[48] J. L. Goldstein and C. T. Caskey, "Peptide chain termination: effect of protein S on ribosomal binding of release factors," *Proc. Natl. Acad. Sci. U. S. A.*, vol. 67, no. 2, pp. 537–543, Oct. 1970, doi: 10.1073/pnas.67.2.537.

[49] S. T. Gregory, "Ribosome Regulation by EF-G and EF-Tu," W. J. Lennarz and M. D. B. T.-E. of B. C. (Second E. Lane, Eds. Waltham: Academic Press, 2013, pp. 122–127.

[50] H. Gao *et al.*, "RF3 Induces Ribosomal Conformational Changes Responsible for Dissociation of Class I Release Factors," *Cell*, vol. 129, no. 5, pp. 929–941, 2007, doi: 10.1016/j.cell.2007.03.050.

[51] A. S. N. Seshasayee, P. Bertone, G. M. Fraser, and N. M. Luscombe, "Transcriptional regulatory networks in bacteria: from input signals to output responses.," *Curr. Opin. Microbiol.*, vol. 9, no. 5, pp. 511–519, Oct. 2006, doi: 10.1016/j.mib.2006.08.007.

[52] C. C. Boutte and S. Crosson, "Bacterial lifestyle shapes stringent response activation.," *Trends Microbiol.*, vol. 21, no. 4, pp. 174–180, Apr. 2013, doi: 10.1016/j.tim.2013.01.002.

[53] K. Liu, A. N. Bittner, and J. D. Wang, "Diversity in (p)ppGpp metabolism and effectors.," *Curr. Opin. Microbiol.*, vol. 24, pp. 72–79, Apr. 2015, doi: 10.1016/j.mib.2015.01.012.

[54] M. Cashel and J. Gallant, "Two compounds implicated in the function of the RC gene of Escherichia coli.," *Nature*, vol. 221, no. 5183, pp. 838–841, Mar. 1969, doi: 10.1038/221838a0.

[55] M. Cashel, “The stringent response,” *Escherichia coli Salmonella typhimulium Cell. Mol. Biol.*, vol. 2, pp. 1458–1496, 1996.

[56] V. Jain, M. Kumar, and D. Chatterji, “ppGpp: stringent response and survival.,” *J. Microbiol.*, vol. 44, no. 1, pp. 1–10, Feb. 2006.

[57] M. Cashel, “The control of ribonucleic acid synthesis in Escherichia coli. IV. Relevance of unusual phosphorylated compounds from amino acid-starved stringent strains.,” *J. Biol. Chem.*, vol. 244, no. 12, pp. 3133–3141, Jun. 1969.

[58] K. Takahashi, K. Kasai, and K. Ochi, “Identification of the bacterial alarmone guanosine 5’-diphosphate 3’-diphosphate (ppGpp) in plants,” *Proc. Natl. Acad. Sci.*, vol. 101, no. 12, pp. 4320–4324, 2004, doi: 10.1073/pnas.0308555101.

[59] S. Masuda, Y. Tozawa, and H. Ohta, “Possible targets of ‘magic spots’ in plant signaling,” *Plant Signal. Behav.*, vol. 3, pp. 1021–1023, Dec. 2008, doi: 10.4161/psb.6766.

[60] B. Field, “Green magic: regulation of the chloroplast stress response by (p)ppGpp in plants and algae.,” *J. Exp. Bot.*, vol. 69, no. 11, pp. 2797–2807, May 2018, doi: 10.1093/jxb/erx485.

[61] W. A. Haseltine and R. Block, “Synthesis of guanosine tetra- and pentaphosphate requires the presence of a codon-specific, uncharged transfer ribonucleic acid in the acceptor site of ribosomes.,” *Proc. Natl. Acad. Sci. U. S. A.*, vol. 70, no. 5, pp. 1564–1568, May 1973, doi: 10.1073/pnas.70.5.1564.

[62] R.-M. Knutsson Jenvert and L. Holmberg Schiavone, “Characterization of the tRNA and ribosome-dependent pppGpp-synthesis by recombinant stringent factor from Escherichia coli.,” *FEBS J.*, vol. 272, no. 3, pp. 685–695, Feb. 2005, doi: 10.1111/j.1742-4658.2004.04502.x.

[63] W. Steinchen and G. Bange, “The magic dance of the alarmones (p)ppGpp,” *Molecular Microbiology*, vol. 101, no. 4. pp. 531–544, 2016, doi: 10.1111/mmi.13412.

[64] Y. Zuo, Y. Wang, and T. A. Steitz, “The mechanism of E. coli RNA polymerase regulation by ppGpp is suggested by the structure of their complex,” *Mol. Cell*, vol. 50, no. 3, pp. 430–436, May 2013, doi: 10.1016/j.molcel.2013.03.020.

[65] S. E. Irving, N. R. Choudhury, and R. M. Corrigan, “The stringent response and physiological roles of (pp)pGpp in bacteria,” *Nat. Rev. Microbiol.*, vol. 19, no. 4, pp. 256–271, 2021, doi: 10.1038/s41579-020-00470-y.

[66] J. D. Keasling, L. Bertsch, and A. Kornberg, “Guanosine pentaphosphate phosphohydrolase of Escherichia coli is a long-chain exopolyphosphatase,” *Proc. Natl. Acad. Sci. U. S. A.*, vol. 90, no. 15, p. 7029—7033, Aug. 1993, doi: 10.1073/pnas.90.15.7029.

[67] G. C. Atkinson, T. Tenson, and V. Hauryliuk, “The RelA/SpoT homolog (RSH) superfamily: distribution and functional evolution of ppGpp synthetases and hydrolases across the tree of life.,” *PLoS One*, vol. 6, no. 8, p. e23479, 2011, doi: 10.1371/journal.pone.0023479.

[68] S. Ronneau and R. Hallez, “Make and break the alarmone: regulation of

(p)ppGpp synthetase/hydrolase enzymes in bacteria.," *FEMS Microbiol. Rev.*, vol. 43, no. 4, pp. 389–400, Jul. 2019, doi: 10.1093/femsre/fuz009.

[69] T. M. Wendrich, G. Blaha, D. N. Wilson, M. A. Marahiel, and K. H. Nierhaus, "Dissection of the mechanism for the stringent factor RelA.," *Mol. Cell*, vol. 10, no. 4, pp. 779–788, Oct. 2002, doi: 10.1016/s1097-2765(02)00656-1.

[70] X. Yang and E. E. Ishiguro, "Involvement of the N terminus of ribosomal protein L11 in regulation of the RelA protein of Escherichia coli.," *J. Bacteriol.*, vol. 183, no. 22, pp. 6532–6537, Nov. 2001, doi: 10.1128/JB.183.22.6532-6537.2001.

[71] L. Aravind and E. V Koonin, "The HD domain defines a new superfamily of metal-dependent phosphohydrolases.," *Trends Biochem. Sci.*, vol. 23, no. 12, pp. 469–472, Dec. 1998, doi: 10.1016/s0968-0004(98)01293-6.

[72] X. Agirrezabala, I. S. Fernández, A. C. Kelley, D. G. Cartón, V. Ramakrishnan, and M. Valle, "The ribosome triggers the stringent response by RelA via a highly distorted tRNA," *EMBO Rep.*, vol. 14, no. 9, pp. 811–816, Sep. 2013, doi: 10.1038/embor.2013.106.

[73] V. Hauryliuk, G. C. Atkinson, K. S. Murakami, T. Tenson, and K. Gerdes, "Recent functional insights into the role of (p)ppGpp in bacterial physiology.," *Nat. Rev. Microbiol.*, vol. 13, no. 5, pp. 298–309, May 2015, doi: 10.1038/nrmicro3448.

[74] T. Hogg, U. Mechold, H. Malke, M. Cashel, and R. Hilgenfeld, "Conformational antagonism between opposing active sites in a bifunctional RelA/SpoT homolog modulates (p)ppGpp metabolism during the stringent response [corrected].," *Cell*, vol. 117, no. 1, pp. 57–68, Apr. 2004, doi: 10.1016/s0092-8674(04)00260-0.

[75] P. Pausch *et al.*, "Structural Basis for Regulation of the Opposing (p)ppGpp Synthetase and Hydrolase within the Stringent Response Orchestrator Rel," *Cell Rep.*, vol. 32, no. 11, p. 108157, Sep. 2020, doi: 10.1016/j.celrep.2020.108157.

[76] K. Syal, H. Joshi, D. Chatterji, and V. Jain, "Novel pppGpp binding site at the C-terminal region of the Rel enzyme from Mycobacterium smegmatis.," *FEBS J.*, vol. 282, no. 19, pp. 3773–3785, Oct. 2015, doi: 10.1111/febs.13373.

[77] H. Xiao, M. Kalman, K. Ikehara, S. Zemel, G. Glaser, and M. Cashel, "Residual guanosine 3',5'-bispyrophosphate synthetic activity of relA null mutants can be eliminated by spoT null mutations.," *J. Biol. Chem.*, vol. 266, no. 9, pp. 5980–5990, Mar. 1991.

[78] A. Battesti and E. Bouveret, "Acyl carrier protein/SpoT interaction, the switch linking SpoT-dependent stress response to fatty acid metabolism.," *Mol. Microbiol.*, vol. 62, no. 4, pp. 1048–1063, Nov. 2006, doi: 10.1111/j.1365-2958.2006.05442.x.

[79] D. Vinella, C. Albrecht, M. Cashel, and R. D'Ari, "Iron limitation induces SpoT-dependent accumulation of ppGpp in Escherichia coli.," *Mol. Microbiol.*, vol. 56, no. 4, pp. 958–970, May 2005, doi: 10.1111/j.1365-2958.2005.04601.x.

[80] A. Battesti and E. Bouveret, "Bacteria possessing two RelA/SpoT-like proteins have evolved a specific stringent response involving the acyl carrier protein-

SpoT interaction.," *J. Bacteriol.*, vol. 191, no. 2, pp. 616–624, Jan. 2009, doi: 10.1128/JB.01195-08.

[81] U. Kanjee, K. Ogata, and W. A. Houry, "Direct binding targets of the stringent response alarmone (p)ppGpp.," *Mol. Microbiol.*, vol. 85, no. 6, pp. 1029–1043, Sep. 2012, doi: 10.1111/j.1365-2958.2012.08177.x.

[82] J. A. Lemos, V. K. Lin, M. M. Nascimento, J. Abranches, and R. A. Burne, "Three gene products govern (p)ppGpp production by Streptococcus mutans.," *Mol. Microbiol.*, vol. 65, no. 6, pp. 1568–1581, Sep. 2007, doi: 10.1111/j.1365-2958.2007.05897.x.

[83] D. H. Wells and S. R. Long, "The Sinorhizobium meliloti stringent response affects multiple aspects of symbiosis.," *Mol. Microbiol.*, vol. 43, no. 5, pp. 1115–1127, Mar. 2002, doi: 10.1046/j.1365-2958.2002.02826.x.

[84] H. Nanamiya *et al.*, "Identification and functional analysis of novel (p)ppGpp synthetase genes in Bacillus subtilis.," *Mol. Microbiol.*, vol. 67, no. 2, pp. 291–304, Jan. 2008, doi: 10.1111/j.1365-2958.2007.06018.x.

[85] W. Eiamphungporn and J. D. Helmann, "The Bacillus subtilis sigma(M) regulon and its contribution to cell envelope stress responses," *Mol. Microbiol.*, vol. 67, no. 4, pp. 830–848, Feb. 2008, doi: 10.1111/j.1365-2958.2007.06090.x.

[86] T. Geiger, B. Kästle, F. L. Gratani, C. Goerke, and C. Wolz, "Two small (p)ppGpp synthases in Staphylococcus aureus mediate tolerance against cell envelope stress conditions.," *J. Bacteriol.*, vol. 196, no. 4, pp. 894–902, Feb. 2014, doi: 10.1128/JB.01201-13.

[87] M. Cao, T. Wang, R. Ye, and J. D. Helmann, "Antibiotics that inhibit cell wall biosynthesis induce expression of the Bacillus subtilis sigma(W) and sigma(M) regulons.," *Mol. Microbiol.*, vol. 45, no. 5, pp. 1267–1276, Sep. 2002, doi: 10.1046/j.1365-2958.2002.03050.x.

[88] P. D. Thackray and A. Moir, "SigM, an Extracytoplasmic Function Sigma Factor of Bacillus subtilis, Is Activated in Response to Cell Wall Antibiotics, Ethanol, Heat, Acid, and Superoxide Stress," *J. Bacteriol.*, vol. 185, no. 12, pp. 3491 LP – 3498, Jun. 2003, doi: 10.1128/JB.185.12.3491-3498.2003.

[89] J. C. Zweers, P. Nicolas, T. Wiegert, J. M. van Dijl, and E. L. Denham, "Definition of the σW Regulon of Bacillus subtilis in the Absence of Stress," *PLoS One*, vol. 7, no. 11, 2012, doi: 10.1371/journal.pone.0048471.

[90] W. Steinchen *et al.*, "Catalytic mechanism and allosteric regulation of an oligomeric (p)ppGpp synthetase by an alarmone.," *Proc. Natl. Acad. Sci. U. S. A.*, vol. 112, no. 43, pp. 13348–13353, Oct. 2015, doi: 10.1073/pnas.1505271112.

[91] M. C. Manav *et al.*, "Structural basis for (p)ppGpp synthesis by the Staphylococcus aureus small alarmone synthetase RelP.," *J. Biol. Chem.*, vol. 293, no. 9, pp. 3254–3264, Mar. 2018, doi: 10.1074/jbc.RA117.001374.

[92] R. H. Silverman and A. G. Atherly, "The search for guanosine tetraphosphate (ppGpp) and other unusual nucleotides in eucaryotes," *Microbiol. Rev.*, vol. 43,

no. 1, pp. 27–41, Mar. 1979, [Online]. Available: https://pubmed.ncbi.nlm.nih.gov/379576.

[93] D. Sun *et al.*, “A metazoan ortholog of SpoT hydrolyzes ppGpp and functions in starvation responses,” *Nat. Struct. Mol. Biol.*, vol. 17, no. 10, pp. 1188–1194, 2010, doi: 10.1038/nsmb.1906.

[94] W. Steinchen *et al.*, “Dual role of a (p)ppGpp- and (p)ppApp-degrading enzyme in biofilm formation and interbacterial antagonism.,” *Mol. Microbiol.*, Jan. 2021, doi: 10.1111/mmi.14684.

[95] C. Maracci and M. V. Rodnina, “Review: Translational GTPases,” *Biopolymers*, vol. 105, no. 8, pp. 463–475, 2016, doi: 10.1002/bip.22832.

[96] P. Milon *et al.*, “The nucleotide-binding site of bacterial translation initiation factor 2 (IF2) as a metabolic sensor.,” *Proc. Natl. Acad. Sci. U. S. A.*, vol. 103, no. 38, pp. 13962–13967, Sep. 2006, doi: 10.1073/pnas.0606384103.

[97] K. Kihira *et al.*, “Crystal structure analysis of the translation factor RF3 (release factor 3),” *FEBS Lett.*, vol. 586, no. 20, pp. 3705–3709, 2012, doi: 10.1016/j.febslet.2012.08.029.

[98] S. S. Chen, E. Sperling, J. M. Silverman, J. H. Davis, and J. R. Williamson, “Measuring the dynamics of E. coli ribosome biogenesis using pulse-labeling and quantitative mass spectrometry,” *Mol. Biosyst.*, vol. 8, no. 12, pp. 3325–3334, Oct. 2012, doi: 10.1039/c2mb25310k.

[99] L. Lindahl, “Intermediates and time kinetics of the in vivo assembly of Escherichia coli ribosomes.,” *J. Mol. Biol.*, vol. 92, no. 1, pp. 15–37, Feb. 1975, doi: 10.1016/0022-2836(75)90089-3.

[100] J. H. Davis and J. R. Williamson, “Structure and dynamics of bacterial ribosome biogenesis,” *Philos. Trans. R. Soc. B Biol. Sci.*, vol. 372, no. 1716, 2017, doi: 10.1098/rstb.2016.0181.

[101] B. Feng *et al.*, “Structural and Functional Insights into the Mode of Action of a Universally Conserved Obg GTPase,” *PLoS Biol.*, vol. 12, no. 5, 2014, doi: 10.1371/journal.pbio.1001866.

[102] J. Czworkowski, J. Wang, T. A. Steitz, and P. B. Moore, “The crystal structure of elongation factor G complexed with GDP, at 2.7 A resolution,” *EMBO J.*, vol. 13, no. 16, pp. 3661–3668, Aug. 1994, [Online]. Available: https://pubmed.ncbi.nlm.nih.gov/8070396.

[103] I. I. Toulokhonov, I. Shulgina, and V. J. Hernandez, “Binding of the transcription effector ppGpp to Escherichia coli RNA polymerase is allosteric, modular, and occurs near the N terminus of the beta’-subunit.,” *J. Biol. Chem.*, vol. 276, no. 2, pp. 1220–1225, Jan. 2001, doi: 10.1074/jbc.M007184200.

[104] M. M. Barker, T. Gaal, C. A. Josaitis, and R. L. Gourse, “Mechanism of regulation of transcription initiation by ppGpp. I. Effects of ppGpp on transcription initiation in vivo and in vitro.,” *J. Mol. Biol.*, vol. 305, no. 4, pp. 673–688, Jan. 2001, doi: 10.1006/jmbi.2000.4327.

[105] S. P. Muench, L. Xu, S. E. Sedelnikova, and D. W. Rice, “The essential GTPase

YphC displays a major domain rearrangement associated with nucleotide binding," *Proc. Natl. Acad. Sci. U. S. A.*, vol. 103, no. 33, pp. 12359–12364, 2006, doi: 10.1073/pnas.0602585103.

[106] A. E. Foucher, J. B. Reiser, C. Ebel, D. Housset, and J. M. Jault, "Potassium Acts as a GTPase-Activating Element on Each Nucleotide-Binding Domain of the Essential Bacillus subtilis EngA," *PLoS One*, vol. 7, no. 10, 2012, doi: 10.1371/journal.pone.0046795.

[107] X. Zhang *et al.*, "Structural insights into the function of a unique tandem GTPase EngA in bacterial ribosome assembly," *Nucleic Acids Res.*, vol. 42, no. 21, pp. 13430–13439, 2014, doi: 10.1093/nar/gku1135.

[108] V. L. Robinson, J. Hwang, E. Fox, M. Inouye, and A. M. Stock, "Domain arrangement of Der, a switch protein containing two GTPase domains," *Structure*, vol. 10, no. 12, pp. 1649–1658, 2002, doi: 10.1016/S0969-2126(02)00905-X.

[109] X. Ji, "Structural insights into cell cycle control by essential GTPase Era.," *Postepy Biochem.*, vol. 62, no. 3, pp. 335–342, 2016.

[110] C. Tu *et al.*, "Structure of ERA in complex with the 3′ end of 16S rRNA: Implications for ribosome biogenesis," *Proc. Natl. Acad. Sci. U. S. A.*, vol. 106, no. 35, pp. 14843–14848, 2009, doi: 10.1073/pnas.0904032106.

[111] A. Razi *et al.*, "Role of Era in assembly and homeostasis of the ribosomal small subunit," *Nucleic Acids Res.*, vol. 47, no. 15, pp. 8301–8317, 2019, doi: 10.1093/nar/gkz571.

[112] H. Yamamoto *et al.*, "EF-G and EF4: Translocation and back-translocation on the bacterial ribosome," *Nat. Rev. Microbiol.*, vol. 12, no. 2, pp. 89–100, 2014, doi: 10.1038/nrmicro3176.

[113] Y. Nishizuka and F. Lipmann, "Comparison of guanosine triphosphate split and polypeptide synthesis with a purified E. coli system.," *Proc. Natl. Acad. Sci. U. S. A.*, vol. 55, no. 1, pp. 212–219, 1966, doi: 10.1073/pnas.55.1.212.

[114] N. Richman and J. W. Bodley, "Ribosomes cannot interact simultaneously with elongation factors EF Tu and EF G.," *Proc. Natl. Acad. Sci. U. S. A.*, vol. 69, no. 3, pp. 686–689, 1972, doi: 10.1073/pnas.69.3.686.

[115] H. R. Bourne, D. A. Sanders, and F. McCormick, "The GTPase superfamily: conserved structure and molecular mechanism.," *Nature*, vol. 349, no. 6305, pp. 117–127, Jan. 1991, doi: 10.1038/349117a0.

[116] S. Hansson, R. Singh, A. T. Gudkov, A. Liljas, and D. T. Logan, "Crystal structure of a mutant elongation factor G trapped with a GTP analogue," *FEBS Lett.*, vol. 579, no. 20, pp. 4492–4497, 2005, doi: 10.1016/j.febslet.2005.07.016.

[117] D. L. Miller, M. Cashel, and H. Weissbach, "The interaction of guanosine 5'-diphosphate, 2' (3')-diphosphate with the bacterial elongation factor Tu.," *Arch. Biochem. Biophys.*, vol. 154, no. 2, pp. 675–682, Feb. 1973, doi: 10.1016/0003-9861(73)90022-2.

[118] G. S. Kushwaha, G. Bange, and N. S. Bhavesh, "Interaction studies on bacterial

stringent response protein RelA with uncharged tRNA provide evidence for its prerequisite complex for ribosome binding," *Curr. Genet.*, vol. 65, no. 5, pp. 1173–1184, 2019, doi: 10.1007/s00294-019-00966-y.

[119] K. S. Winther, M. Roghanian, and K. Gerdes, "Activation of the Stringent Response by Loading of RelA-tRNA Complexes at the Ribosomal A-Site.," *Mol. Cell*, vol. 70, no. 1, pp. 95-105.e4, Apr. 2018, doi: 10.1016/j.molcel.2018.02.033.

[120] A. Brown, I. S. Fernández, Y. Gordiyenko, and V. Ramakrishnan, "Ribosome-dependent activation of stringent control," *Nature*, vol. 534, no. 7606, pp. 277–280, 2016, doi: 10.1038/nature17675.

[121] A. Kuroda, H. Murphy, M. Cashel, and A. Kornberg, "Guanosine tetra- and pentaphosphate promote accumulation of inorganic polyphosphate in Escherichia coli," *J. Biol. Chem.*, vol. 272, no. 34, pp. 21240–21243, 1997, doi: 10.1074/jbc.272.34.21240.

[122] A. Kriel *et al.*, "Direct regulation of GTP homeostasis by (p)ppGpp: a critical component of viability and stress resistance.," *Mol. Cell*, vol. 48, no. 2, pp. 231–241, Oct. 2012, doi: 10.1016/j.molcel.2012.08.009.

[123] C. Lippmann, C. Lindschau, E. Vijgenboom, W. Schröder, L. Bosch, and V. A. Erdmann, "Prokaryotic elongation factor Tu is phosphorylated in vivo.," *J. Biol. Chem.*, vol. 268, no. 1, pp. 601–607, Jan. 1993.

[124] B. Macek *et al.*, "Phosphoproteome analysis of E. coli reveals evolutionary conservation of bacterial Ser/Thr/Tyr phosphorylation.," *Mol. Cell. Proteomics*, vol. 7, no. 2, pp. 299–307, Feb. 2008, doi: 10.1074/mcp.M700311-MCP200.

[125] S. F. F. Pereira, R. L. J. Gonzalez, and J. Dworkin, "Protein synthesis during cellular quiescence is inhibited by phosphorylation of a translational elongation factor.," *Proc. Natl. Acad. Sci. U. S. A.*, vol. 112, no. 25, pp. E3274-81, Jun. 2015, doi: 10.1073/pnas.1505297112.

[126] A. Talavera *et al.*, "Phosphorylation decelerates conformational dynamics in bacterial translation elongation factors.," *Sci. Adv.*, vol. 4, no. 3, p. eaap9714, Mar. 2018, doi: 10.1126/sciadv.aap9714.

[127] A. Sajid *et al.*, "Interaction of Mycobacterium tuberculosis elongation factor Tu with GTP is regulated by phosphorylation," *J. Bacteriol.*, vol. 193, no. 19, pp. 5347–5358, Oct. 2011, doi: 10.1128/JB.05469-11.

[128] B. J. Burnett, R. B. Altman, A. Ferguson, M. R. Wasserman, Z. Zhou, and S. C. Blanchard, "Direct evidence of an elongation factor-Tu/Ts·GTP·Aminoacyl-tRNA quaternary complex," *J. Biol. Chem.*, vol. 289, no. 34, pp. 23917–23927, Aug. 2014, doi: 10.1074/jbc.M114.583385.

[129] J. Yang *et al.*, "Systemic characterization of pppGpp, ppGpp and pGpp targets in Bacillus reveals NahA converts (p)ppGpp to pGpp to regulate alarmone composition and signaling," 2020, doi: 10.1101/2020.03.23.003749.

[130] P. Pausch *et al.*, "Structural basis for (p)ppGpp-mediated inhibition of the GTPase RbgA.," *J. Biol. Chem.*, vol. 293, no. 51, pp. 19699–19709, Dec. 2018, doi: 10.1074/jbc.RA118.003070.

[131] E. S. Honsa *et al.*, “Rela mutant enterococcus faecium with multiantibiotic tolerance arising in an immunocompromised host,” *MBio*, vol. 8, no. 1, pp. 1–12, 2017, doi: 10.1128/mBio.02124-16.

[132] W. Gao *et al.*, “Two novel point mutations in clinical Staphylococcus aureus reduce linezolid susceptibility and switch on the stringent response to promote persistent infection,” *PLoS Pathog.*, vol. 6, no. 6, 2010, doi: 10.1371/journal.ppat.1000944.

[133] M. Khakimova, H. G. Ahlgren, J. J. Harrison, A. M. English, and D. Nguyen, “The stringent response controls catalases in Pseudomonas aeruginosa and is required for hydrogen peroxide and antibiotic tolerance,” *J. Bacteriol.*, vol. 195, no. 9, pp. 2011–2020, 2013, doi: 10.1128/JB.02061-12.

[134] N. Kaldalu, V. Hauryliuk, and T. Tenson, “Persisters-as elusive as ever.,” *Appl. Microbiol. Biotechnol.*, vol. 100, no. 15, pp. 6545–6553, Aug. 2016, doi: 10.1007/s00253-016-7648-8.

[135] A. Hesketh, W. J. Chen, J. Ryding, S. Chang, and M. Bibb, “The global role of ppGpp synthesis in morphological differentiation and antibiotic production in Streptomyces coelicolor A3(2).,” *Genome Biol.*, vol. 8, no. 8, p. R161, 2007, doi: 10.1186/gb-2007-8-8-r161.

[136] J. Mukhopadhyay, E. Sineva, J. Knight, R. M. Levy, and R. H. Ebright, “Antibacterial peptide microcin J25 inhibits transcription by binding within and obstructing the RNA polymerase secondary channel.,” *Mol. Cell*, vol. 14, no. 6, pp. 739–751, Jun. 2004, doi: 10.1016/j.molcel.2004.06.010.

[137] M. F. Pomares, P. A. Vincent, R. N. Farías, and R. A. Salomón, “Protective action of ppGpp in microcin J25-sensitive strains.,” *J. Bacteriol.*, vol. 190, no. 12, pp. 4328–4334, Jun. 2008, doi: 10.1128/JB.00183-08.

[138] K. Sureka *et al.*, “Polyphosphate kinase is involved in stress-induced mprAB-sigE-rel signalling in mycobacteria.,” *Mol. Microbiol.*, vol. 65, no. 2, pp. 261–276, Jul. 2007, doi: 10.1111/j.1365-2958.2007.05814.x.

[139] J. L. Dahl *et al.*, “The role of RelMtb-mediated adaptation to stationary phase in long-term persistence of Mycobacterium tuberculosis in mice.,” *Proc. Natl. Acad. Sci. U. S. A.*, vol. 100, no. 17, pp. 10026–10031, Aug. 2003, doi: 10.1073/pnas.1631248100.

[140] T. P. Primm, S. J. Andersen, V. Mizrahi, D. Avarbock, H. Rubin, and C. E. 3rd Barry, “The stringent response of Mycobacterium tuberculosis is required for long-term survival.,” *J. Bacteriol.*, vol. 182, no. 17, pp. 4889–4898, Sep. 2000, doi: 10.1128/jb.182.17.4889-4898.2000.

[141] D. Nguyen *et al.*, “Active starvation responses mediate antibiotic tolerance in biofilms and nutrient-limited bacteria,” *Science*, vol. 334, no. 6058, pp. 982–986, Nov. 2011, doi: 10.1126/science.1211037.

[142] E. Wexselblatt *et al.*, “ppGpp analogues inhibit synthetase activity of Rel proteins from Gram-negative and Gram-positive bacteria.,” *Bioorg. Med. Chem.*, vol. 18, no. 12, pp. 4485–4497, Jun. 2010, doi: 10.1016/j.bmc.2010.04.064.

[143] E. Wexselblatt *et al.*, “Relacin, a novel antibacterial agent targeting the Stringent Response.,” *PLoS Pathog.*, vol. 8, no. 9, p. e1002925, Sep. 2012, doi: 10.1371/journal.ppat.1002925.

[144] A. Krezel and W. Bal, “A formula for correlating pKa values determined in D2O and H2O.,” *J. Inorg. Biochem.*, vol. 98, no. 1, pp. 161–166, Jan. 2004, doi: 10.1016/j.jinorgbio.2003.10.001.

[145] A. D. Laurie *et al.*, “The role of the alarmone (p)ppGpp in σN competition for core RNA polymerase,” *J. Biol. Chem.*, vol. 278, no. 3, pp. 1494–1503, 2003, doi: 10.1074/jbc.M209268200.

[146] K. Mullis, F. Faloona, S. Scharf, R. Saiki, G. Horn, and H. Erlich, “Specific enzymatic amplification of DNA in vitro: the polymerase chain reaction.,” *Cold Spring Harb. Symp. Quant. Biol.*, vol. 51 Pt 1, pp. 263–273, 1986, doi: 10.1101/sqb.1986.051.01.032.

[147] E. Gasteiger *et al.*, “The Proteomics Protocols Handbook,” *Proteomics Protoc. Handb.*, pp. 571–608, 2005, doi: 10.1385/1592598900.

[148] T. E. Wales, K. E. Fadgen, G. C. Gerhardt, and J. R. Engen, “High-speed and high-resolution UPLC separation at zero degrees Celsius.,” *Anal. Chem.*, vol. 80, no. 17, pp. 6815–6820, Sep. 2008, doi: 10.1021/ac8008862.

[149] S. J. Geromanos *et al.*, “The detection, correlation, and comparison of peptide precursor and product ions from data independent LC-MS with data dependant LC-MS/MS.,” *Proteomics*, vol. 9, no. 6, pp. 1683–1695, Mar. 2009, doi: 10.1002/pmic.200800562.

[150] G.-Z. Li, J. P. C. Vissers, J. C. Silva, D. Golick, M. V Gorenstein, and S. J. Geromanos, “Database searching and accounting of multiplexed precursor and product ion spectra from the data independent analysis of simple and complex peptide mixtures.,” *Proteomics*, vol. 9, no. 6, pp. 1696–1719, Mar. 2009, doi: 10.1002/pmic.200800564.

[151] M. Osorio-Valeriano *et al.*, “ParB-type DNA Segregation Proteins Are CTP-Dependent Molecular Switches,” *Cell*, vol. 179, no. 7, pp. 1512-1524.e15, 2019, doi: https://doi.org/10.1016/j.cell.2019.11.015.

[152] W. Kabsch, “XDS,” *Acta Crystallogr. D. Biol. Crystallogr.*, vol. 66, no. Pt 2, pp. 125–132, Feb. 2010, doi: 10.1107/S0907444909047337.

[153] L. Potterton *et al.*, “CCP4i2: the new graphical user interface to the CCP4 program suite.,” *Acta Crystallogr. Sect. D, Struct. Biol.*, vol. 74, no. Pt 2, pp. 68–84, Feb. 2018, doi: 10.1107/S2059798317016035.

[154] M. D. Winn *et al.*, “Overview of the CCP4 suite and current developments.,” *Acta Crystallogr. D. Biol. Crystallogr.*, vol. 67, no. Pt 4, pp. 235–242, Apr. 2011, doi: 10.1107/S0907444910045749.

[155] P. Evans and G. Murshudov, “How good are my data and what is the resolution?,” *Acta Crystallogr. D. Biol. Crystallogr.*, vol. 69, pp. 1204–1214, Jul. 2013, doi: 10.1107/S0907444913000061.

[156] A. J. McCoy, R. W. Grosse-Kunstleve, P. D. Adams, M. D. Winn, L. C. Storoni,

and R. J. Read, “Phaser crystallographic software.,” *J. Appl. Crystallogr.*, vol. 40, no. Pt 4, pp. 658–674, Aug. 2007, doi: 10.1107/S0021889807021206.

[157] P. D. Adams *et al.*, “PHENIX: a comprehensive Python-based system for macromolecular structure solution,” *Acta Crystallogr. D. Biol. Crystallogr.*, vol. 66, no. Pt 2, pp. 213–221, Feb. 2010, doi: 10.1107/S0907444909052925.

[158] W. L. DeLano, “DeLano,” *PyMOL Mol. Graph. Syst. DeLano Sci. San Carlos, CA, USA*, 2002.

Appendix

Supplementary tables

Table S1. List of oligonucleotides.

Table 2-2 shows the sequence of primers

Primer	Sequence	suggestions
*Ec*EF-Tu-NcoI-F	TTAACCATGGGCTCTAAAGAAAAATTTG AACGTACAAAACCGCACG	Cloning of C-terminal His_6-tagged *E. coli* EF-Tu into pET24d
*Ec*EF-Tu-XhoI-6H-R	TTAACTCGAGTTAGTGGTGATGGTGATG ATGGCCCAGAACTTTAGCAACAACGCC	
*Ec*EF-Ts-NdeI-F	TTAACATATGGCTGAAATTACCGCATC	Cloning of N-terminal His_6-tagged *E. coli* EF-Ts into pET16b
*Ec*EF-Ts-BamHI-R	TTAAGGATCCTTAAGACTGCTTGGACAT C	
*Bs*EF-Tu-PciI-6H-F	TTAAACATGTCACATCACCATCACCATCA CGCTAAAGAAAAATTCGACCGTTCCAAA TC	Cloning of N-terminal His_6-tagged *B. subtilis* EF-Tu into pET24d
*Bs*EF-Tu-XhoI-R	TTAACTCGAGTTACTCAGTGATTGTAGA AACAACG	
*Bs*EngA-Nde-F	TTAACATATGGGTAAACCTGTCGTAGC	Cloning of N-terminal His_6-tagged *B. subtilis* EngA into pET28a
*Bs*EngA-Xho-R	TTAACTCGAGTTATTTTCTAGCTCTTGC	
*Ec*EngA-Nde-F	TTAACATATGGTACCTGTGGTCGCGCTT G	Cloning of N-terminal His_6-tagged *E.coli* EngA into pET28a
*Ec*EngA-Xho-R	TTAACTCGAGTTATTTATTTTTCTTGATG TGCTTC	
*Bs*Era-NcoI-F	TTAACCATGGGCACGAACGAAAGCTTTA AATCAGGATTTG	Cloning of C-terminal His_6-tagged *B. subtilis* Era into pET24d
*Bs*Era-XhoI-6H-R	TTAACTCGAGTTAGTGATGGTGATGGTG ATGATATTCGTCCTCTTTAAAGCCAAAAT C	
*Bs*Era-NcoI-6H-F	TTAACCATGGGCCATCACCATCACCATC ACACGAACGAAAGCTTTAAATCAGGATT TG	Cloning of N-terminal His_6-tagged *B. subtilis* Era into pET24d
*Bs*Era-XhoI-R	TTAACTCGAGTTAATATTCGTCCTCTTTA AAGCCAAAATC	
*Gth*Era-NcoI-F	TTAACCATGGGCAATAAACAGGGATACA AATCAGGATTTG	Cloning of C-terminal His_6-tagged *G. thermodenitrificans* Era into pET24d
*Gth*Era-XhoI-6H-R	TTAACTCGAGTTAGTGATGGTGATGGTG ATGATACTCGTCTTCTCGAAACCCGAAG	
*Gth*Era-NcoI-6H-F	TTAACCATGGGCCATCACCATCACCATC ACAATAAACAGGGATACAAATCAGGATT TG	Cloning of N-terminal His_6-tagged *G. thermodenitrificans* Era into pET24d
*Gth*Era-XhoI-R	TTAACTCGAGTTAATACTCGTCTTCTCGA AACCCGAAG	
*Ec*Era-NcoI-F	TTAACCATGGGCATGAGCATCGATAAAA GTTACTGCGGATTTATTG	

*Ec*Era-XhoI-6H-R	TTAACTCGAGTTAGTGATGGTGATGGTG ATGAAGATCGTCAACGTAACCGAGACTG	Cloning of C-terminal His_6-tagged *E. coli* Era into pET24d
*Ec*Era-NcoI-6H-F	TTAACCATGGGCCATCACCATCACCATC ACAGCATCGATAAAAGTTACTGCGGATT TATTG	Cloning of N-terminal His_6-tagged *E. coli* Era into pET24d
*Ec*Era-XhoI-R	TTAACTCGAGTTAAAGATCGTCAACGTA ACCGAGACTG	
*Ec*EF-G-BamHI-6H-F	TTAAGGATCCACATGCACCATCACCATC ACCATGCTCGTACAACACCCATCG	Cloning of N-terminal His_6-tagged *E. coli* EF-G into pET24d
*Ec*EF-G XhoI-R	TTAACTCGAGTTATTTACCACGGGCTTC AATTACGGC	
*Ec*EF-G-BamHI-F	TTAAGGATCCATGGCTCGTACAACACCC ATCG	Cloning of N-terminal His_6-tagged *E. coli* EF-G into pET24d
*Ec*EF-G XhoI-6H-R	TTAACTCGAGTTAGTGATGGTGATGGTG ATGTTTACCACGGGCTTCAATTAC	

Table S2. List of plasmids.

Vector	Insert	Organism	Affinity tag	Cloning sites
pET-24d(+)	EF-Tu	*E. coli*	C-His_6	NcoI/XhoI
pET-16b(+)	EF-Ts	*E. coli*	N-His_6	NcoI/XhoI
pET-24d(+)	EF-Tu	*B. subtilis*	N-His_6	PciI/XhoI
pET-28a(+)	EngA	*B. subtilis*	N-His_6	NdeI/XhoI
pET-28a(+)	EngA	*E. coli*	N-His_6	NdeI /XhoI
pET-24d(+)	Era	*B. subtilis*	C-His_6	NcoI/XhoI
pET-24d(+)	Era	*B. subtilis*	N-His_6	NcoI/XhoI
pET-24d(+)	Era	*G. thermodenitrificans*	C-His_6	NcoI/XhoI
pET-24d(+)	Era	*G. thermodenitrificans*	N-His_6	NcoI/XhoI
pET-24d(+)	Era	*E. coli*	C-His_6	NcoI/XhoI
pET-24d(+)	Era	*E. coli*	N-His_6	NcoI/XhoI
pET-24d(+)	EF-G	*E. coli*	N-His_6	BamHI/XhoI
pET-24d(+)	EF-G	*E. coli*	C-His_6	BamHI/XhoI